Controlled and uncontrolled inflammatory responses: mechanistic insights and implications for early-phase clinical research

M.C.E. VAN RUISSEN

CONTROLLED AND UNCONTROLLED INFLAMMATORY RESPONSES: MECHANISTIC INSIGHTS AND IMPLICATIONS FOR EARLY-PHASE CLINICAL RESEARCH

Voor papa
Small steps in a big world, heading for …….

Design: Caroline de Lint (caro@delint.nl)
Cover image: M.C.E. van Ruissen

Publication of this thesis was financially supported by the Centre for Human Drug Research (CHDR) foundation in Leiden, the Netherlands.

Controlled and uncontrolled inflammatory responses: mechanistic insights and implications for early-phase clinical research

Proefschrift

ter verkrijging van
de graad van doctor aan de Universiteit Leiden,
op gezag van rector magnificus prof.dr. S. de Rijcke,
volgens besluit van het college voor promoties
te verdedigen op dinsdag 29 september 2026
klokke 13.00 uur

door
Marella Cornelia Elizabeth van Ruissen
geboren te Ede, Nederland
in 1996

PROMOTOR
Prof. dr. J. Burggraaf

CO-PROMOTORES
Dr. M. Moerland
Dr. M.A.A. Jansen

PROMOTIECOMMISSIE
Prof. dr. I. Bot
Prof. dr. A.J. van Zonneveld
Prof. dr. G. Kloppenburg
Dr. J. Aman (*Vrije Universiteit*)

CHAPTER 1 Introduction – 7

SECTION 1 CONTROLLED INFLAMMATORY RESPONSES

CHAPTER 2 Open-label interventional study in healthy volunteers to evaluate NO-mediated vasodilation by dermal allyl isothiocyanate challenge and whole-body heat stress – 17

CHAPTER 3 Proof of pharmacology, safety, and pharmacokinetics of the novel TRPA 1 antagonist BI 1839100: a randomised, placebo-controlled, parallel group, first-in-human study in healthy male participants – 35

CHAPTER 4 Breaking barriers: characterisation of the intradermal lipopolysaccharide challenge as an in vivo model for controlled induction of vascular leakage in healthy volunteers – 59

CHAPTER 5 Advancing clinical drug development: omics-based immunological characterisation of the intradermal lipopolysaccharide-driven human inflammatory response – 83

SECTION 2 UNCONTROLLED INFLAMMATORY RESPONSES

CHAPTER 6 Adverse immunostimulation in early-phase clinical trials: key findings and recommendations based on the investigator's clinical experience – 121

CHAPTER 7 Summary, future directions and conclusion – 137

CHAPTER 8 Nederlandse samenvatting – 153

APPENDICES PhD portfolio – 170
Curriculum vitae – 178

CHAPTER 1

Introduction

PHARMACOLOGICAL CHALLENGE MODELS IN EARLY-PHASE CLINICAL DRUG DEVELOPMENT

Drug development is a time- and money-consuming process that generally takes 10-15 years from drug discovery to market approval and costs $1-2 billion, including the costs of failure, per approved drug.[1-3] Of all drugs that enter the clinical research phase, an estimated 90% fail, with more than 50% attributable to lack of efficacy in clinical studies in patients.[3,4] This indicates the need for implementation of strategies aimed at expanding knowledge about drug efficacy in early clinical drug development. One of these strategies is implementing proof-of-pharmacology assessments in early drug studies. The knowledge gained from such studies may contribute to early termination of drug candidates that do not display signs of efficacy. At the same time this knowledge facilitates efficient advancement of promising drug candidates to later clinical stages by informing the design of future clinical studies, including supporting adequate target, dose, and endpoint selection.[5,6] This approach ultimately reduces drug attrition rates attributable to inefficacy and thereby reduces use of resources and losses of investments.

A practical difficulty in conducting proof-of-pharmacology studies in phase I studies is that healthy participants lack the target disorder. To overcome this problem, pharmacological or physiological challenge models can be used to induce activation of pathophysiological processes related to the mechanism of action of drug candidates.

CONTROLLED INFLAMMATORY RESPONSES

Such challenge models have recently been gaining ground in the field of inflammation.[7-9] Examples include the allyl isothiocyanate (AITC) skin challenge and the intradermal lipopolysaccharide (ID LPS) challenge. These challenges involve transient, mild inflammation induced under controlled conditions by topical administration of the pro-inflammatory agents AITC or LPS, respectively.[7,9,10] These inflammatory models also elicit immune-mediated vascular responses that are relevant to a multitude of diseases targeted by current drug development programmes.[11-13]

AITC

The AITC skin challenge consists of the dermal application of AITC dissolved in mineral oil to the volar forearms. The primary outcome measure is topical vasodilation, quantified as increased perfusion using laser speckle contrast imaging (LSCI).[10] This topical vascular response arises from cutaneous neurogenic inflammation, including vasodilation and leukocyte infiltration, mediated by calcium-dependent neuropeptide release following activation of the transient receptor potential cation channel A1 (TRPA1) channel. TRPA1, expressed in cutaneous sensory nerves, can be activated by various exogenous stimuli such as cold temperature (<17°C) and chemical irritants including mustard oil, cinnamon, and garlic.[14-16] The AITC skin challenge can be applied in early-phase clinical studies to detect the TRPA1-antagonistic pharmacodynamic effects of novel drug candidates targeting TRPA1.[10]

Although this model reproducibly induces vasodilation,[10] the exact underlying mechanisms remain incompletely understood. Moreover, there is no broad practical knowledge base on the pharmacodynamic effects of drug candidates on the AITC skin challenge available yet, as only a single prior clinical study using the AITC skin challenge combined with a TRPA1-antagonist has been published.[17]

LPS

The ID LPS challenge induces a Toll-like receptor 4 (TLR4)-mediated, transient, localised innate immune response by intradermal injection of LPS. This response consists of a vascular component and an inflammatory component, respectively characterised by increased dermal perfusion and erythema, and the recruitment of immune cells and cytokine production. The cellular infiltration follows a temporally ordered pattern of a rapid influx of neutrophils, followed

by influx of monocytes, dendritic cells, and T cells. This response is accompanied by a local increase of cytokines such as interleukin (IL)-1β, IL-6, IL-8, interferon-γ (IFN-γ), and tumour necrosis factor (TNF).[7] Furthermore, topical and systemic administration of corticosteroids attenuate the vascular, especially 6 hours after injection, and the cellular inflammatory responses, mainly 24 hours after injection,[18] indicating the presence of a variety of vasodilatory and inflammatory mechanisms over time targetable by investigational drugs. The available knowledge supports the model's applicability to early-phase clinical trials to study proof-of-pharmacology of anti-inflammatory drug candidates.

Although the immunological clinical endpoints of the ID LPS challenge have been extensively studied, its potential as a model for studying induction of vascular responses, including vascular leakage, and its underlying transcriptomic and proteomic profiles remain largely unexplored.

UNCONTROLLED INFLAMMATORY RESPONSES

Human inflammatory challenge models, such as the AITC skin challenge and ID LPS challenge, are designed to induce mild, transient inflammatory responses in a controlled setting in early-phase clinical studies. In contrast, undesirable inflammatory responses can also occur in an uncontrolled and unpredictable manner during clinical studies.[19,20] These uncontrolled inflammatory responses are referred to as adverse immunostimulation (AIS). AIS can be triggered by investigated drug candidates. Their growing structural complexity, especially of immunomodulatory drugs such as bispecific or Fc-engineered antibodies, has been associated with an increase in AIS in recent years.[20,21] AIS can be categorised into three categories:

1 IGE-mediated hypersensitivity reactions, usually occurring after repeated drug exposure. This reaction arises from basophils and mast cell degranulation following antigen-specific IGE binding to their FcεRI-receptors.[22-24]
2 Complement activation-related pseudo allergy (CARPA), due to unintended activation of the complement cascade after initial drug exposure.[25]
3 Cytokine release syndrome (CRS), characterised by an acute and excessive release of pro-inflammatory mediators (TNF, IL-6, IL-1β, IFN-γ) upon drug exposure. This is followed by widespread immune cell activation and systemic inflammation.[26,27]

The clinical manifestation of AIS is extremely heterogeneous, ranging from mild symptoms (e.g. pruritus and abdominal discomfort) to life-threatening reactions (e.g. hypotension, acute respiratory distress, and multiple organ failure).[28] The often non-specific nature of symptoms complicates detection of early stages of AIS and mild presentations of AIS.[29] Despite the increasing incidence of AIS in early-phase clinical trials with great impact on study participant safety and efficiency of drug development programmes, there is currently no comprehensive evidence-based guidance or framework for its prediction and prevention.

AIM AND STRUCTURE OF THIS THESIS

This thesis describes research ultimately aimed at advancing immunological clinical drug development. The thesis is divided into two sections. First, it mechanistically explores controlled vascular and inflammatory effects of experimental human challenge models used for informing early-phase clinical research with novel therapeutics. Furthermore, it evaluates regulatory considerations and the insights gained from uncontrolled inflammatory effects in clinical trials.

Part 1

Part 1 of this thesis focuses on the pharmacodynamic responses in challenge models in a controlled setting. This section describes the expansion and application of two in vivo challenge models, the AITC skin challenge and the ID LPS challenge, that both induce inflammatory vascular responses. Firstly, chapters 2 and 3 study

the AITC skin challenge. In chapter 2, we examine potential overlap in vasodilatory mechanistic pathways of whole-body heat stress and AITC by combining the two challenges. Chapter 3 presents pharmacodynamic effects of TRPA1-antagonist BI 1839100 on AITC-induced vasodilation in a first-in-human study, aiming to extend our knowledge of the use of the AITC skin challenge within early-phase clinical trials. Secondly, we investigate the ID LPS challenge in chapters 4 and 5. Chapter 4 describes its potential to function as model of vascular hyperpermeability in healthy volunteers, with the aim of using ID LPS to perform early-phase proof-of-pharmacology research with pharmaceuticals targeting endothelial integrity and vascular barrier function. Chapter 5 aims to extend our knowledge on the inflammatory effects of ID LPS by providing an omics-based characterisation of this model.

Part 2

Part 2 examines uncontrolled inflammatory responses in three first-in-human clinical studies of anti-inflammatory investigational medicinal products (IMPs). In each case, the IMPs displayed adverse immunostimulation (AIS) in the early cohorts in these first-in-human studies. This raised safety concerns, which led to modification of the drug development processes. Chapter 6 portrays our perspective on AIS, informed by the available regulatory guidelines and the observed immunostimulatory effects during these three early-phase clinical trials.

Chapter 7 concludes this thesis with a synthesis of the main findings, a general discussion and recommendations for future applications of the studied human challenge models in early-phase clinical pharmacological research.

REFERENCES

1. DiMasi JA, Grabowski HG, Hansen RW. Innovation in the pharmaceutical industry: New estimates of R&D costs. *J Health Econ*. 2016;47:20-33. doi:10.1016/j.jhealeco.2016.01.012
2. Sun D, Gao W, Hu H, Zhou S. Why 90% of clinical drug development fails and how to improve it? *Acta Pharm Sin B*. 2022;12(7):3049-3062. doi:10.1016/j.apsb.2022.02.002
3. Smietana K, Siatkowski M, Møller M. Trends in clinical success rates. *Nat Rev Drug Discov*. 2016;15(6):379-380. doi:10.1038/nrd.2016.85
4. Harrison RK. Phase II and phase III failures: 2013-2015. *Nat Rev Drug Discov*. 2016;15(12):817-818. doi:10.1038/nrd.2016.184
5. Hijma HJ, Groeneveld GJ. Analgesic drug development: proof-of-mechanism and proof-of-concept in early phase clinical studies. *Med Drug Discov*. 2021;10:100083. doi:10.1016/j.medidd.2021.100083
6. Schmidt B. Proof of principle studies. *Epilepsy Res*. 2006;68(1):48-52. doi:10.1016/j.eplepsyres.2005.09.019
7. Buters TP, Hameeteman PW, Jansen IME, et al. Intradermal lipopolysaccharide challenge as an acute in vivo inflammatory model in healthy volunteers. *Br J Clin Pharmacol*. 2022;88(2):680-690. doi:10.1111/bcp.14999
8. van der Kolk T, Assil S, Rijneveld R, et al. Comprehensive, Multimodal Characterization of an Imiquimod-Induced Human Skin Inflammation Model for Drug Development. *Clin Transl Sci*. 2018;11(6):607-615. doi:10.1111/cts.12563
9. Andersen HH, Lo Vecchio S, Gazerani P, Arendt-Nielsen L. Dose-response study of topical allyl isothiocyanate (mustard oil) as a human surrogate model of pain, hyperalgesia, and neurogenic inflammation. *Pain*. 2017;158(9):1723-1732. doi:10.1097/j.pain.0000000000000979
10. Joseph V, Yang X, Gao SS, et al. Development of AITC-induced dermal blood flow as a translational in vivo biomarker of TRPA1 activity in human and rodent skin. *Br J Clin Pharmacol*. 2021;87(1):129-139. doi:10.1111/bcp.14370
11. Wautier JL, Wautier MP. Vascular Permeability in Diseases. *Int J Mol Sci*. 2022;23(7):3645. doi:10.3390/ijms23073645
12. Hajitou A, Pasqualini R, Arap W. Vascular targeting: Recent advances and therapeutic perspectives. *Trends Cardiovasc Med*. 2006;16(3):80-88. doi:10.1016/j.tcm.2006.01.003
13. Chee YJ, Dalan R, Cheung C. The Interplay Between Immunity, Inflammation and Endothelial Dysfunction. *Int J Mol Sci*. 2025;26(4):1708. doi:10.3390/ijms26041708
14. Lippe IT, Stabentheiner A, Holzer P. Participation of nitric oxide in the mustard oil-induced neurogenic inflammation of the rat paw skin. *Eur J Pharmacol*. 1993;232(1):113-120. doi:10.1016/0014-2999(93)90735-z
15. Gouin O, L'Herondelle K, Lebonvallet N, et al. TRPV1 and TRPA1 in cutaneous neurogenic and chronic inflammation: pro-inflammatory response induced by their activation and their sensitization. *Protein Cell*. 2017;8(9):644-661. doi:10.1007/s13238-017-0395-5
16. Aubdool AA, Kodji X, Abdul-Kader N, et al. TRPA1 activation leads to neurogenic vasodilatation: involvement of reactive oxygen nitrogen species in addition to CGRP and NO. *Br J Pharmacol*. 2016;173(15):2419-2433. doi:10.1111/bph.13519
17. Chan P, Ding HT, Liederer BM, et al. Translational and pharmacokinetic-pharmacodynamic application for the clinical development of GDC-0334, a novel TRPA1 inhibitor. *Clin Transl Sci*. 2021;14(5):1945-1954. doi:10.1111/cts.13049
18. Buters TP, Hameeteman PW, Jansen IME, et al. Clinical, Cellular, and Molecular Effects of Corticosteroids on the Response to Intradermal Lipopolysaccharide Administration in Healthy Volunteers. *Clin Pharmacol Ther*. 2022;111(4):964-971. doi:10.1002/cpt.2516
19. Suntharalingam G, Perry MR, Ward S, et al. Cytokine Storm in a Phase 1 Trial of the Anti-CD28 Monoclonal Antibody TGN1412. *N Engl J Med*. 2006;355(10):1018-1028. doi:10.1056/NEJMoa063842
20. Baldo BA. Immune-and Non-Immune-Mediated Adverse Effects of Monoclonal Antibody Therapy: A Survey of 110 Approved Antibodies. *Antibodies*. 2022;11(1):17. doi:10.3390/antib11010017
21. Reijers JAA, Malone KE, Bajramovic JJ, Verbeek R, Burggraaf J, Moerland M. Adverse

immunostimulation caused by impurities: The dark side of biopharmaceuticals. *Br J Clin Pharmacol*. 2019;85(7):1418-1426. doi:10.1111/bcp.13938
22. Reber LL, Hernandez JD, Galli SJ. The pathophysiology of anaphylaxis. *J Allergy Clin Immunol*. 2017;140(2):335-348. doi:10.1016/j.jaci.2017.06.003
23. Castells M. Diagnosis and management of anaphylaxis in precision medicine. *J Allergy Clin Immunol*. 2017;140(2):321-333. doi:10.1016/j.jaci.2017.06.012
24. Maggi E, Vultaggio A, Matucci A. Acute infusion reactions induced by monoclonal antibody therapy. *Expert Rev Clin Immunol*. 2011;7(1):55-63. doi:10.1586/eci.10.90
25. Szebeni J. Complement activation-related pseudoallergy: A new class of drug-induced acute immune toxicity. *Toxicology*. 2005;216(2-3):106-121. doi:10.1016/j.tox.2005.07.023
26. Lee DW, Gardner R, Porter DL, et al. Current concepts in the diagnosis and management of cytokine release syndrome. *Blood*. 2014;124(2):188-195. doi:10.1182/blood-2014-05-552729
27. Kroschinsky F, Stölzel F, von Bonin S, et al. New drugs, new toxicities: Severe side effects of modern targeted and immunotherapy of cancer and their management. *Crit Care*. 2017;21(1):89. doi:10.1186/s13054-017-1678-1
28. van den Noort JA, Meijs AC, Klarenbeek NB, Moerland M. Navigating adverse immunostimulation: A practical guide for clinical researchers. *Br J Clin Pharmacol*. Published online ahead of print September 12, 2025. doi:10.1002/bcp.70268
29. Casagrande S, Sopetto GB, Bertalot G, et al. Immune-Related Adverse Events Due to Cancer Immunotherapy: Immune Mechanisms and Clinical Manifestations. *Cancers (Basel)*. 2024;16(7):1440. doi:10.3390/cancers16071440

SECTION 1

CONTROLLED INFLAMMATORY RESPONSES

CHAPTER 2

Open-label interventional study in healthy volunteers to evaluate NO-mediated vasodilation by dermal allyl isothiocyanate challenge and whole-body heat stress

Published in: J Exp Pharmacol. 2024;16:285-294. DOI:10.2147/JEP.S473217

Marella C.E. van Ruissen[1,2], Sebastiaan J.W. van Kraaij[1,2], Pim Gal[1,2], Wouter A. Bakker[1,2], Hemme J. Hijma[1,2], Geert Jan Groeneveld[1,2], Marieke L. de Kam[1], Jacobus Burggraaf[1,2], Matthijs Moerland[1,2]

1 Centre for Human Drug Research, Leiden, the Netherlands
2 Leiden University Medical Centre, Leiden, the Netherlands

ABSTRACT

Dermal allyl isothiocyanate (AITC) administration and whole-body heat stress (WBHS) are two challenge models used to evaluate physiological mechanisms of vasodilation and pharmacological activity in humans. Their exact vasodilatory mechanisms in humans are not fully elucidated but are likely to be nitric oxide (NO)-mediated. This study aimed to evaluate whether there is overlap in the vasodilatory pathways of dermal AITC application and WBHS by combining the challenges. In this open-label interventional study, healthy volunteers underwent dermal administration of AITC twice: once under basal conditions and once during WBHS. Dermal blood flow (DBF) was non-invasively measured using laser speckle contrast imaging on four occasions, corresponding to the following situations: baseline, WBHS only, AITC only, and WBHS combined with AITC. A total of 12 male volunteers, aged 18–61 years, participated in the study. Compared to baseline, following AITC application, DBF increased by 63.43 AU (baseline: 32.55, 95% CI [17.78, 47.31] AU, AITC only: 95.97, 95% CI [81.21, 110.7] AU, $p < 0.0001$). During WBHS, the increase in DBF after AITC was 42.76 AU (WBHS only: 87.25, 95% CI [72.49, 102.0] AU, WBHS+AITC: 130.0, 95% CI [115.2, 144.8] AU, $p < 0.0001$). The combination of WBHS and AITC resulted in a lower DBF than the sum of the DBF responses to AITC and WBHS when applied separately (ED 20.67, 95% CI [−3.532, 44.88], $p = 0.0916$). This might point towards the presence of an interaction between the vasodilatory mechanisms of AITC application and WBHS, possibly indicating overlap in their nitric oxide synthase (NOS)-driven vasodilatory pathways.

INTRODUCTION

A large variety of pharmacodynamic models and human challenges are used in clinical research to unravel (patho)physiological mechanisms, mimic pathological conditions, and evaluate the pharmacological effects of newly developed drug candidates.[1–6] Two such challenges are the allyl isothiocyanate (AITC) skin challenge and whole-body heat stress (WBHS). WBHS is a technique commonly used to study mechanisms of vasodilation.[7–10] It involves passively increasing core body temperature to 38–39°C by exposing healthy volunteers to heat either with warm water suits or in baths, which induces a dermal vasodilatory response.[8,10] The recently developed AITC skin challenge based on dermal administration of AITC leads to vasodilation through agonism of the transient receptor potential cation channel A1 (TRPA1).[11,12] This challenge has been shown to be suitable for use in early-phase clinical trials investigating TRPA1-antagonists.[13] Both challenges induce dermal vasodilation, which has been demonstrated to be objectively quantifiable as (changes in) dermal blood flow (DBF) using several imaging techniques, including laser speckle contrast imaging (LSCI).[14,15] The physiological pathways leading to vasodilation in these challenges are not yet fully understood.

Nitric oxide (NO) has a role in various physiological processes, including acting as potent vasodilator. Its production is catalysed by three isoforms of nitric oxide synthase (NOS): neuronal, inducible, and endothelial NOS (nNOS, iNOS, eNOS). The primary function of nNOS involves NO-related vasodilation via nitrergic nerves, synaptic signalling, and central regulation of blood pressure. iNOS plays a signalling role in immune-mediated vasodilation and shaping the immune response, while eNOS induces endothelium-dependent vasodilation.[16–18] Despite the lack of knowledge about the exact vasodilatory mechanisms of the AITC challenge and WBHS, it is known that their responses are at least partly mediated by TRPA1-agonistic activity influencing the NO system.[9,19,20] Hypothetically, there may be overlap in their vasodilatory mechanisms. However, data substantiating this hypothesis are lacking.

This study evaluated the vasodilatory response following a combined WBHS and AITC challenge, compared to the response to each challenge alone. The AITC skin challenge and WBHS were combined in the same study participants, allowing the identification of a potential overlap in their vasodilatory pathways. Theoretical outcomes comprised (1) a full overlap, resulting in no increase in skin perfusion following an AITC challenge during WBHS, (2) a partial overlap, resulting in a partially additive effect of AITC, or (3) no overlap, resulting in a full additive effect of an AITC challenge in a WBHS background (Figure 1).

MATERIALS AND METHODS

This study was conducted in accordance with the principles of the Declaration of Helsinki and the Dutch Act on Medical Research involving Human Subjects (WMO) between 23 November 2021 and 12 January 2022 at the Centre for Human Drug Research, Leiden, The Netherlands. The study, submitted at ToetsingOnline (NL79322.056.21) and prospectively registered on 16 November 2021 in the WHO-recognised Overview of Medical Research in The Netherlands (NL-OMON50731) registry, was approved by an independent Medical Ethics Committee (Medisch Ethische Toetsingscommissie van de Stichting Beoordeling Ethiek Biomedisch Onderzoek, Assen, The Netherlands).

Study design and participants

This was an open-label interventional study. Before any study-related procedure, all participants provided written informed consent. Healthy, non-smoking volunteers aged 18–65 years, without a prior history of acute or chronic medical conditions and treatments, were eligible for participation after successfully completing a medical screening consisting of a full medical history, physical examination, and laboratory testing. Only male participants were eligible to minimise variability in DBF measurements due to known inter-sex differences in AITC responses.[11,21] Participants with a history of skin disorders, food allergies (specifically to mustard), or post-inflammatory hyperpigmentation, and participants unable to undergo WBHS were excluded. Participants refrained from the use of medications or illicit drugs and from vitamin, mineral, herbal, or dietary supplements from respectively 14 days and 7 days prior to AITC administration until the end of the study. Participants refrained from alcohol and caffeine-containing products from 24 hours prior to AITC administration until the end of the study.

For the AITC skin challenge, GMP-grade AITC (Ofichem BV, Ter Apel, The Netherlands), dissolved in mineral oil was dispensed by the Leiden University Medical Centre pharmacy (Leiden, The Netherlands), was used. On two occasions, 25 µL of 15% AITC was topically applied to the skin within an 11mm O-ring: under basal conditions to one volar forearm (AITC only), and subsequently during WBHS to the contralateral volar forearm (WBHS+AITC) (Figure 2). The selected volume and concentration of AITC have previously been demonstrated to induce a robust DBF increase while having a tolerable safety profile.[11]

During WBHS, participants were submerged up to their shoulders in a 40°C water bath (NetSpa, Rousset, France) until their core temperature reached 38°C (WBHS only and WBHS+AITC) (Figure 2). Core body temperature was measured during WBHS with an ingested capsulated thermometer (BodyCap, Hérouville Saint-Clair, France).

Vascular endpoints

DBF, expressed in arbitrary units (AU), was measured continuously for 5 minutes before and 15 minutes after the first AITC application and for 10 minutes before and 15 minutes after the second AITC application in temperature-controlled rooms between 20 and 24°C using LSCI (PeriCam PSI NR System, Perimed AB, Järfälla, Sweden) (Figure 2). LSCI recordings of the target area on the ventral forearms were captured using dedicated software (PIMSoft, Perimed AB, Järfälla, Sweden).[22] The maximum DBF, measured as mean blood flow in a 30-second time frame around the peak of perfusion, was used as the primary endpoint for the vasodilatory effects.

Statistics

All safety and statistical calculations were conducted with SAS version 9.4 for Windows or newer (SAS Institute INC., Cary, North Carolina, United States of America). Baseline characteristics were summarised by descriptive statistics (N, mean, SD) in the case of continuous demographic variables. Qualitative demographic characteristics (e.g. sex, race) were summarised by counts and percentages. DBF was evaluated at baseline, and vascular responses were evaluated after AITC only, WBHS only and WBHS+AITC within the O-ring. To further substantiate the data, a pre-specified secondary analysis was performed on skin responses that extended outside the borders of the O-ring. For this secondary response, standardised skin areas were selected based on the largest AITC-induced response in DBF among all participants. DBF was summarised per condition and graphically represented in Tukey boxplots as mean and median with minimum and maximum. DBF was analysed with a mixed effects model with fixed factor treatment and random factor participant, and results were presented as estimated differences and estimated means, both with 95% confidence interval (95% CI). Contrasts within the model were calculated between baseline and AITC only, baseline and WBHS only, and baseline and WBHS+AITC. To estimate the difference between the combined WBHS+AITC effect and the addition of the separate WBHS only and AITC only effects, the contrast between (WBHS+AITC - baseline) and ((WBHS only - baseline) + (AITC only - baseline)) was calculated within the model.

RESULTS

Baseline demographics

Twelve healthy participants, aged between 18 and 61 years, participated in the study. All included participants were male, white, and had normal vital signs and haemoglobin levels. Baseline demographics are provided in Table 1.

TABLE 1 **Baseline characteristics.**

Baseline characteristics	(N = 12)
Age (years)	33.6 (16.2)
Sex, N (%)	
Male	12 (100%)
Race, N (%)	
White	12 (100%)
Ethnicity, N (%)	
Not Hispanic or Latino	12 (100%)
Heart rate (beats per minute)	60 (10)
Temperature (°C)	36.7 (0.3)
Systolic blood pressure (mmHg)	120 (11)
Diastolic blood pressure (mmHg)	74 (9)
Respiratory rate (breaths per minute)	14 (2)
BMI (KG/M^2)	24.1 (3.3)
Haemoglobin (MMOL/L)	9.4 (0.5)

Abbreviations: BMI, body mass index; mmHg, millimetres of mercury.

AITC induces a robust vasodilatory response

The AITC skin challenge was performed under basal conditions to characterise the AITC-mediated vasodilatory response. This dermal application of AITC induced an increase in DBF lasting for at least 15 minutes (end of measurement), with the 30-second peak occurring approximately 1-4 minutes after application. A typical curve is depicted in Figure 3. DBF within the O-ring increased significantly from 32.55 (95% CI [17.78, 47.31]) AU at baseline to a maximum of 95.97 (95% CI [81.21, 110.7]) AU, $p < 0.0001$ (Figure 4, Table 2).

TABLE 2 **DBF responses within the O-ring under the studied conditions.**

Intervention	LSM maximum flow in AU (95% CI)	ED in AU vs. baseline (95% CI)	*p*-value vs. baseline
Baseline	32.55 (17.78, 47.31)	-	-
AITC only	95.97 (81.21, 110.7)	63.43 (46.31, 80.54)	<0.0001
WBHS only	87.25 (72.49, 102.0)	54.71 (37.59, 71.82)	<0.0001
WBHS+AITC	130.0 (115.2, 144.8)	97.47 (80.35, 114.6)	<0.0001

Notes: DBF was measured using LSCI at baseline, after AITC administration (AITC only), during WBHS (WBHS only), and after AITC administration during WBHS (WBHS+AITC). Abbreviations: AITC, allyl isothiocyanate; AU, arbitrary units; ED, estimated difference; LSCI, laser speckle contrast imaging; LSM, least squares means; WBHS, whole-body heat stress; 95% CI, 95% confidence interval.

Dermal blood flow is augmented to a lesser extent by AITC application during WBHS than by AITC application without WBHS

The AITC skin challenge was combined with WBHS to evaluate their combined vasodilatory response. The observed peak in DBF occurred 0.5-3 minutes after the AITC application. Figure 5 illustrates a typical curve of the augmented basal flow due to WBHS and the vasodilatory response after AITC administration. The maximal DBF increased significantly from 32.55 at baseline to 87.25 (95% CI [72.49, 102.0]) AU during WBHS only (ED 54.71, 95% CI [37.59, 71.82] AU, $p < 0.0001$), and subsequently to a maximum of 130.0 (95% CI [115.2, 144.8]) AU after AITC challenge (ED 97.47, 95% CI [80.35, 114.6] AU, $p < 0.0001$) (Figure 4, Table 2). The combination of WBHS and AITC resulted in a lower DBF than theoretically possible based on the sum of the DBF responses to AITC and WBHS when applied separately (ED 20.67, 95% CI [−3.532, 44.88] AU, $p = 0.0916$) (Figure 4). Comparable effects were observed in the secondary analysis (Table 3).

TABLE 3 DBF under the studied conditions, in the area corresponding to the largest AITC-induced vasodilatory response among all participants.

Intervention	LSM maximum flow in AU (95% CI)	ED in AU vs. baseline (95% CI)	*p*-value (vs. baseline)
Baseline	28.94 (20.67, 37.21)	-	-
AITC only	47.08 (38.81, 55.35)	18.14 (8.90, 27.37)	0.0003
WBHS only	81.19 (72.92, 89.46)	52.25 (43.02, 61.49)	<0.0001
WBHS+AITC	104.9 (96.62, 113.2)	75.94 (66.71, 85.18)	<0.0001

Notes: DBF was measured using LSCI at baseline, after AITC administration (AITC only), during WBHS (WBHS only), and after AITC administration during WBHS (WBHS+AITC). Abbreviations: AITC, allyl isothiocyanate; AU, arbitrary units; ED, estimated difference; LSCI, laser speckle contrast imaging; LSM, least squares means; WBHS, whole-body heat stress; 95% CI, 95% confidence interval.

DISCUSSION

This clinical study demonstrates a robust increase in DBF, indicating vasodilation, after the topical dermal application of 15% AITC. The observations were in line with two recent papers by Joseph et al. and Chan et al.[11,13] Furthermore, a clear increase in skin perfusion upon WBHS was observed, with vasodilatory increases similar to those previously reported by Gemae et al. and Luetkemeier et al.[10,23] Our study is the first to combine AITC application and WBHS to evaluate additive effects of, and overlap in, the vasodilatory pathways of both challenges in humans. It showed that the combination of

WBHS and AITC led to an enhanced DBF compared to each of the challenges alone, but to a lower DBF than the sum of both challenge responses, indicating a partial overlap in the underlying vasodilatory mechanisms (Figure 1D).

The observed partially additive effects of AITC on WBHS responses may indicate a partial overlap in underlying vasodilatory mechanisms between WBHS and AITC. Both challenges are known to mediate vasodilation through the NO pathway, which might explain the observations in this study. A ceiling effect in the physiological vasodilatory capacity of the dermal circulation cannot be fully excluded, for example, related to technical limitations in the detection of extreme vasodilation by LSCI. However, previous research in other pharmacological challenge models using the same recording method and analysis settings demonstrated higher DBF values (up to 110 AU higher) than in our study, suggesting that the combined effects of AITC and WBHS did not reach maximal vasodilatory capacity (data on file). Other theoretical explanations for the partial additive effect of AITC on WBHS responses are of a pharmacokinetic nature: a higher DBF during WBHS could drive more efficient local AITC absorption or clearance, thereby respectively enhancing or limiting TRPA1 stimulation and AITC-driven DBF. However, since there is no apparent faster increase after AITC application and no apparent faster resolution of the AITC-induced vasodilatory response in a WBHS background, a more efficient local AITC absorption or clearance due to heating does not seem to play a role.

Currently, limited knowledge is available about the exact contribution of specific mechanisms of vasodilation and NOS isoforms involved in both challenges in humans. However, for TRPA1 agonism, NOS, specifically nNOS, has been identified as a relevant driver of downstream vasodilatory effects. For example, vasodilation induced by cinnamaldehyde (CA), another TRPA1 agonist, has been studied

in mice and humans. Significant reductions in DBF response to CA were observed in mice administered nitro-L-arginine methyl ester (L-NAME), a non-specific NOS inhibitor, prior to dermal application of CA. To investigate NOS isoform involvement, nNOS was selectively inhibited using S-methyl-L-thiocitrulline (SMTC), which significantly reduced CA-induced DBF. This highlights the role of nNOS in TRPA1-mediated vasodilation.[24] In healthy volunteers, administration of L-NAME prior to CA infusion through dermal microdialysis significantly reduced CA-induced vasodilation.[25] Furthermore, the vasodilatory mechanisms of WBHS have been studied in humans, also showing NOS involvement. Administration of L-NAME significantly lowered WBHS-driven skin perfusion.[9,20] Intradermal administration of two specific nNOS-inhibitors, 7-nitroindazol (7-NI) and Nω-propyl-l-arginine (NPLA), during WBHS significantly attenuated the dermal vasodilatory response to WBHS in healthy volunteers, underlining the involvement of nNOS in the WBHS response.[7,26] Based on this, we hypothesise that nNOS involvement in both challenge models specifically explains the overlap in vasodilatory response observed in our study.

The influence of other downstream activated vasodilatory mediators, such as hydrogen sulphide (H_2S) through TRPA1 agonism, on the development of the vasodilatory response after TRPA1 activation by AITC cannot be ruled out.[24,25,27] However, based on the presented (pre)clinical research on TRPA1 antagonists and mechanistic reasoning, it is most likely that the direct agonistic effect of AITC on TRPA1 initiates the vasodilatory response measured in this study through NO signalling and that other vasodilatory mediators arise secondary to the AITC stimulus.[9,20,24–26]

Although our study does not include a WBHS-only group, specific NOS-related biomarkers, or an intervention blocking specific NOS pathways, it does provide insight into mechanistic overlap between the AITC and WBHS responses, potentially aiding further characterisation and application of these challenge models for the pharmacodynamic evaluation of future vascular drugs. To provide further insight into the vasodilatory mechanisms of both challenges and examine the involvement of nNOS, it would be interesting to conduct future studies that included vasodilation induced by AITC skin challenge and WBHS combined with the addition of a specific nNOS blocker, such as 7-NI. However, there are currently no facilities that produce GMP-grade 7-NI for the purpose of exploratory clinical studies.

CONCLUSION

In conclusion, this is the first study combining AITC and WBHS, demonstrating an enhanced skin response for the combined challenges compared to the individual challenge responses and suggesting a potential mechanistic overlap in the underlying NO-mediated vasodilatory mechanisms. Both challenges, combined or separately, are considered useful for evaluating the pharmacodynamic effects of NO-targeted drugs. An extended evaluation of the exact vasodilatory mechanisms involved in both challenges may further increase their value.

FIGURE 1 **Theoretical DBF responses to AITC, WBHS, and the combination of AITC and WBHS over time.** (A) DBF after dermal administration of AITC. (B) DBF during WBHS. (C–E) DBF under the combination of AITC and WBHS. Hypotheses comprise full overlap (C), partial overlap (D), and no overlap (E) in vasodilatory mechanisms. Synergism of the DBF response by WBHS+AITC is theoretically possible, but mechanistically unlikely and therefore not included.

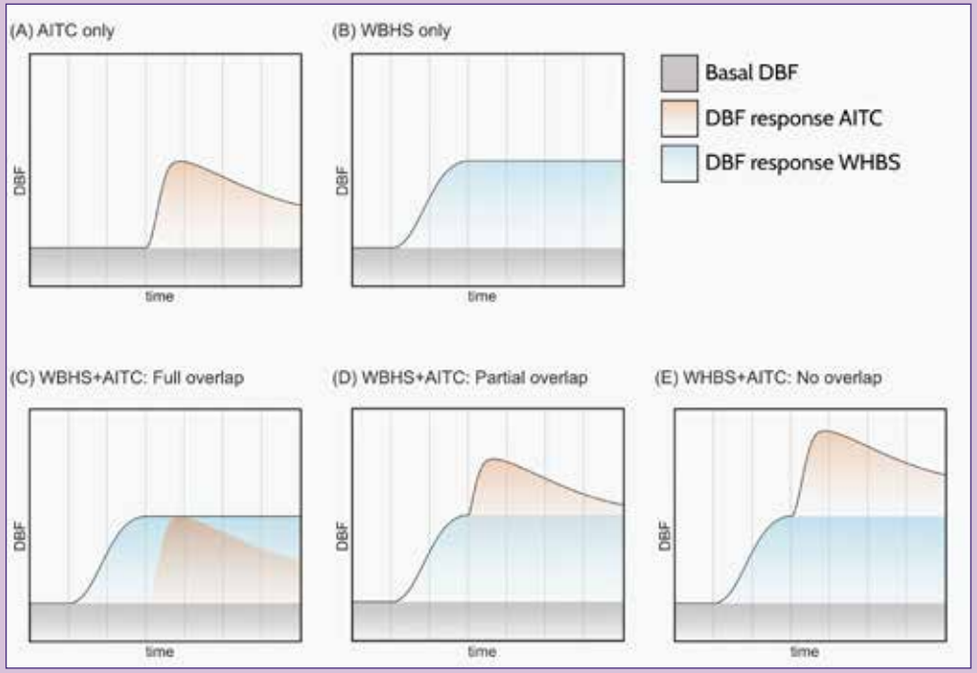

Abbreviations: AITC, allyl isothiocyanate; DBF, dermal blood flow; WBHS, whole-body heat stress.

FIGURE 2 **Schematic representation of the study design.** (A) Measurement of DBF using LSCI for a duration of 5 minutes at baseline and 15 minutes after AITC application. (B) Measurement of DBF using LSCI for a duration of 10 minutes during WBHS and 15 minutes after combination with the AITC application. In both (A) and (B), 25 µL of 15% AITC was administered within an 11mm O-ring to the volar forearm.

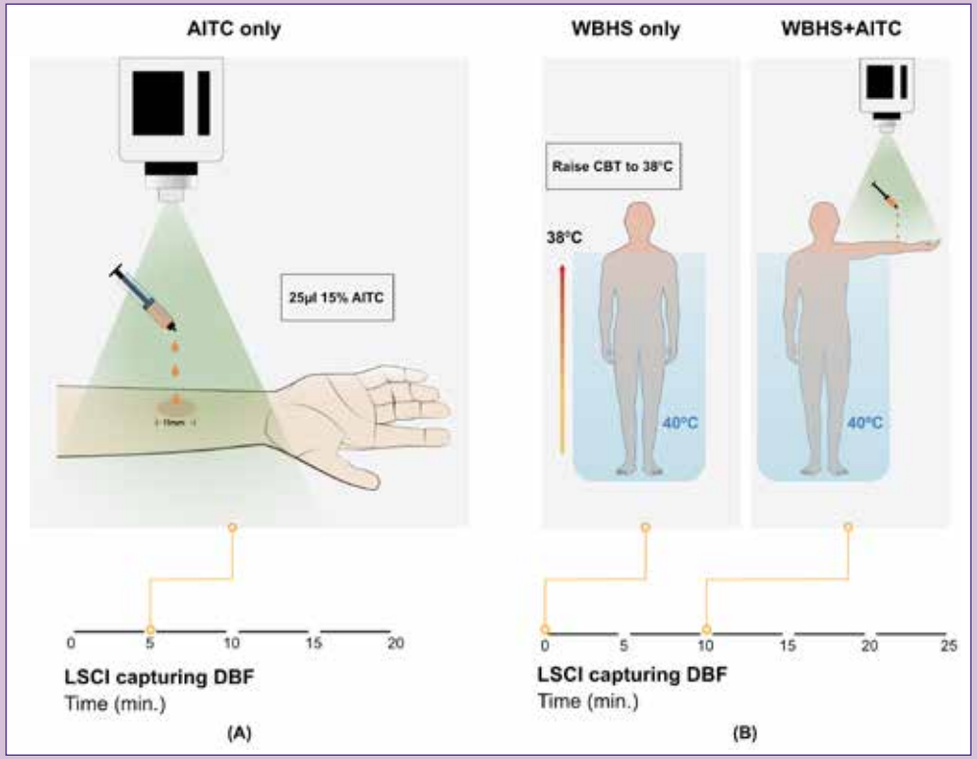

Abbreviations: AITC, allyl isothiocyanate; CBT, core body temperature; DBF, dermal blood flow; WBHS, whole-body heat stress.

FIGURE 3 **Exemplary response of an individual to AITC.** (A) Visual representation of DBF within the O-ring in AU after AITC administration; 1 = O-ring. (B) DBF expressed in AU at baseline and in response to AITC administration at 5 minutes, as measured by LSCI.

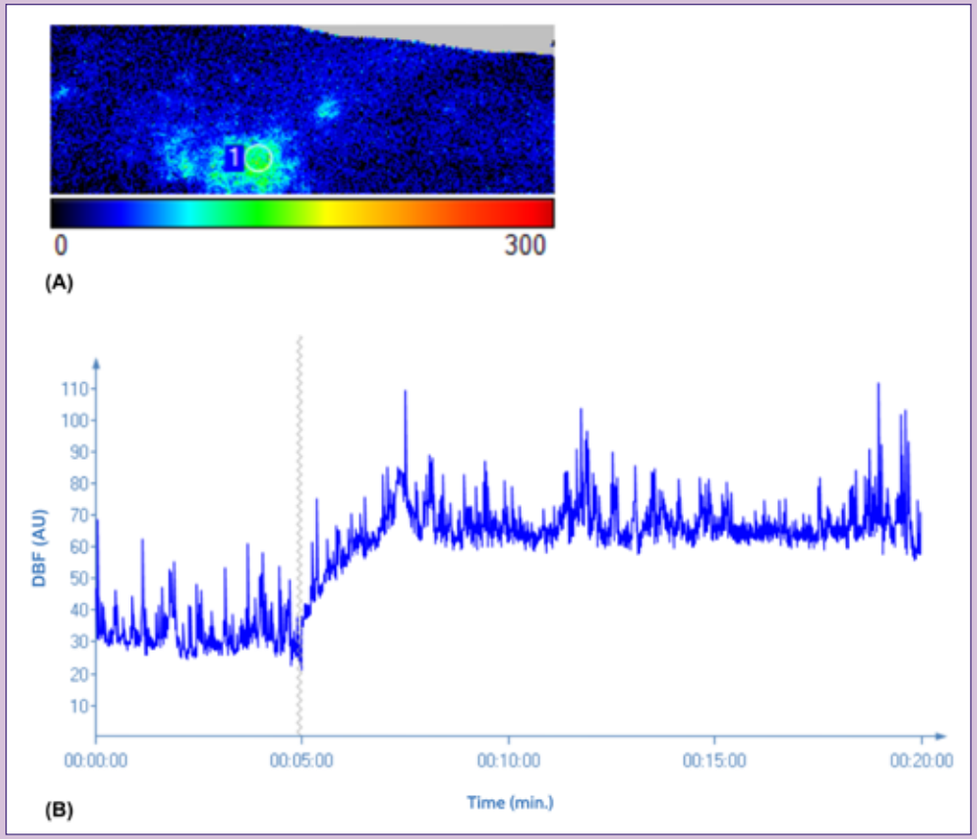

Abbreviations: AITC, allyl isothiocyanate; AU, arbitrary units; DBF, dermal blood flow; LSCI, laser speckle contrast imaging.

FIGURE 4 **Tukey boxplot representing DBF within the O-ring under the studied conditions.** DBF was measured using LSCI, and statistical analysis of AITC, WBHS, and WBHS+AITC compared to baseline report *p*-values <0.0001, as indicated with an *.

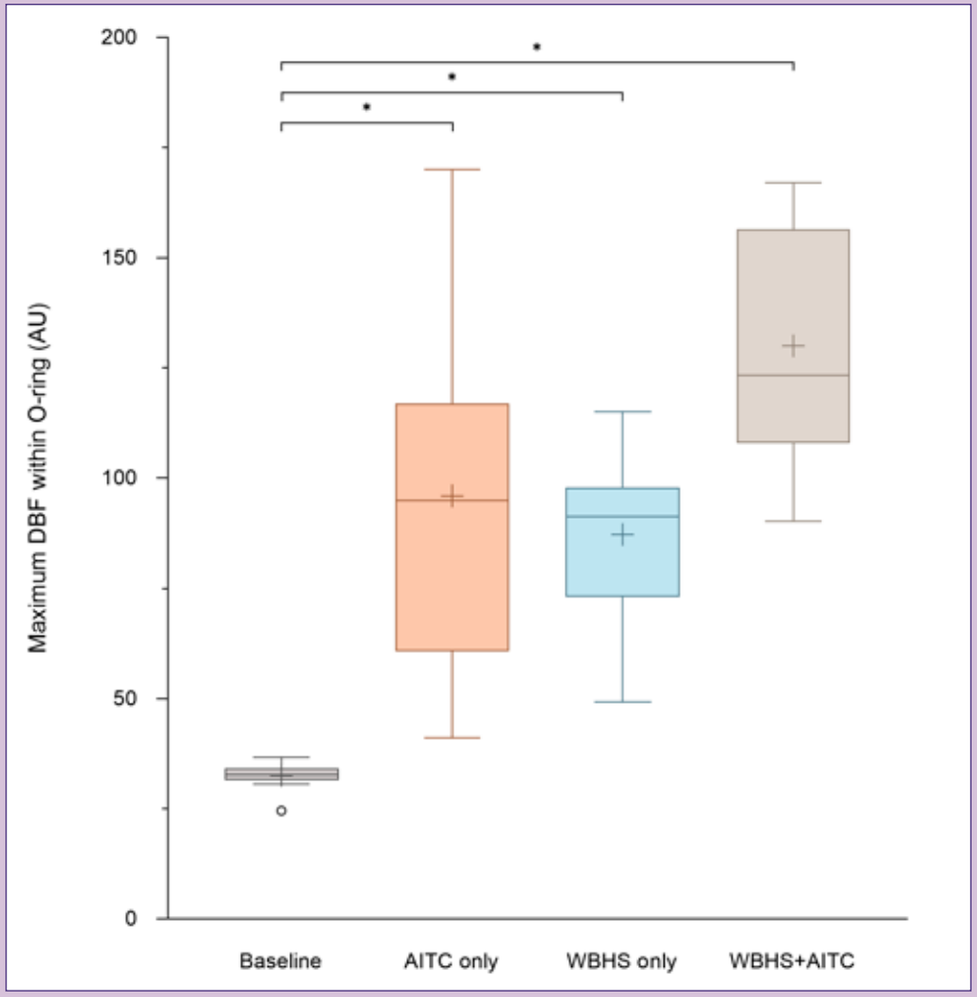

Abbreviations: AITC, allyl isothiocyanate; AU, arbitrary units; DBF, dermal blood flow; LSCI, laser speckle contrast imaging; WBHS, whole-body heat stress.

FIGURE 5 **Exemplary response of an individual to AITC during WBHS.** (A) Visual representation of DBF within the O-ring in AU after AITC administration during WBHS; 1 = O-ring. (B) DBF expressed in AU during WBHS and in response to AITC administration at 10 minutes, as measured by LSCI.

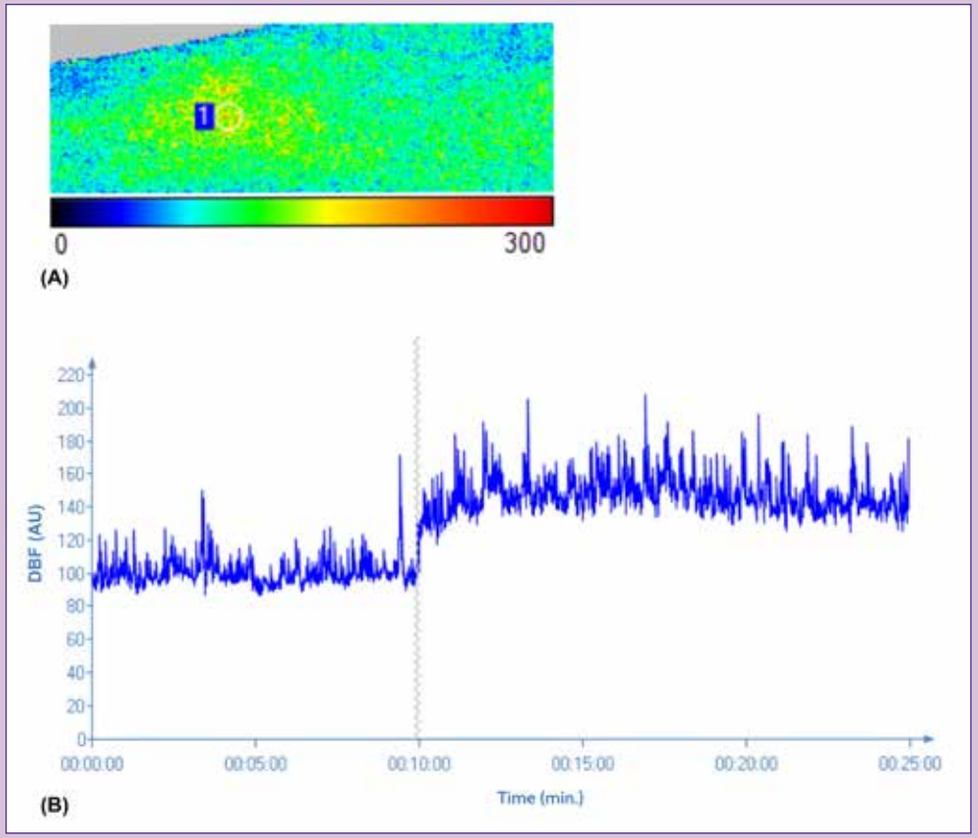

Abbreviations: AITC, allyl isothiocyanate; AU, arbitrary units; DBF, dermal blood flow; LSCI, laser speckle contrast imaging; WBHS, whole-body heat stress.

REFERENCES

1. van der Kolk T, Assil S, Rijneveld R, et al. Comprehensive, multimodal characterization of an imiquimod-induced human skin inflammation model for drug development. *Clin Transl Sci*. 2018;11(6):607-615. doi:10.1111/cts.12563
2. Buters TP, Hameeteman PW, Jansen IME, et al. Intradermal lipopolysaccharide challenge as an acute in vivo inflammatory model in healthy volunteers. *Br J Clin Pharmacol*. 2022;88(2):680-690. doi:10.1111/bcp.14999
3. Van Dongen MGJ, Geerts BF, Bhanot S, et al. Characterization of a standardized glucagon challenge test as a pharmacodynamic tool in pharmacological research. *Horm Metab Res*. 2014;46(4):269-273. doi:10.1055/s-0033-1363223
4. Vanmolkot FHM, Van Der Schueren BJEP, De Hoon JNJM. Calcitonin gene-related peptide-induced vasodilation in the human forearm is antagonized by CGRP8-37: Evaluation of a human in vivo pharmacodynamic model. *Clin Pharmacol Ther*. 2006;79(3):263-273. doi:10.1016/j.clpt.2005.11.005
5. Stephens DP, Charkoudian N, Benevento JM, Johnson JM, Louis Saumet J, Johnson JM. The influence of topical capsaicin on the local thermal control of skin blood flow in humans. *Am J Physiol Regul Integr Comp Physiol*. 2001;281(3):894-901. doi:10.1152/ajpregu.2001.281.3.R894
6. Roestenberg M, Hoogerwerf MA, Ferreira DM, Mordmüller B, Yazdanbakhsh M. Experimental infection of human volunteers. *Lancet Infect Dis*. 2018;18(10):e312-e322. doi:10.1016/S1473-3099(18)30177-4
7. Kellogg DL, Zhao JL, Wu Y. Neuronal nitric oxide synthase control mechanisms in the cutaneous vasculature of humans in vivo. *J Physiol*. 2008;586(3):847-857. doi:10.1113/jphysiol.2007.144642
8. Kellogg Jr DL, Zhao JL, Wu Y, et al. Antagonism of soluble guanylyl cyclase attenuates cutaneous vasodilation during whole body heat stress and local warming in humans. *J Appl Physiol*. 2011;110:1406-1413. doi:10.1152/japplphysiol.00702.2010
9. Wong BJ. Sensory nerves and nitric oxide contribute to reflex cutaneous vasodilation in humans. *Am J Physiol Regul Integr Comp Physiol*. 2013;304(8):651-656. doi:10.1152/ajpregu.00464.2012.
10. Gemae MR, Akerman AP, McGarr GW, et al. Myths and methodologies: Reliability of forearm cutaneous vasodilatation measured using laser-Doppler flowmetry during whole-body passive heating. *Exp Physiol*. 2021;106(3):634-652. doi:10.1113/EP089073
11. Joseph V, Yang X, Gao SS, et al. Development of AITC-induced dermal blood flow as a translational in vivo biomarker of TRPA1 activity in human and rodent skin. *Br J Clin Pharmacol*. 2021;87(1):129-139. doi:10.1111/bcp.14370
12. Lippe IT, Stabentheiner A, Holzer P. Participation of nitric oxide in the mustard oil-induced neurogenic inflammation of the rat paw skin. *Eur J Pharmacol*. 1993;232(1):113-120. doi:10.1016/0014-2999(93)90735-z
13. Chan P, Ding HT, Liederer BM, et al. Translational and pharmacokinetic-pharmacodynamic application for the clinical development of GDC-0334, a novel TRPA1 inhibitor. *Clin Transl Sci*. 2021;14(5):1945-1954. doi:10.1111/cts.13049
14. Guven G, Dijkstra A, Kuijper TM, et al. Comparison of laser speckle contrast imaging with laser Doppler perfusion imaging for tissue perfusion measurement. *Microcirculation*. 2023;30(1):e12795. doi:10.1111/micc.12795
15. Chaseling GK, Crandall CG, Gagnon D. Skin blood flow measurements during heat stress: technical and analytical considerations. *Am J Physiol Regul Integr Comp Physiol*. 2020;318(1):R57-R69. doi:10.1152/ajpregu.00177.2019
16. Förstermann U, Sessa WC. Nitric oxide synthases: Regulation and function. *Eur Heart J*. 2012;33(7):829-837. doi:10.1093/eurheartj/ehr304
17. Bogdan C. Nitric oxide and the immune response NO production in the immune system. *Nat Immunol*. 2001;(10):907-916. doi:10.1038/ni1001-907
18. Bruckdorfer R. The basics about nitric oxide. *Mol Aspects Med*. 2005;26(1-2):3-31. doi:10.1016/j.mam.2004.09.002
19. Andrei SR, Ghosh M, Sinharoy P, Damron DS. Stimulation of TRPA1 attenuates ischemia-induced cardiomyocyte cell death through an eNOS-mediated

mechanism. *Channels*. 2019;13(1):192-206. doi:10.1080/19336950.2019.1623591
20. Holowatz LA, Houghton BL, Wong BJ, et al. Nitric oxide and attenuated reflex cutaneous vasodilation in aged skin. *Am J Physiol Heart Circ Physiol*. 2003;284(5):H1662-H1667. doi:10.1152/ajpheart.00871.2002
21. Bartley EJ, Fillingim RB. Sex differences in pain: A brief review of clinical and experimental findings. *Br J Anaesth*. 2013;111(1):52-58. doi:10.1093/bja/aet127
22. Heeman W, Steenbergen W, van Dam GM, Boerma EC. Clinical applications of laser speckle contrast imaging: a review. *J Biomed Opt*. 2019;24(08):1. doi:10.1117/1.jbo.24.8.080901
23. Luetkemeier MJ, Allen DR, Huang M, et al. Skin tattooing impairs sweating during passive whole body heating. *J Appl Physiol*. 2020;129(5):1033-1038. doi:10.1152/japplphysiol.00427.2019
24. Aubdool AA, Kodji X, Abdul-Kader N, et al. TRPA1 activation leads to neurogenic vasodilatation: involvement of reactive oxygen nitrogen species in addition to CGRP and NO. *Br J Pharmacol*. 2016;173(15):2419-2433. doi:10.1111/bph.13519
25. McGarr GW, King KE, Cassan CJM, Janetos KMT, Fujii N, Kenny GP. Involvement of nitric oxide synthase and reactive oxygen species in TRPA1-mediated cutaneous vasodilation in young and older adults. *Microvasc Res*. 2023;145:104443. doi:10.1016/j.mvr.2022.104443
26. Kellogg DL, Zhao JL, Wu Y. Roles of nitric oxide synthase isoforms in cutaneous vasodilation induced by local warming of the skin and whole body heat stress in humans. *J Appl Physiol*. 2009;107(5):1438-1444. doi:10.1152/japplphysiol.00690.2009
27. Pozsgai G, Hajna Z, Bagoly T, et al. The role of transient receptor potential ankyrin 1 (TRPA1) receptor activation in hydrogen-sulphide-induced CGRP-release and vasodilation. *Eur J Pharmacol*. 2012;689(1-3):56-64. doi:10.1016/j.ejphar.2012.05.053

CHAPTER 3

Proof of pharmacology, safety, and pharmacokinetics of the novel TRPA1 antagonist BI 1839100: a randomised, placebo-controlled, parallel group, first-in-human study in healthy male participants

Published in: Clin Transl Sci. 2025;18(8):e70290. DOI:10.1111/cts.70290

Marella C.E. van Ruissen[1,2], Sebastiaan J.W. van Kraaij[1,2], Jana Wolfova[3], Franziska E. Hermann[4], Yanick Botilde[5], Lutz Wollin[4], Naomi B. Klarenbeek[1,2]

1 Centre for Human Drug Research, Leiden, the Netherlands
2 Leiden University Medical Centre, Leiden, the Netherlands
3 Boehringer Ingelheim International GMBH, Ingelheim am Rhein, Germany
4 Boehringer Ingelheim Pharma GMBH & CO. KG, Biberach an der Riss, Germany
5 Venn Life Sciences ED BV, Breda, the Netherlands

ABSTRACT

BI 1839100 is a selective antagonist of transient receptor potential cation channel A1 (TRPA1). Topically applied TRPA1-agonistic allyl isothiocyanate (AITC), which induces non-invasively measurable increased dermal blood flow (DBF), is known as a skin challenge model to assess TRPA1-target engagement and pharmacodynamic (PD) activity of TRPA1 inhibitors. This study aims to support the pharmacological rationale of BI 1839100 based on preclinical evidence and to test its safety, pharmacokinetic (PK) profile, and PD effects using an AITC skin challenge in a phase I first-in-human clinical study. In vitro and in vivo experiments were conducted in human TRPA1-overexpressing human embryonal kidney (HEK)293 cells and mice, respectively. Exposure to BI 1839100 and AITC demonstrated a BI 1839100 exposure-related reduction in AITC-induced CA^{2+} increase in HEK293 cells and skin oedema in mice. Healthy male participants, aged 18–45 years, were randomised within ten cohorts in the single-ascending dose part (n = 80) and two cohorts in the PD part (n = 32). All received single doses of BI 1839100/placebo followed by safety and PK measurements. In the PD part, participants underwent an AITC skin challenge twice; at baseline and at time to peak drug concentration after BI 1839100/placebo administration. No significant imbalance in occurrence of adverse events was detected between single doses of BI 1839100 up to 300 MG and placebo, and PK profiles were dose-proportional in the 40–300 MG range. BI 1839100 demonstrated a dose-dependent inhibitory effect on DBF after the AITC skin challenge, indicating TRPA1-targeted pharmacological activity and supporting further clinical development of BI 1839100 for a broad range of TRPA1 antagonistic applications.

INTRODUCTION

The mammalian transient receptor potential channel superfamily, including 28 members, is present in the majority of tissues in the human body and serves a wide variety of physiologic functions ranging from olfaction to angiogenesis.[1] The transient receptor potential cation channel A1 (TRPA1) is predominantly located on sensory neurons and fibroblasts and thereby plays an important role in pain perception, vasodilation, and immune cell recruitment in response to various endogenous and exogenous irritants.[2-8] The involvement of TRPA1 in sensory, vascular, and immunologic processes has inevitably led to its association with the pathogenesis of a wide range of diseases.[6-8] Examples include associations with pain disorders and with the pathogenesis of dermal pruritic disorders, including atopic dermatitis, and lung diseases such as allergic rhinitis, asthma and chronic obstructive pulmonary disease.[1,9,10] Given the role of TRPA1 in the pathogenesis of many diseases, its pharmacological targeting has gained attention in recent years. As such, numerous drug candidates have emerged in the early phases of drug development, aiming to modulate TRPA1 activity to potentially provide relief for the associated diseases.[9-12]

Simultaneously, with growing interest in TRPA1-targeting drugs, a pharmacological model aimed at early-phase testing of TRPA1-target engagement and pharmacodynamic (PD) activity was developed. This 'AITC skin challenge' model uses topical dermal application of allyl isothiocyanate (AITC) as exogenous irritant to selectively activate TRPA1. TRPA1 activation induces a vasodilatory response, which can be quantified as the intensity and size of enhanced dermal blood flow (DBF) by laser speckle contrast imaging (LSCI).[13] By performing the AITC skin challenge both before and after exposure to TRPA1-targeting compounds, the effects of the compound on the vasodilatory response to AITC can be assessed. In previous phase I clinical studies, this model has proven to be efficacious in demonstrating proof of pharmacologic principles of TRPA1 antagonists.[14,15]

BI 1839100, a small molecule inhibitor that selectively antagonises TRPA1, is a new drug candidate aiming to modify disease through TRPA1. Preclinical studies indicated that BI 1839100 displays low

protein binding, formation of relevant metabolites by hepatic metabolism, and a toxicologically safe profile for further exploration in humans. In this paper, we present preclinical evidence supporting the pharmacological rationale of BI 1839100 and a phase I, first-in-human study aimed at evaluating the safety, tolerability, and pharmacokinetic (PK) profile of BI 1839100 in healthy male participants. Furthermore, the AITC skin challenge was used to explore proof of pharmacological principle by assessing PD effects of BI 1839100.

MATERIALS AND METHODS

Preclinical studies

The preclinical explorations were conducted at Boehringer Ingelheim Pharma GMBH & CO. KG, Biberach an der Riss, Germany, where BI 1839100 was synthesised.

EFFECT OF BI 1839100 ON AITC-INDUCED CA^{2+}-INCREASE IN HUMAN TRPA1-OVEREXPRESSING HEK293 CELLS

To assess the efficacy of BI 1839100 to inhibit AITC-induced CA^{2+} increase, human TRPA1-overexpressing human embryonal kidney (HEK)293 cells were pre-incubated with increasing concentrations of BI 1839100 (0.03–10000 NM) and subsequently stimulated with 100 µM AITC. Human TRPA1-overexpressing HEK293 cells were plated in a 384 poly-D-lysin black/clear plate (Biocoat #4663, Corning, Kaiserslautern, Germany) using an incubator. The FLIPR® calcium 6-QF assay kit (#R8190, Molecular Devices, Sunnyvale, CA, USA) was used to measure calcium fluorescence. For each plate, dye loading buffer (total of 10 mL) was prepared by dissolving one vial of Component A with saline ($CACL_2$/$MGCL_2$, 20 mM HEPES, 0.1% BSA, pH 7.4). Cell plates were removed from the incubator and 20 µL of dissolved Component A was added per well. Subsequently, plates were incubated for 2 hours at 37°C, 5% CO_2, and then cooled to room temperature for 15 minutes prior to read-out. The plates containing HEK293 cells, AITC (100 µM) (#377430, Sigma-Aldrich, St. Louis, MO, USA), and BI 1839100 (0.00001–10 µM) were placed in the FLIPR Tetra® System (Molecular Devices, Sunnyvale, CA, USA). The compound was incubated for 15 minutes before AITC was added. Throughout the following 10 minutes, fluorescence measurement was performed at 515–575 NM emission and 470–495 NM excitation. Raw data were analysed using ScreenWorks software (Molecular Devices). After baseline subtraction, the area under the curve (AUC) of the relative light units was determined.

EFFECT OF BI 1839100 ON AITC-INDUCED EAR OEDEMA IN MICE

To further address the efficacy of BI 1839100 as a TRPA1 antagonist in vivo, a mouse model of AITC-induced skin oedema was assessed. All animal experiments were conducted in accordance with German national guidelines and legal regulations and approved by the Medical Review and Ethics Committee Regierungspräsidium (Tübingen, Germany) (permit numbers: 15-001-01, 15-001-03 and 15-016-02).

Eight 10-week-old, test-naive, female Balb/c mice weighing 18–23 G (Charles River Laboratories International INC., Sulzfeld, Germany) were housed in isolated ventilated cages of constant temperature (22°C ± 2°C) and humidity (60% ± 15%) under a 12-hour light-dark cycle in groups of up to six. They were allowed free access to water and standard food.

BI 1839100 was dissolved in 0.5% hydroxyethyl cellulose (Merck Schuchardt OHG, Hohenbrunn, Germany) containing 0.01% Tween20 (Acros Organics, NJ, USA) and applied by oral gavage at specified time points prior to the AITC skin challenge at doses of 0.003, 0.01, 0.03, 0.1, 0.3, 1, 3, and 10 MG/KG. Five minutes prior to the AITC skin challenge, animals were briefly anaesthetised with isoflurane (3-4% v/v) (Abbott GMBH, Wiesbaden, Germany) and 0.1 mL of 2% Evans blue (#E2129, Sigma-Aldrich, St. Louis, MO, USA) diluted in 0.9% saline was injected into the tail vein. Five µL of 5% AITC (#377430, Sigma-Aldrich, St. Louis, MO, USA) dissolved in paraffin oil (Merck Schuchardt OHG, Hohenbrunn, Germany) was applied to the inner and outer surface of the right ear and simultaneously, 5 µL paraffin oil was applied to the inner and outer surface of the left ear as a negative control. Animals were constantly monitored during induction and maintenance of anaesthesia, and the level of narcotic adjusted to maintain optimal depth of anaesthesia.

Mice were euthanised 30 minutes after the AITC skin challenge by intraperitoneal pentobarbital injection (160 MG/KG Narcoren®)

(Merial GMBH, Halbergmoos, Germany). Ear tissue biopsies were taken from both ears using a tissue punch (⌀8 mm). The Evans blue was extracted by incubating the ear tissue in 0.5 mL of formamide (#F7503, Sigma-Aldrich, St. Louis, MO, USA) at 65°C overnight with gentle agitation (450 RPM). The following day the absorbance in the supernatant was measured at 620 NM using a spectrophotometer. Furthermore, blood samples from the retro-orbital plexus were collected into ethylenediamine tetra-acetic acid (EDTA) tubes under terminal anaesthesia. Samples were centrifuged at 1500 RPM for 5 minutes at 4°C, and the plasma aspirated and stored at -80°C prior to analysis of BI 1839100 concentrations.

Clinical study

The phase I clinical study was conducted from 30 May 2022 to 14 June 2023 at the Centre for Human Drug Research (Leiden, the Netherlands) after approval prior to any clinical study activity by the Medical Review and Ethics Committee of the BEBO foundation

(Assen, The Netherlands). Before any study-related procedures, all participants provided written informed consent. The study was conducted in accordance with the principles of the Helsinki Declaration of 1975 (as revised in 1983), the International Council on Harmonisation Good Clinical Practice (ICH-GCP), and the Dutch Act on Medical Research involving Human Participants (WMO). The study was registered at toetsingonline.nl (NL81007.056.22), clinicaltrials.gov (NCT05354453), and in EudraCT (2021-006294-27).

STUDY DESIGN AND TREATMENTS

This was a phase I, randomised, placebo-controlled study. The study participants were blinded to treatment allocation, but not to dose level. It consisted of two parts: a single-ascending dose (SAD) part and a PD AITC skin challenge part. The SAD part consisted of ten cohorts of eight participants who were randomised to BI 1839100 or placebo (6:2). Sentinel dosing was performed in every cohort by dosing the first two participants with BI 1839100 and placebo (1:1) at least 23 hours before the remainder of the cohort.

In the AITC skin challenge part of the study, participants were divided into two dosing cohorts of 16 participants and randomised to BI 1839100 or placebo (8:8). All participants in this part of the study underwent the AITC skin challenge. They received 30-second topical applications of 25 µL 15% Good Manufacturing Practice (GMP)-manufactured AITC dissolved in mineral oil (Laboratorium Ofichem BV, Ter Apel, The Netherlands) within an 11 mm O-ring on two application areas on the same forearm on two occasions: once at baseline and once around the median time to peak drug concentration (T_{max}), derived from the PK results from the corresponding dose groups in the SAD part, following BI 1839100 administration (Figure 1).

During both parts, doses were administered in tablet form after an overnight fast of at least 10 hours. In the first cohort of the SAD part, BI 1839100 was administered orally suspended in 25 mL Macrogol 400.

STUDY PARTICIPANTS

Healthy male participants aged 18–45 years with a body mass index (BMI) of 18.5–31.9 KG/M^2 were eligible for inclusion in this trial. Health status was verified by performing medical screening, including medical history, physical examination, vital signs, 12-lead electrocardiogram (ECG), alcohol breath analysis, and clinical laboratory tests (serum chemistry, haematology, coagulation, infectious serology, urine drug screen, and urinalysis). Participants were excluded if they had undergone surgery that could interfere with the PK of BI 1839100, or if any relevant concomitant disease or disorder was present. In the AITC skin challenge part, participants with food allergies (specifically to mustard), dermal abnormalities on the forearms preventing them from undergoing the AITC skin challenge, and participants with a history of post-inflammatory hyperpigmentation were excluded. Additionally, participants who exhibited an increase in AITC-induced DBF of < 100% based on interim analysis during baseline measurement were excluded from the AITC skin challenge part, in accordance with previous research.[15] Detailed information on in- and exclusion criteria is available in Supplementary Table S1.

Participants were not enrolled in the study if they had a history of drug abuse. Participants refrained from the use of medications for 30 days prior to, and COVID-19 vaccinations from 7 days prior to BI 1839100 administration until the end of the study. Furthermore, they were not allowed to consume alcohol and products containing

grapefruit, Seville orange, and St. John's wort from 7 days prior to BI 1839100 administration until at least 3 days thereafter. Caffeine-containing dietary products were to be avoided from 4 hours prior to BI 1839100 administration until 4 hours thereafter.

DOSE LEVEL JUSTIFICATION

The 0.5 MG starting dose was based on the predicted human therapeutic dose, including a safety factor, derived from PK simulations using the data from the AITC-induced TRPA1-mediated skin oedema model in mice. Additionally, this dose was ~600–1600-fold lower than the safe estimated starting doses based on the no-observed-adverse-effect-level approaches in the most sensitive species recommended by the U.S. Food and Drug Administration and International Council for Harmonisation guidelines.[16,17]

Subsequent dose levels were confirmed in dose escalation meetings based on a documented review of all safety measurements, all available PK data, including PK data from the previous dose level, and estimated PK extrapolated from previous cohorts. Decreasing escalation factors from 4.0 to 1.5 were used. Based on preliminary data indicating higher clearance and shorter $t_{1/2}$ than predicted based on interspecies scaling, three additional dose levels were added during trial conduct, leading to a total of ten cohorts, to expand options for further development. The dose of 40 MG in the AITC part was selected based on integrated data from preclinical PK/PD models and emerging PK data extrapolations from the SAD part, the dose of 120 MG was also selected based on PD data from the 40 MG cohort. The safety and tolerability of the AITC part dose levels were first established in the SAD part. The administered dose levels are described in Supplementary Figure S1.

SAFETY ASSESSMENTS

Safety and tolerability of BI 1839100 were monitored in-house during both parts of the study by collecting adverse events (AEs), performing physical examinations, and assessing vital signs, 12-lead ECGs, and laboratory parameters (i.e., full blood count, biochemistry, and urinalysis) at set intervals up to 72 hours and telemetry up to 8 hours after dosing. A follow-up visit occurred 5–10 days after dosing. Participants were monitored continuously throughout the study for AEs, coded according to MEDDRA version 26.0, and concomitant medication use.

PHARMACOKINETIC ASSESSMENTS

Plasma PK sampling was performed prior to BI 1839100 administration and at time points 10 minutes, 20 minutes, 45 minutes, 1 hour, 1 hour 20 minutes, 1 hour 40 minutes, 2 hours, 2 hours 20 minutes, 2 hours 40 minutes, 3 hours, 4 hours, 6 hours, 8 hours, 10 hours, 12 hours, 24 hours, 36 hours, 48 hours, 72 hours post-BI 1839100 administration in both parts. Plasma concentrations of BI 1839100 were measured using a validated liquid chromatography tandem mass spectrometry (LC-MS/MS) assay (lower limit of quantification [LLOQ] 1.00 NMOL/L). Urine PK sampling occurred until 48 hours after dosing, divided in intervals of 0–4 hours, 4–8 hours, 8–12 hours, 12–24 hours, and 24–48 hours. The urine BI 1839100 concentrations were determined by a validated LC-MS/MS assay (LLOQ 10.0 NMOL/L). Analyses were performed by Nuvisan GMBH (Neu-Ulm, Germany). Details on these assays can be found in Supplementary Table S2.

PHARMACODYNAMIC ASSESSMENTS

During the AITC skin challenge part of the study, PD activity of BI 1839100 was assessed by measuring the DBF, expressed in perfusion units (PU). The DBF was measured continuously for 5 minutes before and 15 minutes after AITC application in temperature-controlled rooms between 20°C and 24°C using LSCI (PeriCam PSI NR System, Perimed AB, Järfälla, Sweden) as previously described.13 LSCI recordings of the target areas, defined as the 11 mm O-ring and the size of the individual vascular responses to AITC on the ventral forearm, were captured with the use of dedicated software (PimSoft, Perimed AB, Järfälla, Sweden) (Figure 1).

STATISTICS: IN VITRO STUDY

Data for the in vitro assays are presented as mean values ± standard deviation for triplicate measurements. BI 1839100 concentrations were log transformed and plotted against response. A non-linear curve fit was applied using "log (inhibitor) vs response (4 parameter)"

using GraphPad Prism version 8.01 for Windows (GraphPad Software, La Jolla, CA, USA). Values for 90% maximal effect concentration (EC_{90}) and half maximal inhibitory concentration (IC_{50}) were calculated from the curve fit.

STATISTICS: IN VIVO STUDY

Data from the in vivo study are presented as individual values of n = 5 animals per group. The percentage inhibition of Evans blue presence in biopsies was calculated from the mean value in the positive group according to the formula:

$$\%inhibition = \left(100 - \left(\frac{mean\ BI1839100\ treated\ positive\ control - mean\ vehicle\ treated\ negative\ control}{mean\ vehicle\ treated\ positive\ control - mean\ vehicle\ treated\ negative\ control}\right)\right) * 100$$

STATISTICS: CLINICAL STUDY

All statistical analyses were conducted according to a statistical analysis plan written before database lock. All safety and statistical programming was conducted using SAS version 9.4 for Windows (SAS Institute INC., Cary, NC, USA). The non-compartmental analysis was performed using Phoenix WinNonlin software (Version 8.1, Certara USA INC., Princeton, NJ, USA).

The sample size for the SAD part was based on the common use of eight participants per cohort in this type of SAD study, which is generally considered sufficient for the exploratory evaluation of single-dose safety and PK. The sample size of the AITC skin challenge part was based on sample sizes in previous research in which an AITC skin challenge was used as pharmacological model.[15] All participants who were treated with at least one dose of BI 1839100 were included in the safety analysis, and of those participants who provided at least one PK endpoint and one PD endpoint were included in the PK analysis and PD analysis, respectively. Descriptive statistics were calculated for the endpoints in both the SAD and the AITC skin challenge part, which were evaluated separately. No statistical hypothesis testing was performed, and the confidence interval was considered as interval estimates for treatment effects.

Safety data

Treatment-emergent adverse events (TEAEs) were summarised, and percentages calculated by treatment, system organ class, preferred term, severity, and BI 1839100 relatedness as judged by the investigator. ECG, safety laboratory results, and vital signs were summarised similarly. The number and percentage of out-of-range values were calculated by treatment and time point.

Pharmacokinetic data

BI 1839100 PK parameters were calculated for all dose levels in plasma (area under the curve from 0 to infinite [$AUC_{0-\infty}$], peak drug concentration [C_{max}], T_{max}, and half-life [$T_{½}$]) and urine (cumulative amount of BI 1839100 excreted [AE] and cumulative fraction of BI 1839100 excreted [FE]). Dose proportionality of C_{max} and $AUC_{0-\infty}$ in plasma was explored in the SAD part of the study by graphical checks and by using a power model describing the functional relationship between the dose level and PK endpoint on a log scale.

Pharmacodynamic data

The basal DBF and maximum DBF after AITC application were described. The change from baseline (CFB) in the AITC-induced DBF was analysed using analysis of covariance (ANCOVA), including factors for treatment and baseline value as covariates. The respective values were log-transformed (natural logarithm) prior to fitting the model. The DBF inhibition was calculated according to the formula: (1-((gMean CFB active)/(gMean CFB placebo)))*100. A post hoc analysis based on clinical observations was performed to assess the maximum DBF and size of the vascular response to AITC, including its flare (defined as maximum size of vascular response*maximum DBF), before and after BI 1839100 administration.

RESULTS

Preclinical studies

BI 1839100 ATTENUATED AITC-INDUCED CA^{2+} INCREASE IN HUMAN TRPA1-OVEREXPRESSING HEK293 CELLS

BI 1839100 inhibited CA^{2+} influx in HEK293 cells in a concentration-dependent manner, with an IC_{50} value of 92 NM and IC_{90} of 563 NM. Maximal inhibition of AITC-induced CA^{2+} influx was achieved at 1 µM of BI 1839100 (Supplementary Figure S2A).

BI 1839100 INHIBITED AITC-INDUCED EAR OEDEMA IN MICE

BI 1839100 inhibited AITC-induced skin oedema in a dose-dependent manner when dosed 30 minutes prior to AITC skin challenge. The IC_{50} value was 4 nM and the IC_{90} value was 54 nM (Supplementary Figure S2B).

Clinical study

BASELINE CHARACTERISTICS AND PARTICIPANT DISPOSITION

In this study, a total of 112 male healthy participants (SAD part n = 80, AITC skin challenge part n = 32) aged 18–45 years with a BMI between 18.5 and 30.9 kg/m^2 were included. Detailed baseline characteristics are depicted in Supplementary Table S3. In both the SAD and the AITC skin challenge part, all participants completed the study as planned per protocol (Supplementary Figure S1). In the AITC skin challenge part, six planned participants were excluded per protocol from participation before BI 1839100 administration due to insufficient dermal blood flow response to AITC (<100% increase).

SAFETY AND TOLERABILITY

In both parts of the study, there were no deaths, serious adverse events (SAEs) or severe TEAEs that were considered related to BI 1839100 (Table 1). One SAE (somnolence leading to a car accident) was reported in the follow-up period by a participant receiving 40 mg BI 1839100. This SAE was considered unrelated to BI 1839100 and did not lead to study discontinuation. The incidence of mild-to-moderate TEAEs ranged between 16.7%–66.7%, independent of the assigned dose group and study part. The most commonly reported AEs in the SAD part were headache (11.3%), fatigue (13.8%), dizziness (5.0%), and somnolence (6.3%), and the most common AE in the AITC skin challenge part was headache (21.9%). Besides an isolated, asymptomatic mild alanine aminotransferase increase in one participant during the follow-up visit 6 days after dosing, which normalised during the retest 11 days after dosing, no clinically significant changes from baseline related to BI 1839100 or trends were observed in the vital signs, 12-lead ECGs, telemetry, physical examination, or the clinical laboratory results. A full overview of the frequency of all AEs per participant can be found in Supplementary Tables S4 and S5.

TABLE 1 Summary of treatment-emergent adverse events per dose group.

		SAD											AITC skin challenge		
Dose level (MG)	**Placebo**	**0.5**	**2**	**5**	**10**	**20**	**40**	**70**	**120**	**200**	**300**	**Placebo**	**40**	**120**
Number of participants	20	6	6	6	6	6	6	6	6	6	6	16	8	8
Participants with any TEAE, n (%)	11 (55.0)	3 (50.0)	1 (16.7)	2 (33.3)	3 (50.0)	2 (33.3)	3 (50.0)	1 (16.7)	3 (50.0)	4 (66.7)	3 (50.0)	5 (31.3)	3 (37.5)	4 (50.0)
Participants with any mild TEAE, n (%)	11 (55.0)	3 (50.0)	1 (16.7)	1 (16.7)	3 (50.0)	2 (33.3)	3 (50.0)	1 (16.7)	3 (50.0)	4 (66.7)	3 (50.0)	5 (31.3)	3 (37.5)	4 (50.0)
Participants with any moderate TEAE, n (%)	0 (0.0)	0 (0.0)	0 (0.0)	1 (16.7)	0 (0.0)	0 (0.0)	0 (0.0)	0 (0.0)	0 (0.0)	0 (0.0)	0 (0.0)	0 (0.0)	0 (0.0)	0 (0.0)
Participants with any severe TEAE, n (%)	0 (0.0)	0 (0.0)	0 (0.0)	0 (0.0)	0 (0.0)	0 (0.0)	0 (0.0)	0 (0.0)	0 (0.0)	0 (0.0)	0 (0.0)	0 (0.0)	0 (0.0)	0 (0.0)
Participants with any drug-related TEAE	11 (55.0)	3 (50.0)	1 (16.7)	2 (33.3)	3 (50.0)	1 (16.7)	2 (33.3)	1 (16.7)	2 (33.3)	4 (66.7)	2 (33.3)	2 (12.5)	3 (37.5)	3 (37.5)
Participants with any TEAE leading to study discontinuation, n (%)	0 (0.0)	0 (0.0)	0 (0.0)	0 (0.0)	0 (0.0)	0 (0.0)	0 (0.0)	0 (0.0)	0 (0.0)	0 (0.0)	0 (0.0)	0 (0.0)	0 (0.0)	0 (0.0)
Participants with any AESI, n (%)	0 (0.0)	0 (0.0)	0 (0.0)	0 (0.0)	0 (0.0)	0 (0.0)	0 (0.0)	0 (0.0)	0 (0.0)	0 (0.0)	0 (0.0)	0 (0.0)	0 (0.0)	0 (0.0)
Participants with any SAE, n (%)	0 (0.0)	0 (0.0)	0 (0.0)	0 (0.0)	0 (0.0)	0 (0.0)	0 (0.0)	0 (0.0)	0 (0.0)	0 (0.0)	0 (0.0)	0 (0.0)	0 (0.0)	0 (0.0)

Note: All adverse events occurring up to 48 H (2 days) after administration of study drug were assigned to treatment. Abbreviations: AESI, treatment-emergent adverse event of special interest; AITC, allyl isothiocyanate; FIH, first-in-human; H, hours; MG, milligram; SAD, single-ascending dose; SAE, serious treatment-emergent adverse event; TEAE, treatment-emergent adverse event.

TABLE 2 Summary statistics of pharmacokinetic parameters for BI 1839100 after single oral administration (gMean (gCV[%])).

	SAD										AITC skin challenge		
Dose level (MG)	**0.5**	**2**	**5**	**10**	**20**	**40**	**70**	**120**	**200**	**300**	**40**	**120**
Cmax (NMOL/L)	16.0 (19.1)	80.1 (19.8)	139 (22.8)	351 (40.4)	597 (19.0)	1030 (20.1)	1650 (24.2)	2850 (6.65)	4770 (20.0)	6220 (37.4)	1100 (14.9)	3020 (13.2)
Tmax[a] (h)	0.77 (0.33-1.00)	0.88 (0.33-1.67)	1.50 (0.75-2.00)	1.50 (0.75-2.33)	2.51 (1.67-3.00)	1.67 (0.33-2.67)	1.33 (0.75-4.00)	1.70 (0.75-2.67)	1.67 (0.75-4.00)	3.34 (0.75-4.02)	1.17 (0.75-3.00)	1.67 (1.00-4.00)
$AUC_{0-\infty}$ (NMOL·H/L)	63.0 (12.5)	316 (16.6)	636 (17.9)	1570 (29.2)	3290 (29.7)	5620 (15.7)	9060 (17.9)	17700 (17.2)	28700 (13.8)	42300 (31.2)	5380 (25.8)	17100 (14.1)
T½ (h)	2.78 (8.67)	2.65 (6.99)	3.03 (35.5)	3.68 (14.6)	3.96 (10.9)	3.64 (10.5)	3.66 (17.4)	4.10 (17.4)	4.21 (26.6)	4.45 (22.5)	3.94 (10.5)	4.12 (7.64)

Abbreviations: AITC, allyl isothiocyanate; $AUC_{0-\infty}$, area under the curve from 0 to infinite; Cmax, peak drug concentration; SAD, single-ascending dose; T½, half-life; Tmax, time to peak drug concentration. [a]Median (range).

Pharmacokinetic analyses

PLASMA

Following administration of single oral doses of 0.5–300 MG of BI 1839100 in the fasted state, BI 1839100 quickly reached its maximum plasma concentration. The peak concentration increased with the dose, with geometric mean C_{max} ranging from 16.0–6220 NMOL/L and a median T_{max} ranging from 0.77–3.34 H. The $AUC_{0-\infty}$ also increased with increasing BI 1839100 dose (Figure 2; Table 2). After reaching maximum plasma concentrations, BI 1839100 was rapidly eliminated, with a geometric mean terminal elimination $T_{½}$ of 2.8–4.5 H and $T_{½}$ tended to increase with the dose (Table 2). The increase in exposure was confirmed to be dose proportional over the whole dose range in the SAD part of the study for the $AUC_{0-\infty}$ ($AUC_{0-\infty}$: β 1.006, 90% CI [0.982–1.029]), while the C_{max} was slightly less than dose proportional (C_{max}: β 0.918, 90% CI [0.891–0.945]). However, when restricting the analysis to the 40–300 MG dose range, the increase in C_{max} was dose proportional as well (β 0.921, 90% CI [0.824–1.017]) (Supplementary Table S6).

Urine

The cumulative amount of BI 1839100 excreted in urine (AE) increased with increasing dose (Supplementary Figure S3A). However, the cumulative fraction excreted in urine (FE) decreased with dose. After 48 H, less than 20% of the dose of BI 1839100 was excreted unchanged in urine for the highest dose groups (120–300 MG), while for the lower dose groups (0.5–20 MG) this ranged between 30% and 40% (Supplementary Figure S3B).

PHARMACODYNAMIC ANALYSES – PROOF OF PHARMACOLOGY

To assess TRPA1 target engagement of BI 1839100, AITC skin challenges were performed prior to and after dosing of BI 1839100. |A typical curve of the vascular response to AITC before and after dosing is depicted in Figure 3.

Prior to dosing of BI 1839100, the basal DBF, maximum DBF after AITC application, and size of the dermal response were comparable among treatment groups, as was the basal DBF after dosing of BI 1839100 (Table 3). Post-AITC application, 40 MG and 120 MG of BI 1839100 reduced the AITC-induced increased DBF by 57% and 67%, respectively, compared to the placebo participants (Table 3). Furthermore, the size of the dermal vasodilatory response was reduced in the BI 1839100 groups as compared to the response sizes during the baseline AITC skin challenge (Placebo: −0.4 CM^2, 40 MG: −13.6 CM^2, 120 MG: −23.8 CM^2) (Table 3; Figure 4A). An inhibiting effect of BI 1839100 on TRPA1-mediated AITC-induced vasodilation was also observed for the maximum DBF and the flare after AITC application (Figure 4B,C).

TABLE 3 **Geometric mean (range) of pharmacodynamic measures during AITC skin challenge per dose group.**

	AITC skin challenge		
Dose level (MG)	**Placebo**	**40**	**120**
PRE-DOSE			
AUC basal DBF[a] (PU*300S)	7602.2	7872.4	7721.3
AUC maximum DBF[b] (PU*30S)	2503.9	2677.2	2712.9
AITC-induced %CFB[c] (range)	225.4 (107-331)	232.0 (96-482)	247.7 (129-321)
Response size (CM^2)	17.7	20.2	27.9
POST-DOSE			
AUC basal DBF (PU*300S)	7975.3	7682.2	7495.4
AUC maximum DBF (PU*30S)	2694.3	1636.3	1388.0
AITC-induced %CFB (range)	232.0 (92-500)	99.9 (36-281)	75.4 (29-189)
%Inhibition of DBF by BI 1839100	N/A	56.9	67.5
Response size (CM^2)	17.3	6.6	4.1

Abbreviations: AITC, allyl isothiocyanate; AUC, area under the curve; CFB, change from baseline; CM^2, square centimetre; DBF, dermal blood flow; MG, milligram; N/A, not applicable; PU, perfusion unit; S, seconds. [a]Basal DBF = AUC over 300 S. [b]Maximum DBF = AUC over 30 S. [c]Minal analyses can differ from the interim analysis on Day-1, potentially leading to a %-CFB < 100%.

DISCUSSION

The described preclinical explorations demonstrated exposure-related inhibitory activity by the TRPA1 antagonist BI 1839100 on AITC-induced CA^{2+} increase in TRPA1-overexpressing HEK293 cells and on AITC-induced skin oedema in mice, providing a rationale for clinical assessment.

The main safety and tolerability findings of the clinical study were mild TEAEs of headache and fatigue, without a clear dose dependency. No BI 1839100-related deaths or SAEs were observed. No adverse events of special interest (AESIs), defined as potential severe drug-induced liver injury in this study, were seen. No significant imbalance in adverse events between treatment groups and no indication of increased risk by administration of BI 1839100 up to 300 MG was detected. This overall favourable safety profile is in line with results reported in other early clinical research with TRPA1 antagonists, such as GDC-0334, which include only mild-to-moderate TEAEs without SAEs or AESIs.[14]

PK data showed a dose-proportional increase in exposure parameters. A reduction in fractional excretion of BI 1839100 in urine (FE), accompanied by an increasing $t_{½}$, was observed in the higher dose groups, suggesting saturation of renal excretion. Compared to human PK predictions based on preclinical data, the observed clearance was higher and half-life shorter, resulting in an estimated human exposure in the range of 10-fold lower than originally anticipated. However, the parameters remained in the acceptable range for potential future clinical application, for instance in a multi-daily dosing scheme.

TRPA1-target engagement of BI 1839100 was demonstrated by its dose-dependent inhibitory effect on the DBF increases during the AITC skin challenge. Specifically, there was inhibition of both the size and intensity of the AITC-induced dermal vasodilatory response. However, due to the low number of participants, no significant association between BI 1839100 concentration and PD could be detected in PK/PD analysis. Demonstrating proof of pharmacology in early clinical studies is beneficial for guiding study design, dose selection, and disease target in the later stages of the clinical development process.[18,19] Balestrini et al., successfully performed a study with an AITC skin challenge test, showing a dose-dependent inhibition of DBF with the TRPA1 antagonist GDC-0334, eventually reaching full inhibition.[15] Bamps et al., used cinnamaldehyde instead of AITC to demonstrate TRPA1-mediated DBF inhibition of the TRPA1-antagonist LY3526318, but did not reach full inhibition.[20] The present study confirms the value of the AITC skin challenge test in showing pharmacological activity of TRPA1 antagonists in humans.

The ability of BI 1839100 to inhibit TRPA1 agonism by AITC was also tested in an in vitro study using AITC stimulation of HEK293 cells, which were overexpressing human TRPA1. In this study, BI 1839100 inhibited intracellular calcium influx with IC_{50} and IC_{90} values of 92 NM and 563 NM, respectively. Based on this data, full inhibition of the AITC-induced vasodilatory response in humans by BI 1839100 in our trial was predicted. However, the maximal inhibition achieved in the presented study was 67% for the 120 MG BI 1839100 dose group. The incomplete translatability highlights the relevance of performing human in vivo challenges to aid in mapping PD effects of novel therapeutics and their dose selection in later stages of the drug development process.

There are several potential explanations for the observed translational discrepancy. First of all, due to the limited number of doses tested, we cannot exclude the possibility that higher inhibition can be achieved at higher doses of BI 1839100. Furthermore, the AITC skin challenge assumes direct vasodilation mediated by TRPA1 agonism. However, AITC can display off-target activity and secondary pathway activation leading to vasodilation. For example, it is known that AITC initiates transient receptor potential cation channel subfamily V member 1 (TRPV1) signalling and subsequent induction of mild vasodilation.[13] It was observed that in TRPA1 knock out rats, AITC induced an increase in DBF, albeit less than in TRPA1-wildtype rats.[13] Furthermore, it can be hypothesised that TRPA1 agonism induces secondary activation of nuclear factor kappa-light-chain-enhancer of activated B-cells (NF-KB) signalling[21] and inhibits voltage-gated CA^{2+} in vascular smooth muscle cells,[22] both leading to vasodilation. It is possible that these pharmacodynamics factors depend on the administered AITC dose, but in this study only one standardised AITC dose was administered, precluding the possibility of assessing these effects. The PK-related factors might consist of individual participant T_{max} variability, as compared to the T_{max} derived from the data from the SAD part of the study, or lower exposure to BI 1839100 in the skin compared to the systemic circulation. However, extensive BI 1839100 exposure around T_{max} and substantial inhibitory effects on DBF were observed, suggesting that purely PK-related reasons do not entirely explain the observed partial inhibition.

Limitations

The most important limitation of this study is the conduct of only two dose levels in the AITC skin challenge part of the study. Based on the acquired data, it is unknown whether more extensive inhibition of AITC-induced vasodilation can be achieved by BI 1839100. This prevents us from estimating the exact dose–response relationship. Furthermore, the study was performed in a single-blind fashion, which may have affected the interpretation of reported AEs. To prevent assessment bias, the post hoc analysis of the imaging data was performed by a blinded assessor.

CONCLUSION

In conclusion, BI 1839100 is a potent TRPA1 antagonist with demonstrated in vitro and in vivo efficacy on AITC-induced effects. In the first-in-human study, single doses of BI 1839100 did not increase the risk of adverse events in the healthy male participants and demonstrated limited variability and dose-proportional PK profiles. Furthermore, the displayed dose-dependent TRPA1-target engagement using the AITC skin challenge potentiates BI 1839100 for a broad range of TRPA1 antagonistic applications, including modulating vasodilation resulting from TRPA1 agonism. These findings provide a basis for advancing BI 1839100 into further stages of clinical development, marking it as a promising candidate for therapeutic applications targeting TRPA1.

SUPPORTING INFORMATION

Supplementary figures: https://pmc.ncbi.nlm.nih.gov/articles/instance/12292558/bin/CTS-18-e70290-s001.docx

Supplementary tables: https://pmc.ncbi.nlm.nih.gov/articles/instance/12292558/bin/CTS-18-e70290-s002.docx

FIGURE 1 **Set-up of the AITC skin challenge.** (A) AITC skin challenge prior to dosing of BI 1839100. (B) AITC skin challenge at median T_{max} after dosing of BI 1839100. The depicted PK-curve is for illustrative purposes only and does not represent true PK exposures measured in this study. In both (A) and (B), DBF was measured using LSCI for a duration of 5 MIN. at baseline and 15 MIN. after AITC application. 25 µL of 15% AITC was administered to the volar forearm within an 11 mm O-ring.

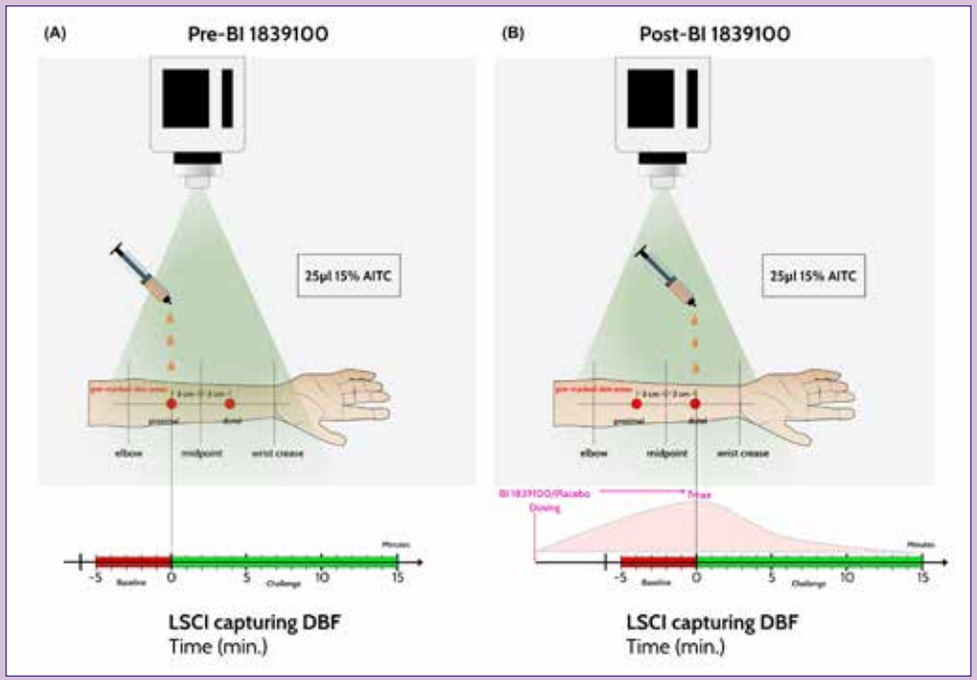

Abbreviations: AITC, allyl isothiocyanate; DBF, dermal blood flow; LSCI, laser speckle contrast imaging; MIN., minutes; PK, pharmacokinetic.

FIGURE 2 **BI 1839100 geometric mean plasma concentration-time profiles after single oral administration (semi-log scale).** (A) SAD part. (B) AITC skin challenge part.

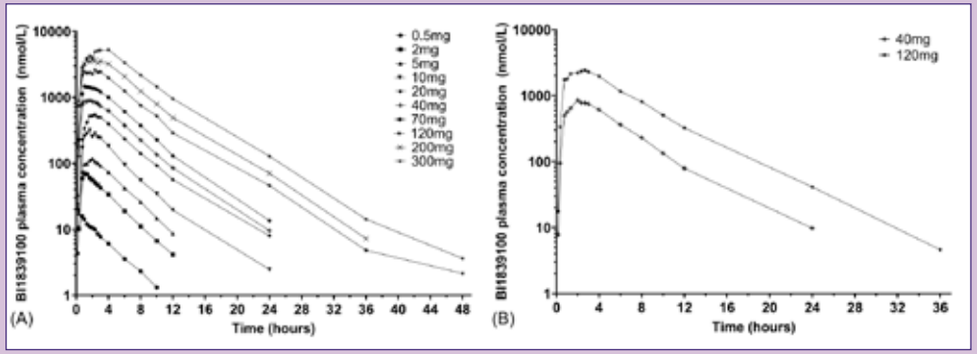

Abbreviations: AITC, allyl isothiocyanate; SAD, single-ascending dose.

FIGURE 3 **Representative displays of AITC-induced DBF on the forearm of study participants.** (A) Visual representation of DBF within the O-ring in PU after AITC administration before dosing of BI 1839100; 1 = O-ring. (B) DBF expressed in PU at baseline and in response to AITC administration (t = 05:00 MIN.) before dosing of BI 1839100, as measured by LSCI. (C) Visual representation of DBF within the O-ring in PU after AITC administration at median T_{max} after dosing of BI 1839100 (120 MG); 1 = O-ring. (D) DBF expressed in PU at baseline and in response to AITC administration (t = 05:00 MIN.) at median T_{max} after dosing of BI 1839100, as measured by LSCI.

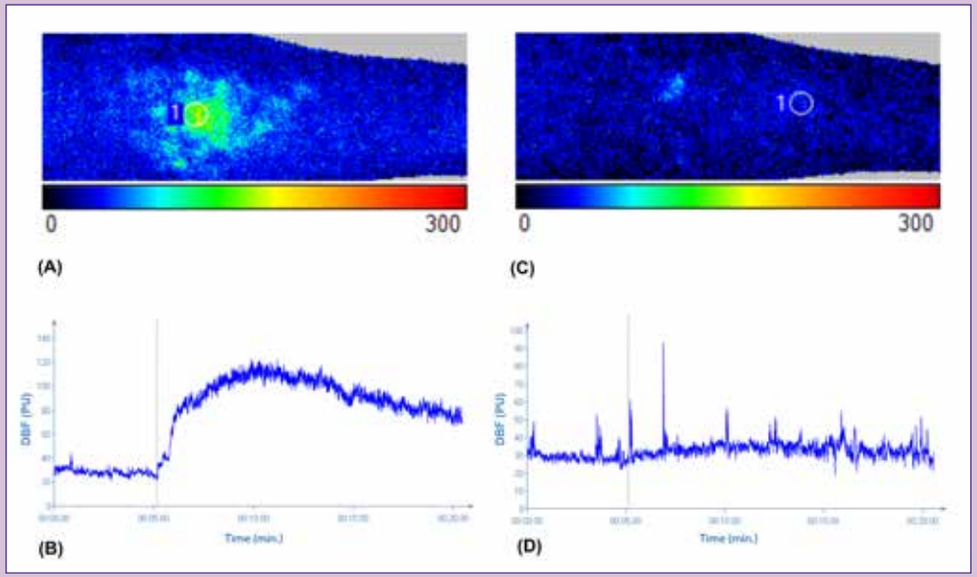

Abbreviations: AITC, allyl isothiocyanate; DBF, dermal blood flow; LSCI, laser speckle contrast imaging; MIN., minutes; T_{max}, time to peak drug concentration; PU, perfusion units.

FIGURE 4 **Pharmacodynamic measures of AITC skin challenge per treatment group.** (A) CFB in mean (SD) DBF response size (CM^2) as measured by LSCI after AITC application pre-BI 1839100 and post-BI 1839100 per treatment group. (B) CFB in mean (SD) of the maximum DBF as measured by LSCI after AITC application pre-BI 1839100 and post-BI 1839100 per treatment group. (C) CFB in mean (SD) flare (surface*maximum DBF) as measured by LSCI after AITC application pre-BI 1839100 and post-BI 1839100 per treatment group.

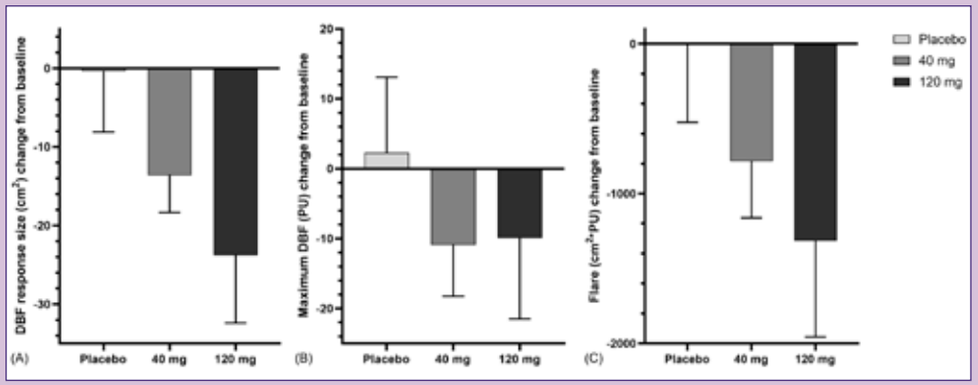

Abbreviations: AITC, allyl isothiocyanate; CFB, change from baseline; CM^2, square centimetre; DBF, dermal blood flow; LSCI, laser speckle contrast imaging; PU, perfusion units; SD, standard deviation.

REFERENCES

1. Zhang M, Ma Y, Ye X, Zhang N, Pan L, Wang B. TRP (transient receptor potential) ion channel family: structures, biological functions and therapeutic interventions for diseases. *Signal Transduc Target Ther*. 2023;8(1):261. doi: 10.1038/s41392-023-01464-x
2. Bautista DM, Jordt SE, Nikai T, et al. TRPA1 mediates the inflammatory actions of environmental irritants and proalgesic agents. *Cell*. 2006;124(6):1269-1282. doi: 10.1016/j.cell.2006.02.023
3. Bandell M, Story GM, Hwang SW, et al. Noxious cold ion channel TRPA1 is activated by pungent compounds and bradykinin. *Neuron*. 2004;41(6):849-857. doi: 10.1016/S0896-6273(04)00150-3
4. Shimizu S, Takahashi N, Mori Y. TRPs as chemosensors (ROS, RNS, RCS, gasotransmitters). *Handb Exp Pharmacol*. 2014;223:767-794. doi:10.1007/978-3-319-05161-1_3
5. Wei Y, Cai J, Zhu R, Xu K, Li H, Li J. Function and therapeutic potential of transient receptor potential ankyrin 1 in fibrosis. *Front Pharmacol*. 2022;13:1014041. doi:10.3389/fphar.2022.1014041
6. Aubdool AA, Graepel R, Kodji X, et al. TRPA1 is essential for the vascular response to environmental cold exposure. *Nat Commun*. 2014;5(1): 5732. doi:10.1038/ncomms6732
7. Aubdool AA, Kodji X, Abdul-Kader N, et al. TRPA1 activation leads to neurogenic vasodilatation: involvement of reactive oxygen nitrogen species in addition to CGRP and NO. *Br J Pharmacol*. 2016;173(15):2419-2433. doi:10.1111/bph.13519
8. Viana F. TRPA1 channels: molecular sentinels of cellular stress and tissue damage. *J Physiol*. 2016;594(15):4151-4169. doi:10.1113/JP270935
9. Hu Z, Zhang Y, Yu W, et al. Transient receptor potential ankyrin 1 (TRPA1) modulators: Recent update and future perspective. *Eur J Med Chem*. 2023;257:115392. doi:10.1016/j.ejmech.2023.115392
10. Maglie R, Souza Monteiro de Araujo D, Antiga E, Geppetti P, Nassini R, De Logu F. The Role of TRPA1 in Skin Physiology and Pathology. *Int J Mol Sci*. 2021;22(6):3065. doi:10.3390/ijms22063065
11. Eberhardt MJ, Filipovic MR, Leffler A, et al. Methylglyoxal activates nociceptors through transient receptor potential channel A1 (TRPA1): a possible mechanism of metabolic neuropathies. *J Biol Chem*. 2012;287(34):28291-28306. doi:10.1074/jbc.M111.328674
12. Koivisto A-P, Belvisi MG, Gaudet R, Szallasi A. Advances in TRP channel drug discovery: from target validation to clinical studies. *Nat Rev Drug Discov*. 2022;21(1):41-59. doi:10.1038/s41573-021-00268-4
13. Joseph V, Yang X, Gao SS, et al. Development of AITC-induced dermal blood flow as a translational in vivo biomarker of TRPA1 activity in human and rodent skin. *Br J Clin Pharmacol*. 2021;87(1):129-139. doi:10.1111/bcp.14370
14. Chan P, Ding HT, Liederer BM, et al. Translational and pharmacokinetic-pharmacodynamic application for the clinical development of GDC-0334, a novel TRPA1 inhibitor. *Clin Transl Sci*. 2021;14(5):1945-1954. doi:10.1111/cts.13049
15. Balestrini A, Joseph V, Dourado M, et al. A TRPA1 inhibitor suppresses neurogenic inflammation and airway contraction for asthma treatment. *J Exp Med*. 2021;218(4):e20201637. doi:10.1084/jem.20201637
16. US Food & Drug Administration. Estimating the Maximum Safe Starting Dose in Initial Clinical Trials for Therapeutics in Adult Healthy Volunteers. https://www.fda.gov/regulatory-information/search-fda-guidance-documents/estimating-maximum-safe-starting-dose-initial-clinical-trials-therapeutics-adult-healthy-volunteers. Accessed July 9, 2024.
17. European Medicines Agency. ICH M3 (R2) Non-clinical safety studies for the conduct of human clinical trials for pharmaceuticals - Scientific guideline. https://www.ema.europa.eu/en/ich-m3-r2-non-clinical-safety-studies-conduct-human-clinical-trials-pharmaceuticals-scientific-guideline. Accessed July 9, 2024.
18. Hijma HJ, Groeneveld GJ. Analgesic drug development: proof-of-mechanism and proof-of-concept in early phase clinical studies. *Med Drug Discov*. 2021;10:100083. doi:10.1016/j.medidd.2021.100083
19. Schmidt B. Proof of principle studies. *Epilepsy Res*. 2006;68(1):48-52. doi:10.1016/j.eplepsyres.2005.09.019

20. Bamps D, Blockeel AJ, Dreesen E, et al. TRPA1 Antagonist LY3526318 Inhibits the Cinnamaldehyde-Evoked Dermal Blood Flow Increase: Translational Proof of Pharmacology. *Clin Pharmacol Ther*. 2023;114(5):1093-1103. doi: 10.1002/cpt.3024
21. Yao K, Dou B, Zhang Y, et al. Inflammation-the role of TRPA1 channel. *Front Physiol*. 2023;14:1093925. doi:10.3389/fphys.2023.1093925
22. Alvarez-Collazo J, Alonso-Carbajo L, López-Medina AI, et al. Cinnamaldehyde inhibits L-type calcium channels in mouse ventricular cardiomyocytes and vascular smooth muscle cells. *Pflugers Arch*. 2014;466(11):2089-2099. doi:10.1007/s00424-014-1472-8

CHAPTER 4

Breaking barriers: characterisation of the intra-dermal lipopolysaccharide challenge as an in vivo model for controlled induction of vascular leakage in healthy volunteers

Published in: Clin Pharmacol Ther. Published online November 15, 2025. doi:10.1002/cpt.70126

Marella C.E. van Ruissen[1,2], Menno van Diemen[1,2], Liza Botros[1,2], Ingrid Tomljanovic[3], Hind Achbo[1], Dimitra Eleftheriou[1,4], Paul W. Schenk[2], Naomi B. Klarenbeek[1,2], Derek W. Gilroy[5], Manon A. A. Jansen[1,2], Matthijs Moerland[1,2]

1 Centre for Human Drug Research, Leiden, the Netherlands
2 Leiden University Medical Centre, Leiden, the Netherlands
3 Department of Urology, Erasmus University Medical Centre, Rotterdam, The Netherlands
4 Division of Systems Pharmacology and Pharmacy, Leiden Academic Centre for Drug Research, Leiden, The Netherlands
5 Department of Experimental & Translational Medicine, Division of Medicine, University College London, London, United Kingdom

ABSTRACT

Vascular leakage and its associated phenomena vasodilation and endothelial activation are pathophysiological features of various diseases. Multiple drug candidates targeting these phenomena are in development, necessitating translational models to demonstrate proof-of-pharmacology and proof-of-mechanism in early-phase clinical trials. This single-centre experimental study evaluated the intradermal lipopolysaccharide (ID LPS) challenge model as a tool to induce and characterise vascular leakage in healthy participants. Eight participants (male:female = 4:4) received ID LPS in the volar forearms, followed by serial pharmacodynamic assessments including imaging and suction blister induction up to 9 hours after injection. ID LPS administration resulted in significant increases in skin perfusion ($p < 0.0001$), erythema ($p = 0.0013$) and skin volume ($p = 0.0008$), indicating initial stages of inflammation and fluid extravasation. Blister fluid analysis revealed elevated extravascular concentrations of albumin ($p = 0.0011$), total protein ($p < 0.0001$), and neutrophils ($p = 0.0342$), supporting the presence of vascular leakage. Moreover, the expression of endothelial activation markers VCAM-1 ($p = 0.0015$), ICAM-1 ($p = 0.0004$), ITGB1 ($p = 0.01$) and E-selectin ($p = 0.0218$) increased significantly. Disruption of endothelial cell-cell integrity was supported by increased expression of VE-cadherin ($p = 0.0002$) in blister fluid. These findings support the applicability of the ID LPS model for induction of vascular leakage in humans. This model holds potential as a translational tool for evaluating the pharmacodynamic responses of vascular leakage-targeting drugs in early clinical development.

INTRODUCTION

The vascular endothelium is a dynamic, semi-permeable layer lining all blood vessels that regulates barrier function and vasomotor tone. Vascular leakage is a hallmark feature of numerous acute and chronic conditions, including prevalent infectious, inflammatory, and malignant diseases, such as sepsis and arthritis.[1] Within these conditions, endothelial barrier dysfunction and vascular integrity loss occur through a variety of mechanisms. Although vascular leakage significantly contributes to morbidity and disease progression, development of drugs specifically targeting vascular leakage within these diseases remains highly challenging.[2-4]

Encouragingly, multiple vascular leakage-targeting drug candidates with various mechanisms of action (MoA) are under investigation in clinical trials.[5] These drugs aim to reduce vascular leakage by stabilising the endothelial barrier function. This effect is mainly induced by enhancing endothelial cell-cell junctions via the angiopoietin-Tie2 pathway, but various other mechanisms are also being explored.[3] Examples of such drugs in the clinical phase include razuprotafib (AKB-9778), which activates Tie2 via VE-PTP inhibition, and nesvacumab (REGN910), which binds and inactivates the Tie2 receptor ligand Ang2.[6-8] Furthermore, registered drugs are being investigated for repurposing for treatment of vascular leakage. One such example is imatinib, which targets ABL-family kinases that mediate vascular permeability.[9]

Given the unmet medical need for vascular leakage-targeting drugs for a wide range of diseases,[3,4] development of methodologies allowing evaluation of proof-of-pharmacology and proof-of-mechanism for these drugs in early-phase clinical studies would be valuable. Collecting such pharmacological knowledge aids translation from preclinical to clinical settings, allows early dose optimisation, and may help in the identification of potential safety concerns and therapeutic options. This ultimately leads to optimisation of future clinical trial designs.[10,11]

Despite the availability of well-established animal models for vascular leakage,[12-17] experimental models applicable to humans focusing

on this purpose are yet to be developed. The intradermal lipopolysaccharide (ID LPS) challenge model could fill this gap. LPS, a Toll-like receptor 4 (TLR4) agonist, is an established clinical model used to induce acute and transient inflammation in the skin, and its cellular inflammatory profile has been extensively studied. The model allows direct assessment of immune responses via suction blister fluid and non-invasive imaging techniques. This method allows serial sampling of tissue responses over time under highly controlled conditions. The relatively low burden for study participants enhances its practical feasibility and applicability.[18]

Besides an acute inflammatory response, LPS is also known to drive a vascular response in animal models, including increased expression of endothelial adhesion molecules, the release of vasoactive mediators, and disruption of endothelial barrier integrity via TLR4 signalling.[19,20] Similarly, in the clinical setting intravenously administered LPS has activated biomarkers for endothelial and vascular activation, such as vascular cell adhesion molecule 1 (VCAM-1) as well as vascular endothelial growth factor (VEGF).[21,22] Currently limited data are available on potential vascular effects induced by ID LPS in humans, but it is known that locally increased perfusion and erythema occur as markers of vasodilation post-LPS injection, which suggests the involvement of endothelial barrier dysfunction at a microvascular level.[18] Given these data and the physiological interplay between inflammation and the vasculature, including neutrophil extravasation upon endothelial activation,[23] it can be envisioned that ID LPS elicits vascular leakage in humans.

The objective of this study was to characterise ID LPS as a human challenge model for vascular leakage, including key features such as endothelial activation and plasma extravasation, with the aim of establishing its suitability for application in early-phase clinical research. By integrating data on clinical hallmarks of vascular activation and permeability (skin perfusion, erythema, and skin volume) with protein and neutrophil contents of interstitial fluid from LPS-inflamed regions, we aim to characterise vascular leakage within this model and to establish a unique translational tool that can be used to test drug candidates that target features of vascular leakage in a wide range of diseases, bridging preclinical and clinical pharmacological research.

METHODS

This study was conducted from June 2024 to February 2025 at the Centre for Human Drug Research (Leiden, The Netherlands) in accordance with the principles of the Declaration of Helsinki (as revised in 1983) and the Dutch Medical Research Involving Human Subjects Act (WMO). The protocol was approved by the independent Medical Ethics Committee of the Stichting Beoordeling Ethiek Biomedisch Onderzoek (BEBO, Assen, The Netherlands) and was prospectively registered in the EU Clinical Trials Register (2024-512377-27-00). All participants provided written informed consent prior to the initiation of any study-related procedures.

Participants

Healthy men and women, aged 18-45 years, were eligible for inclusion in this study if no clinically significant abnormal findings were obtained during a standardised screening procedure consisting of medical history, physical examination, 12-lead ECG, alcohol breath analysis and clinical laboratory testing (i.e., serum chemistry, haematology, coagulation, urine drug screening, and urinalysis). Participants who previously participated in an LPS challenge study within the last year, and participants with a history of pathological scar formation, dermatologic conditions, or autoimmune diseases were excluded from participation. Furthermore, participants with a Fitzpatrick skin type >III were excluded given their increased risk of pathological scar formation after the invasive measurements conducted in this study. The use of vitamins was not permitted from 7 days (or 5 half-lives, whichever was longer) prior to dosing until study completion. For concomitant medication, topical treatments, and vaccinations, a window of 14 and 30 days, respectively, prior to dosing until the end of the study was imposed. Throughout the study, participant safety was monitored through recording adverse events (AEs), vital signs (i.e., heart rate and blood pressure), and laboratory testing (including complete blood count and C-reactive protein).

Study design and treatments

This single-centre experimental challenge study aimed to establish ID LPS administration as a model for vascular leakage and included eight healthy volunteers in an equal male-to-female ratio (1:1). Participants received three ID LPS injections of 5 NG each, administered to designated treatment areas on the volar forearms. An additional site on the volar forearms served as untreated control (Figure 1). The LPS dose was chosen based on previous observations that a dose of 5 NG induces an acute inflammatory response based on cytokine expression and neutrophil influx, with only mild systemic effects on leukocyte counts and tolerable, mild, transient topical adverse events.[18,24] The inflammatory response at 5 NG has been shown to be modifiable by anti-inflammatory drugs.[25] Therefore we argued that 5 NG LPS would induce sufficient inflammation to produce objectifiable vascular leakage within this model.

Non-invasive measures to assess features of vasodilation and vascular leakage

DERMAL IMAGING–VASODILATION AND FLUID EXTRAVASATION

Dermal imaging was conducted at regular intervals on a designated skin area on the forearms to characterise vasodilation by local assessments of skin perfusion and erythema and to characterise fluid extravasation by assessing skin volume (Figure 1). All procedures were performed in temperature (20–24°C)- and humidity (40-60%)-controlled rooms and prior to any blister formation. Skin perfusion was quantified using laser speckle contrast imaging (PeriCam PSI NR System, Perimed AB, Järfälla, Sweden) and dedicated image capturing software (PimSoft, Perimed AB, Järfälla, Sweden) at baseline and at 0.25, 0.5, 0.75, 1, 1.5, 2, 3, 4, 6, and 9 hours after LPS injection. Skin erythema and volume were measured using multispectral imaging (Antera 3D, Miravex, Ireland) at the same time points (Figure 1).

Invasive measures to assess features of vascular leakage

BLISTER FLUID–PROTEIN LEAKAGE

Suction blisters were induced at the designated areas on the forearms at baseline, 0.5, 4, and 9 hours post-LPS injection (Figure 1) following the method described by Buters et al.[18] to determine the presence of vascular leakage based on extravascular albumin and total protein concentrations in interstitial fluid over time. After blister induction, blister fluid was collected in a Sarstedt tube containing 50 µL 3% sodium citrate (Sigma-Aldrich, St. Louis, MO, USA) in phosphate buffered saline (Gibco, Thermo Fisher Scientific, Waltham, MA, USA) and kept on ice. After the tube was centrifuged, the supernatant was collected and then frozen at -80°C for protein analysis at the clinical laboratory of the Leiden University Medical Centre (Department of Clinical Chemistry and Laboratory Medicine, LUMC, Leiden, The Netherlands). All protein concentrations were measured using a Cobas® c502 automated analyser (Roche Diagnostics International AG, Rotkreuz, Switzerland) with the applicable assays obtained from Roche Diagnostics. Albumin concentration was determined using the immunoturbidimetric Tina-quant Albumin Gen. 2 (ALBT2) assay (catalogue number 04469658190) in CSF mode (measuring range 0.036 - 4.8 G/L) upon manual 4-fold dilution with 0.9% NACL (Versylene Fresenius, Fresenius Kabi AG, Bad Homburg, Germany). Total protein concentration was determined using the turbidimetric Total Protein Urine/CSF Gen. 3 (TPUC3) assay (catalogue number 03333825190, measuring range 0.04 - 2.0 G/L) upon manual 12-fold dilution with 0.9% NACL. Parallel blood samples were obtained in 3.5 mL SST tubes (BD, Franklin Lakes, NJ, USA) to assess corresponding serum protein levels using the colorimetric Albumin Gen. 2 (ALB2) assay (catalogue number 03183688122, measuring range 2.0 - 160 G/L) for albumin concentrations and colorimetric Total Protein Gen. 2 (TP2) assay (catalogue number 03183734190, measuring range 2.0 - 120 G/L) for total protein concentrations.

Invasive measures to assess endothelial activation

BLISTER FLUID - ENDOTHELIAL ACTIVATION MARKERS

The Olink Explore 384 Cardiometabolic Panel (Olink Proteomics AB, Uppsala, Sweden) was used to examine the relative changes in protein expression of a range of proteins related to endothelial activation and endothelial cell-cell integrity in the obtained blister fluids. This is a multiplex immunoassay based on proximity extension assay technology which reports normalised protein expression (NPX), an arbitrary unit on a $\log_2$ scale.[26]

BLISTER FLUID–NEUTROPHIL EXTRAVASATION

Neutrophil extravasation was measured in cell pellets from centrifuged blister fluid. The living cells were stained with the following fluorescent antibodies to classify them as neutrophils: CD45, Siglec8, CD66b (details in Supplementary Table S1). Subsequently, flow cytometry analysis was performed on a MACSQuant 16.3 analyzer (Miltenyi Biotec BV, Leiden, The Netherlands).

Statistical analysis

SAMPLE SIZE AND BASELINE CHARACTERISTICS

No formal statistical considerations were applied to calculate the sample size in this study. However, based on prior experience in early-phase clinical pharmacology trials using in vivo challenge models and given the application of these models in this setting, a sample size of eight participants is considered adequate. Therefore we adopted the same approach in this study. Baseline characteristics were summarised using descriptive statistics: means and standard deviations (SDs) for continuous variables, and frequencies and percentages for categorical variables (e.g., sex, skin type).

PHARMACODYNAMIC ASSESSMENTS

The pharmacodynamic endpoints (dermal imaging parameters, protein concentrations from blister fluid, and neutrophil counts from blister fluid) were summarised over time (n, mean, SD), and time profiles were graphically represented. The repeated pharmacodynamic measurements, defined as having more than one post-baseline measurement, were analysed using a mixed-effects model with treatment, time, and their interaction (treatment × time) as fixed effects, and participant as a random effect. Least squares means (LSM) were estimated for each time point and tested for statistical significance compared to baseline with a *p*-value of 0.05 as threshold. The contrast of interest calculated within the model was baseline versus peak after ID LPS injection. All statistical analyses were performed using SAS version 9.4 for Windows or newer (SAS Institute Inc., Cary, NC, USA).

Pharmacodynamic analyses of Olink protein expression in blister fluid (endothelial markers) were conducted using R statistical software version 4.4.2. Repeatedly measured endpoints for Olink protein expression were summarised using boxplots depicting NPX. The relative changes in expression over time were analysed using the Skillings-Mack test followed by the Eisinga, Heskes, Pelzer & Te Grotenhuis post-hoc test on data from participants with complete observations (n = 7), defined as not yielding any panel-specific outlier samples for the Olink Cardiometabolic panel. Unless otherwise specified, the statistical significance threshold across all analyses was set at 0.05 and a Benjamini–Hochberg correction was applied to account for multiple testing.

RESULTS

Baseline characteristics and participant safety

A total of eight healthy volunteers (males: n = 4, females: n = 4), aged 19-31 years, were enrolled in this study. All participants had Fitzpatrick scores I, II or III, and demonstrated normal vital signs and laboratory values, including haemoglobin levels and white blood cell counts. Detailed baseline characteristics are presented in Supplementary Table S2. No relevant AEs or clinically significant abnormalities in vital signs and laboratory testing were observed in any of the participants, in line with previous studies using ID LPS.[18,25]

Non-invasive measures to assess features of vasodilation and vascular leakage

DERMAL IMAGING – VASODILATION

Skin perfusion increased after ID LPS injection following a biphasic pattern, with an initial peak (56.5 ± 19.3 AU) at one hour and the highest observed peak (77.2 ± 19.8 AU) at four hours post-injection (Figure 2D). Erythema followed an ascending trend as well, albeit more variable than skin perfusion, reaching its peak (10.3 ± 2.0 AU) at nine hours after LPS (Figure 2E). The observations of the peaks in skin perfusion and erythema were statistically significant when compared to baseline for both parameters (Table 1). Exemplary clinical figures reflecting these measurements over time are depicted in Figures 2A and 2B.

DERMAL IMAGING – FLUID EXTRAVASATION

An increase in skin volume was seen immediately after administering the ID LPS solution. Subsequently, a statistically significant second peak in skin volume (17.7 ± 18.4 mm^3) was observed at four hours after injection, coinciding with the observed peak in skin perfusion (Table 1). The skin volume then returned towards baseline, while skin perfusion reached a plateau (Figure 2F). Corresponding clinical figures are presented in Figure 2C.

TABLE 1 Statistical analysis for the baseline vs. the peak of the non-invasive and invasive measurements of vasodilation, vascular leakage and endothelial activation.

	LSM Estimate change from baseline	95% CI (lower, upper)	*p*-value
NON-INVASIVE MEASUREMENTS – VASODILATION AND FLUID EXTRAVASATION			
Skin perfusion (AU)*	42.6	29.6, 55.6	< 0.0001
Erythema (AU)**	2.6	1.3, 3.9	0.0013
Skin volume (mm^3)*	15.3	7.4, 23.3	0.0008
INVASIVE MEASUREMENTS – PROTEINS (G/L)			
Albumin**	5.9	2.8, 9.0	0.0011
Total protein**	12.1	8.0, 16.3	<0.0001
INVASIVE MEASUREMENTS – NEUTROPHILS (NUMBER OF CELLS IN 100 µL BLISTER FLUID)			
Neutrophils (CD45+/CD66b+/ Siglec8- cells)**	942	82, 1801	0.0342

*AU = arbitrary units, CI = confidence interval, LSM = least squares means / *Baseline vs. peak at 4 hours after ID LPS injection / **Baseline vs. peak at 9 hours after ID LPS injection Invasive measures to assess features of vascular leakage*

BLISTER FLUID – PROTEIN LEAKAGE

Albumin was measured in blister fluid as a marker for local vascular leakage. A time-dependent statistically significant increase in mean albumin contents of blister fluid, from 11.3 G/L at baseline to a maximum of 17.3 G/L, was observed nine hours after dosing of LPS (Figure 3A, Table 1). Similar data and trends were observed for total protein concentrations in blister fluid (Figure 3A, Table 1). These increases were irrespective of albumin and total protein concentration in blood, as those concentrations did not vary over time (albumin least-squares mean change from baseline -0.3, 95% CI [-0.7, 0.1] G/L, $p = 0.0879$, total protein least-squares mean change from baseline -0.2, 95% CI [-1.1, 0.7] G/L, $p = 0.5919$) (Figure 3B).
A composite plot that comprehensively demonstrates the time-courses of the effects of ID LPS on vasodilation, fluid extravasation and protein leakage can be found in Supplementary Figure S1.

Invasive measures to assess endothelial activation

BLISTER FLUID – ENDOTHELIAL ACTIVATION MARKERS

The Olink Cardiometabolic panel measured the expression of 369 proteins. Within this manuscript we focus on the proteins indicating endothelial activation and proteins related to endothelial junctional integrity. The proteins indicating endothelial activation were vascular cell adhesion molecule 1 (VCAM-1), intercellular adhesion molecule 1 (ICAM-1), integrin β-1 (ITGB1) and E-selectin, all of which significantly increased over time after ID LPS with a peak at nine hours post-dose (Figure 4A). Endothelial cell-cell junctions were significantly altered after ID LPS as well, illustrated by increased expression of VE-cadherin as indicator of adherens junctions and a decreased expression of endothelial cell-selective adhesion molecule (ESAM) (Figure 4B).

BLISTER FLUID – NEUTROPHIL EXTRAVASATION

The presence of neutrophils in blister fluid was assessed to underline the classical cascade of rolling, adhesion, crawling and transmigration, initiated upon interaction with the activated endothelial cells. In our study, ID LPS injection induced an influx of neutrophils into the blister fluid. This followed a similar pattern as the protein extravasation, with a peak at 9 hours post-LPS injection (942, 95% CI [82, 1802] cells 100 µL of blister fluid, $p = 0.0342$) (Figure 4C, Table 1).

DISCUSSION AND CONCLUSION

In this study we aimed to characterise the ID LPS challenge in humans as a localised vascular leakage model. This application represents a valuable translational tool for early-phase clinical pharmacological studies evaluating the effects of vascular leakage-targeting compounds. By integrating data collected from dermal imaging techniques and analyses of biomarkers from blister fluid, we show that the ID injection of LPS elicited endothelial activation and vascular leakage. Approximately one hour after the injection, clinical signs of increased skin perfusion and erythema marked the onset of the vascular response to LPS. This vascular response further increased over time, while skin volume, as measure of oedema, and protein leakage were also initiated and peaked at nine hours post-injection, indicating the presence of additional LPS-induced vascular leakage. Olink data further substantiated these findings revealing endothelial activation and loss of endothelial cell-cell integrity in response to ID LPS in a similar time course.

It is known that increased perfusion and erythema, as measures of vasodilation, are consistent with early signs of inflammation and can contribute to capillary leakage by various mechanisms, for example increasing the number of perfused vessels and local vascular pressure.[27,28] The local vascular responses in our study, characterised by increased skin perfusion and erythema, are in agreement with this knowledge and with observations from two other clinical studies that focused on the effects of ID LPS on the inflammatory response.[18,25]

Our study adds to the available clinical data on ID LPS by extensively profiling early effects of ID LPS and by objectifying the presence of increased skin volume after ID LPS. Importantly, the observation that skin volume decreased while perfusion remained elevated following their simultaneous peak suggests that skin volume is not solely attributable to enhanced perfusion. Rather, the increase and subsequent decrease in skin volume can be explained by the presence of vascular leakage after ID LPS injection, as vascular barrier restoration and interstitial fluid clearance after an inflammatory stimulus reduce oedema, irrespective of skin perfusion.[29,30] An alternative explanation for the resolution of skin volume could be that the 3D multispectral imaging technique's sensitivity limits do not allow for detection of subtle changes. However, prior research has demonstrated relevant changes in a similar effect range over time using the same technique.[31,32]

Furthermore, blister fluid analysis provided direct biochemical evidence of loss of vascular barrier function and leakage, since albumin and total protein levels were significantly increased at LPS-challenged sites. Albumin leakage is a well-established marker of endothelial permeability in in vivo models for vascular leakage in rodent skin, lungs, and brain.[33–36] In humans, under normal circumstances, suction blister fluid contains protein concentrations comparable to those of interstitial fluid.[37] Fluid that actively leaks through a disrupted endothelial barrier contains high protein concentrations.[30] This highlights the relevance of our observations that protein concentrations increased after ID LPS and supports the use of ID LPS as model of vascular leakage. Furthermore, we observed that the peaks in protein concentrations did not coincide with the peak in skin volume. This discrepancy is not unexpected, given that interstitial fluid is mainly reabsorbed within hours, while clearance of proteins is a much slower process, with proteins in interstitial fluid having a half-life of 20-29 hours (depending on the health status of the skin).[18,38–40]

An additional novel finding in our study was the relative increase in expression of endothelial activation markers, namely VCAM-1, ICAM-1, ITGB1 and E-selectin, and altered levels of cell-cell junction markers, namely VE-cadherin and ESAM, in the blister fluid. VCAM-1, ICAM-1, ITGB1 and E-selectin are proteins present on the luminal surface of endothelial cells. They promote leukocyte extravasation and are upregulated under inflammatory circumstances.[23,41] Furthermore, under these conditions, they may subsequently be shed and circulate in the bloodstream.[42,43] Therefore, the observed increase of these proteins in blister fluid combined with increased numbers of neutrophils suggests endothelial activation after ID LPS. VE-cadherin is the main contributor to adherens junctions, while ESAM is part of the tight junctions between endothelial cells. The increased expression of VE-cadherin, which can also be shed under inflammatory

conditions, serves as an indicator of disintegration of endothelial cell-cell interactions and a decline in endothelial integrity.[44-46] The effects of inflammation on ESAM expression and whether it is internalised or shed have not yet been elucidated in literature. Finally, it is important to stress that these pathophysiological processes observed in our ID LPS model are also observed in the pathophysiology of a wide range vascular leakage-related diseases, including sepsis, arthritis and cancer,[47-50] which further supports the potential value of our model for future use in early-phase research with pharmaceuticals targeting vascular leakage in such diseases.

The intravenous LPS challenge is widely used as a human endotoxemia model, and therefore data are available on the systemic effects of LPS. However, there are only two studies describing outcome measures related to vascular leakage. These describe dose-dependent increases in E-selectin, VCAM-1 and ICAM-1 in a study administering 0.5-2 NG/KG LPS intravenously to healthy volunteers and VEGF increases in another clinical study administering 20 IU/KG LPS intravenously.[21,22] Our local dermal data are consistent with these observations. However, limitations of the systemic challenges include the impact on healthy volunteers, including temporary side effects such as fever, nausea and headaches, and the fact that non-invasive imaging and sequential local interstitial fluid collection to study the direct effects of systemic LPS on the vasculature in peripheral tissue are impossible.[51] Our ID LPS model has the major advantage that it allows for controlled, high-precision localised assessment of vascular leakage over time, without the logistical and safety limitations of a systemic LPS challenge.

When comparing the imaging data with the data from blister fluid, there is a high degree of similarity in the observed trends and time course of the effects, indicating interplay between several aspects of vascular leakage. Figure 5 presents the integration of these aspects based on theoretical knowledge and the findings from our study. The figure describes the vascular effects of the ID LPS model and the outcomes that can be measured in the setting of clinical trials. While preclinical assays for vascular leakage such as Evans blue-dyed protein extravasation in rodents and in vitro endothelial barrier models provide insights into the MoA of investigational drugs, these insights are limited due to interspecies differences and the lack of presence of all aspects of the human biology in culture systems. By collecting pharmacodynamic data in humans early in the clinical phase, an assessment of proof-of-pharmacology and proof-of-mechanism of new investigational vascular leakage-targeting drugs can be made. Thereby bridging the gap between preclinical and clinical stages.

While our novel application of the ID LPS model provides valuable insights into localised vascular leakage, several limitations must be acknowledged. First, the model reflects an acute innate immune stimulus and may not capture the complexity of chronic vascular inflammation or systemic microvascular pathology present in chronic diseases. Secondly, while the 5 NG LPS dose, chosen based on prior knowledge on inflammation and tolerability, does provide insights into vascular leakage induced by LPS, this study did not evaluate an LPS dose-response relationship and we cannot exclude the possibility that a higher LPS dose might induce enhanced effects on vascular leakage. However, safety and tolerability of study participants is of utmost importance and is safeguarded at the 5 NG dose. Thirdly, it must be acknowledged that the variability displayed by the parameters differs, with some (perfusion, skin volume) yielding enough power to individually demonstrate treatment effects with small group sizes (n = 6-10) while others (erythema) do not. Despite this variability, the integration of the presented parameters and their complementary contribution to several aspects of vascular leakage increase the overall signal-to-noise ratio and the applicability of the model. Additionally, it would be beneficial to investigate the effects of a vascular leakage-targeting drug in this model. However, no such compounds have been registered yet, thereby preventing this benchmarking. For application of this model beyond early-phase clinical pharmacological trials further studies expanding the knowledge on the effects of ID LPS in a broader population should be conducted.

In conclusion, we demonstrated that the ID LPS model is suitable for controlled induction of vascular leakage. A wide range of therapeutic agents targeting endothelial activation and vascular leakage, for example conventional immunosuppressants or Ang-Tie2

axis-, sphingosine-1-phosphate signalling- and adherens junction integrity-targeting agents that have shown preventive effects on models of vascular leakage in vitro and in vivo, could be effectively evaluated using this framework.[3,52,53] Therefore, this unique model can be applied in proof-of-mechanism studies for pharmaceuticals targeting endothelial integrity and vascular barrier function.

SUPPORTING INFORMATION

Supplementary tables and figures: https://ascpt.onlinelibrary.wiley.com/action/downloadSupplement?doi=10.1002%2Fcpt.70126&file=cpt70126-sup-0001-Supinfo.pdf

FIGURE 1 **Schematic representation of the study design and schedule of assessments.** In this experimental clinical study eight healthy volunteers received a total of three ID LPS injections to designated areas on the volar forearms. One ID LPS-injected site on the arm served as area for non-invasive imaging prior to LPS injection (baseline) and repeatedly from 0.25 up to 9 hours thereafter. Imaging consisted of recording skin perfusion using laser speckle contrast imaging and capturing erythema and skin volume using multispectral imaging. For albumin, total protein and Olink protein analysis, blister fluid was collected from suction blisters induced at all areas on the arms at baseline and at 0.5, 4, and 9 hours after ID LPS injection. Blood samples for albumin and total protein analysis were taken simultaneously with blister induction.

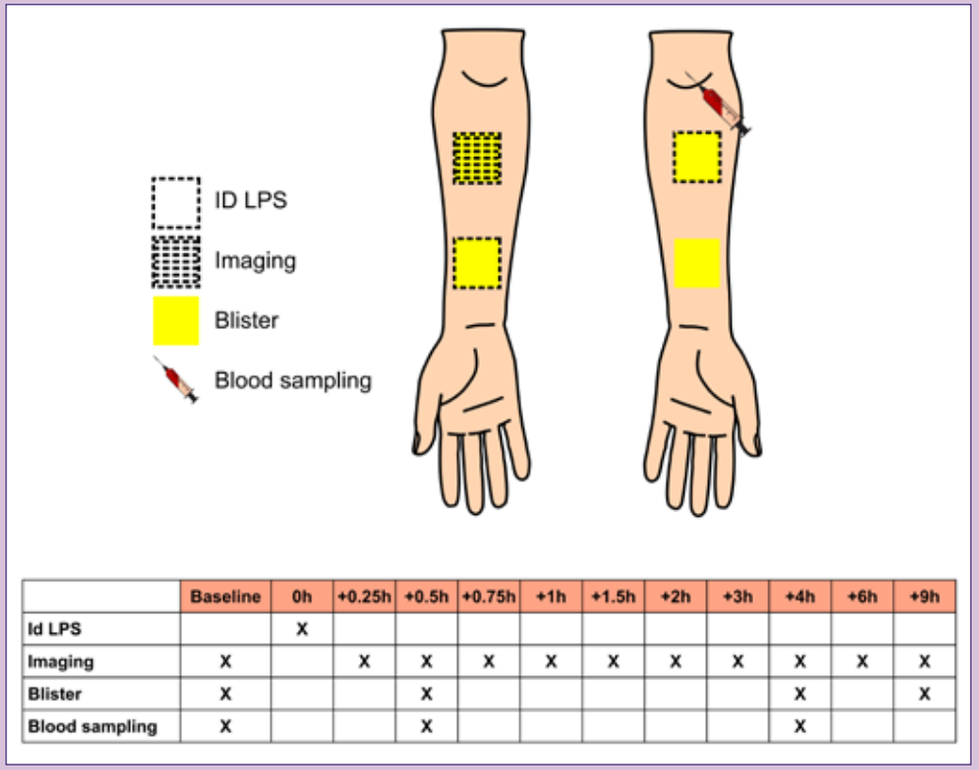

	Baseline	0h	+0.25h	+0.5h	+0.75h	+1h	+1.5h	+2h	+3h	+4h	+6h	+9h
Id LPS		X										
Imaging	X		X	X	X	X	X	X	X	X	X	X
Blister	X			X						X		X
Blood sampling	X			X						X		

Abbreviations: H, hour; ID, intradermal; LPS, lipopolysaccharide.

FIGURE 2 **Non-invasive quantification of local dermal responses to ID LPS to assess vasodilation and vascular leakage.** Skin perfusion was non-invasively assessed using laser speckle contrast imaging, and erythema, and skin volume were evaluated using the Antera 3D camera. (A-C) Representative clinical imaging data from a participant demonstrating the observed local response in (A) skin perfusion, (B) erythema, and (C) skin volume at 0.5, 4, and 9 hours after id LPS injection as compared to baseline. (D-F) Group summary data (n = 8) showing mean ± SD change from baseline in (D) skin perfusion, (E) erythema, and (F) skin volume over time after ID LPS injection.

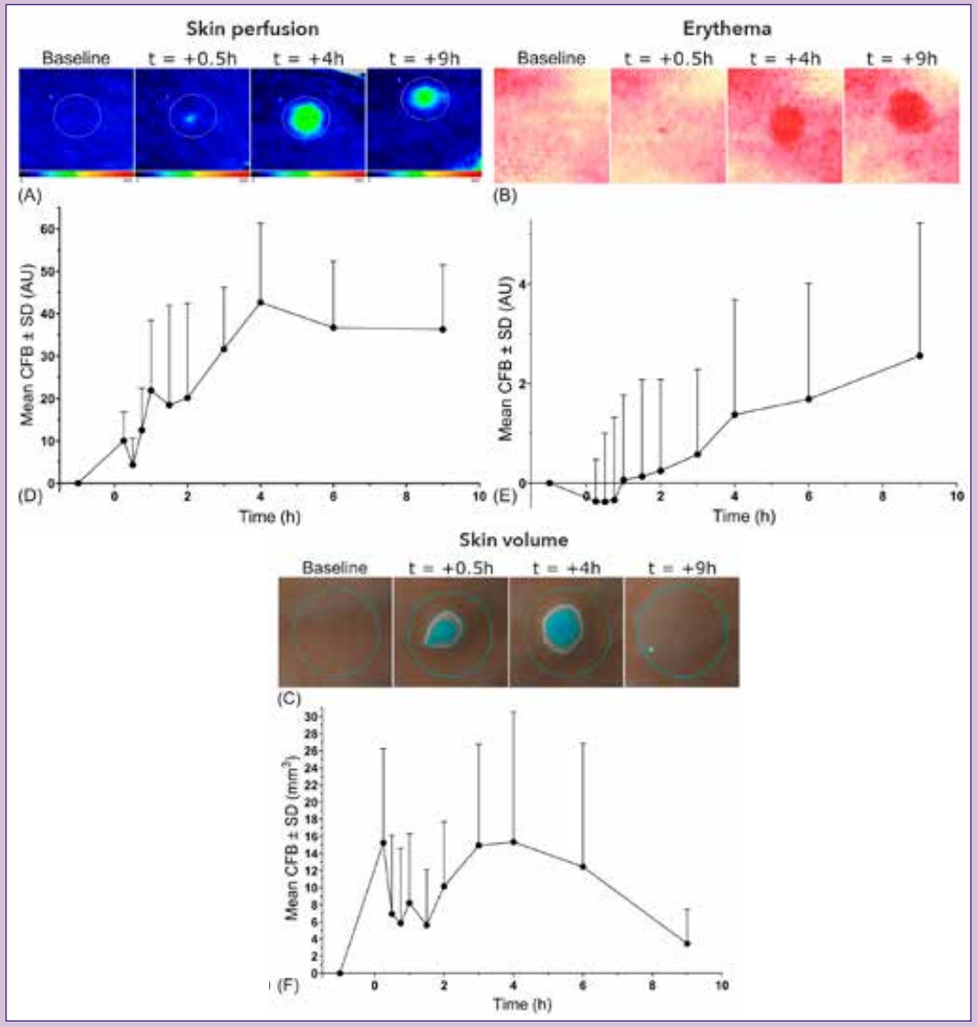

Abbreviations: AU, arbitrary unit; CFB, change from baseline; H, hours; LPS, lipopolysaccharide.

FIGURE 3 **ID LPS-induced increases of protein contents in local blister fluid as measure of vascular leakage.** (A) Concentrations of albumin and total protein (G/L, mean ± SD) in blister fluid at baseline prior to LPS injection, and at three LPS injected-skin areas at 0.5, 4, and 9 hours after ID LPS injection. (B) Corresponding serum albumin and total protein concentrations (G/L, mean ± SD) measured from blood samples collected in parallel with the induction of the suction blisters.

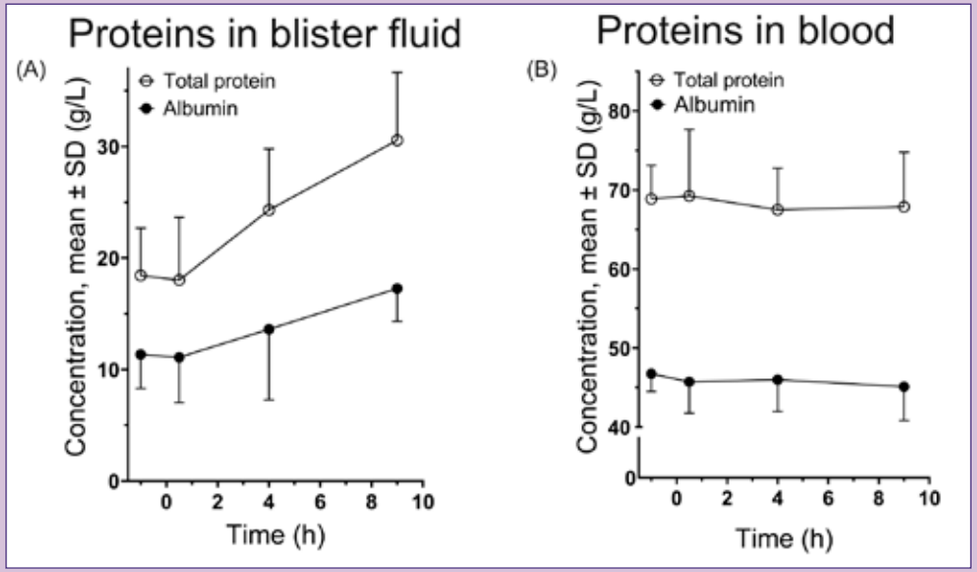

Abbreviations: LPS, lipopolysaccharide.

FIGURE 4 **ID LPS-induced alterations in endothelial activation and endothelial junction markers in local blister fluid.** (A) NPX values representing the expression of proteins associated with endothelial activation (VCAM-1, ICAM-1 and E-selection) in blister fluid at baseline and at 0.5, 4, and 9 hours after ID LPS injection. (B) NPX values for proteins associated with endothelial cell-cell interaction (VE-cadherin and endothelial surface adhesion marker [ESAM]) in blister fluid collected from skin suction blisters on a designated control area (baseline) and on three LPS-injected sites (0.5, 4, and 9 hours after injection) on the volar forearms. (C) Quantification (individual values and mean ± SD) of neutrophil infiltration at the designated skin area at baseline prior to LPS injection, and at three LPS injected-skin areas at 0.5, 4, and 9 hours after ID LPS injection. Neutrophils were measured as the absolute number of CD45+/CD66b+/Siglec8- cells in 100 µL blister fluid using flow cytometry.
Each boxplot in (A) and (B) represents the median, interquartile range (IQR), and 1.5*IQR (whiskers) NPX for each protein. Asterisks indicate levels of statistical significance as analysed using the Eisinga, Heskes, Pelzer & Te Grotenhuis post-hoc test. *: $p < 0.05$, **: $p < 0.01$, ***: $p < 0.001$.

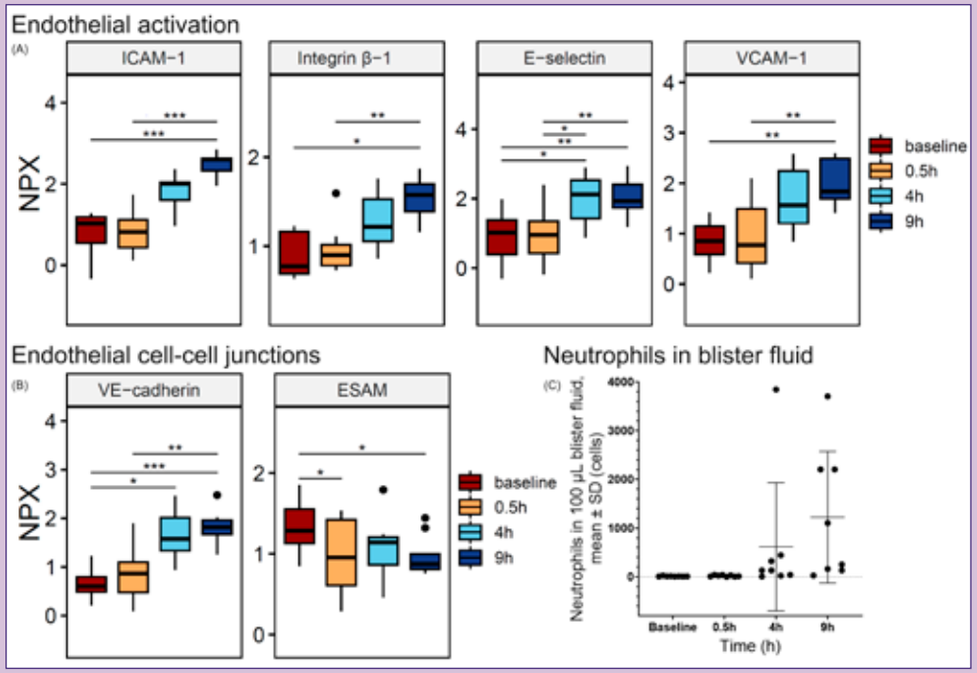

Abbreviations: ESAM, endothelial surface adhesion marker; ICAM-1, intercellular adhesion molecule 1; NPX, normalised protein expression;VCAM-1, vascular cell adhesion molecule 1.

FIGURE 5 **Schematic representation of the effects of an intradermal LPS challenge on vascular leakage and potential read-outs.** This figure displays a cross section of part of the dermis, the vascular wall and part of the vascular lumen. (A) The inflammatory challenge is initiated by the intradermal injection of LPS into the skin of healthy volunteers. (B) The ID LPS injection elicits an innate inflammatory response characterised by vasodilation (increased perfusion and erythema), leukocyte attraction, and endothelial activation. (C) Furthermore, the endothelium is activated (e.g., VCAM-1 and ICAM-1), leading to extravasation of neutrophils, and vascular integrity is altered by disintegration of tight junctions and the extravasation of fluids and proteins (e.g., albumin). Non-invasive available experimental read-outs for the described processes are imaging of vasodilation by laser speckle contrast imaging, and erythema and skin volume as measure of fluid extravasation by Antera 3D camera. Invasive experimental read-outs are analysis of local suction blister fluid by laboratory assays for albumin and total protein, Olink proteomics for endothelial markers, and flowcytometry for neutrophil extravasation.

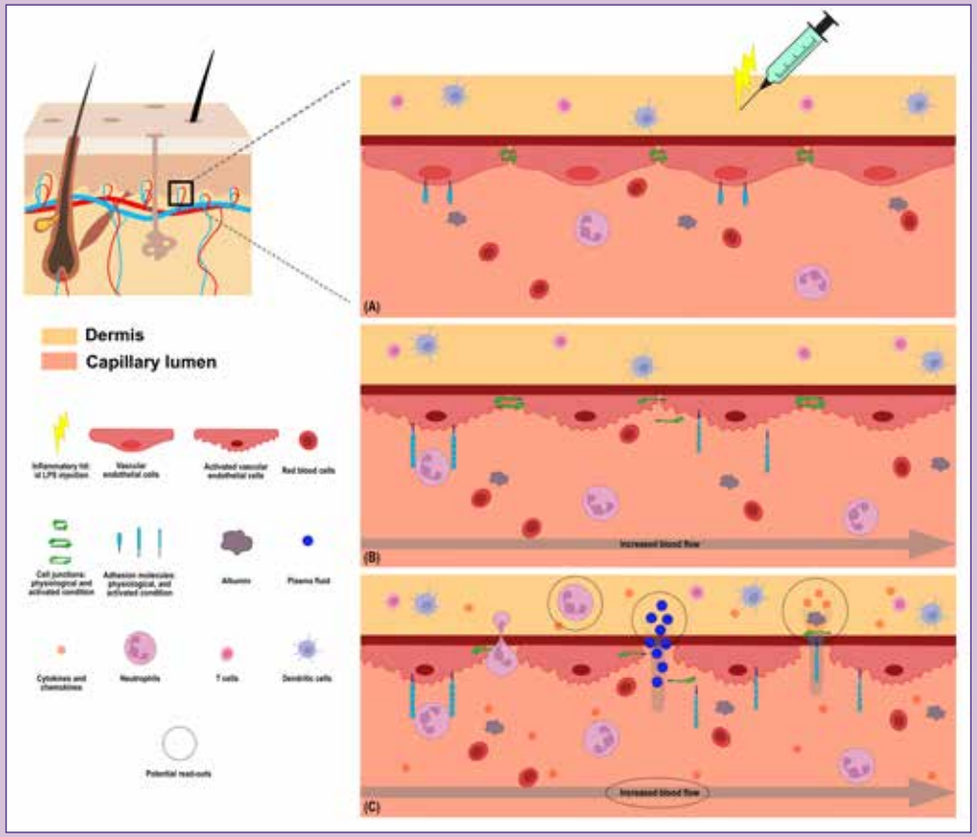

Abbreviations: ICAM-1, intercellular adhesion molecule 1; LPS, lipopolysaccharide; VCAM-1, vascular cell adhesion molecule 1.

REFERENCES

1. Wautier JL, Wautier MP. Vascular Permeability in Diseases. *Int J Mol Sci*. 2022;23(7):3645. doi:10.3390/ijms23073645
2. Park-Windhol C, D'Amore PA. Disorders of Vascular Permeability. *Annu Rev Path*. 2016;11:251–281. doi:10.1146/annurev-pathol-012615-044506
3. Darwish I, Conrad Liles W. Emerging therapeutic strategies to prevent infection-related microvascular endothelial activation and dysfunction. *Virulence*. 2013;4(6):572-582. doi:10.4161/viru.25740
4. Okada Y. Potential Therapeutic Strategies and Drugs That Target Vascular Permeability in Severe Infectious Diseases. *Biol Pharm Bull*. 2024;47(3):549-555. doi:10.1248/bpb.b24-00028
5. Hajitou A, Pasqualini R, Arap W. Vascular targeting: Recent advances and therapeutic perspectives. *Trends Cardiovasc Med*. 2006;16(3):80-88. doi:10.1016/j.tcm.2006.01.003
6. ClinicalTrials.gov. Evaluation of the Safety and Efficacy of Razuprotafib in Hospitalized Subjects With Coronavirus Disease 2019 (RESCUE). Identifier: NCT04511650. https://clinicaltrials.gov/study/NCT04511650?term=RESCUE%20razuprotafib&rank (2023). Accessed April 24, 2025.
7. Goel S, Gupta N, Walcott BP, et al. Effects of vascular-endothelial protein tyrosine phosphatase inhibition on breast cancer vasculature and metastatic progression. *J Natl Cancer Inst*. 2013;105(16):1188-1201. doi:10.1093/jnci/djt164
8. Papadopoulos KP, Kelley RK, Tolcher AW, et al. A phase i first-in-human study of nesvacumab (REGN910), a fully human anti-angiopoietin-2 (Ang2) monoclonal antibody, in patients with advanced solid tumors. *Clin Cancer Res*. 2016;22(6):1348-1355. doi:10.1158/1078-0432.CCR-15-1221
9. Aman J, Van Bezu J, Damanafshan A, et al. Effective treatment of edema and endothelial barrier dysfunction with imatinib. *Circulation*. 2012;126(23):2728-2738. doi:10.1161/CIRCULATIONAHA.112.134304
10. Chen C. Opportunities and pitfalls in clinical proof-of-concept: principles and examples. *Drug Discov Today*. 2018;23(4):776-787. doi:10.1016/j.drudis.2018.01.045
11. Schmidt B. Proof of principle studies. *Epilepsy Res*. 2006;68(1):48-52. doi:10.1016/j.eplepsyres.2005.09.019
12. Jiang S, Xia R, Jiang Y, Wang L, Gao F. Vascular endothelial growth factors enhance the permeability of the mouse blood-brain barrier. *PLoS One*. 2014;9(2):e86407. doi:10.1371/journal.pone.0086407
13. Li XY, Donaldson K, MacNee W. Lipopolysaccharide-induced alveolar epithelial permeability the role of nitric oxide. *Am J Respir Crit Care Med*. 1998;157:1027-1033. doi:10.1164/ajrccm.157.4.9605080
14. Ashina K, Tsubosaka Y, Nakamura T, et al. Histamine induces vascular hyperpermeability by increasing blood flow and endothelial barrier disruption in vivo. *PLoS One*. 2015;10(7):e0132367. doi:10.1371/journal.pone.0132367
15. Chen XL, Nam JO, Jean C, et al. VEGF-Induced Vascular Permeability Is Mediated by FAK. *Dev Cell*. 2012;22(1):146-157. doi:10.1016/j.devcel.2011.11.002
16. Zarban AA, Chaudhry H, Maselli D, et al. Enhancing Techniques for Determining Inflammatory Edema Formation and Neutrophil Accumulation in Murine Skin. *JID Innov*. 2023;3(1):100154. doi:10.1016/j.xjidi.2022.100154
17. Scheppke L, Aguilar E, Gariano RF, et al. Retinal vascular permeability suppression by topical application of a novel VEGFR2/Src kinase inhibitor in mice and rabbits. *J Clin Invest*. 2008;118(6):2337-2346. doi:10.1172/JCI33361
18. Buters TP, Hameeteman PW, Jansen IME, et al. Intradermal lipopolysaccharide challenge as an acute in vivo inflammatory model in healthy volunteers. *Br J Clin Pharmacol*. 2022;88(2):680-690. doi:10.1111/bcp.14999
19. Wang M, Feng J, Zhou D, Wang J. Bacterial lipopolysaccharide-induced endothelial activation and dysfunction: a new predictive and therapeutic paradigm for sepsis. *Eur J Med Res*. 2023;28(1):339. doi:10.1186/s40001-023-01301-5
20. Stierschneider A, Wiesner C. Shedding light on the molecular and regulatory mechanisms of TLR4 signaling in endothelial cells under physiological and inflamed conditions. *Front Immunol*. 2023;14. doi:10.3389/fimmu.2023.1264889
21. Mittermayer F, Pleiner J, Schaller G, et al. Marked increase in vascular endothelial growth factor concentrations during Escherichia coli endotoxin-induced acute inflammation in humans. *Eur J Clin Invest*. 2003;33(9):758-761. doi:10.1046/j.1365-2362.2003.01192.x
22. van Poelgeest EP, Dillingh MR, de Kam M, et al. Characterization of immune cell, endothelial, and renal responses upon experimental human endotoxemia. *J Pharmacol Toxicol Methods*. 2018;89:39-46. doi:10.1016/j.vascn.2017.10.004
23. Filippi MD. Neutrophil transendothelial migration: Updates and new perspectives. *Blood*. 2019;133(20):2149-2158. doi:10.1182/blood-2018-12-844605
24. Basran A, Jabeen M, Bingle L, et al. Roles of neutrophils in the regulation of the extent of human inflammation through delivery of IL-1 and clearance of chemokines. *J Leukoc Biol*. 2013;93(1):7-19. doi:10.1189/jlb.0512250
25. Buters TP, Hameeteman PW, Jansen IME, et al. Clinical, Cellular, and Molecular Effects of Corticosteroids on the Response to Intradermal Lipopolysaccharide Administration in Healthy Volunteers. *Clin Pharmacol Ther*. 2022;111(4):964-971. doi:10.1002/cpt.2516
26. Olink Proteomics AB. Assay data. https://olink.com/knowledge/documents. Accessed April 24, 2025.
27. Punchard NA, Whelan CJ, Adcock I. The Journal of Inflammation. *J Inflamm*. 2004;1(1):1. doi:10.1186/1476-9255-1-1
28. Curry FRE, Adamson RH. Vascular permeability modulation at the cell, microvessel, or whole organ level: Towards closing gaps in our knowledge. *Cardiovasc Res*. 2010;87(2):218-229. doi:10.1093/cvr/cvq115
29. Scallan J, Huxley VH, Korthuis RJ. Chapter 1: Fluid Movement Across the Endothelial Barrier. In Capillary Fluid Exchange: Regulation, Functions, and Pathology. (Morgan & Claypool Life Sciences, San Rafael, CA, USA; 2010).
30. Scallan J, Huxley VH, Korthuis RJ. Chapter 4: Pathophysiology of Edema Formation. In: Capillary Fluid Exchange: Regulation, Functions, and Pathology. (Morgan & Claypool Life Sciences, San Rafael, CA, USA; 2010).
31. Shaiek A, Monot M, Rubert V, et al. In vitro and in vivo validation of a new three-dimensional fringe projection-based device (AEVA-HE) dedicated to skin surface mapping. *Skin Res Technol*. 2023;29(2):e13209. doi:10.1111/srt.13209
32. Adatto M. Clinical evaluation of the efficacy of fractional radiofrequency for the treatment and reduction of stretch marks: A prospective study. *J Cosmet Dermatol*. 2023;22(1):214-221. doi:10.1111/jocd.15463
33. Radu M, Chernoff J. An in vivo assay to test blood vessel permeability. *J Vis Exp*. 2013;(73):e50062. doi:10.3791/50062-v
34. Iuvone T, D'Acquisto F, Van Osselaer N, Di Rosa M, Carnuccio R, Herman AG. Evidence that inducible nitric oxide synthase is involved in LPS-induced plasma leakage in rat skin through the activation of nuclear factor-κB. *Br J Pharmacol*. 1998;123(7):1325-1330. doi:10.1038/sj.bjp.0701730
35. Dallal MM, Chang SW. Evans blue dye in the assessment of permeability-surface area product in perfused rat lungs. *J Appl Physiol*. 1994;77(2):1030-1035. doi:10.1152/jappl.1994.77.2.1030
36. Rosengren L, Persson L, Johansson B. Enhanced blood-brain barrier leakage to evans blue-labelled albumin after air embolism in ethanol-intoxicated rats. *Acta Neuropathol*. 1977;38(2):149-152. doi:10.1007/BF00688562
37. Vermeer BJ, Reman FC, Van Gent CM. The determination of lipids and proteins in suction blister fluid. *J Invest Dermatol*. 1979;73(4):303-305. doi:10.1111/1523-1747.ep12531833
38. Staberg B, Klemp P, Aasted M, Worm AM, Lund P. Lymphatic albumin clearance from psoriatic skin. *J Am Acad Dermatol*. 1983;9(6):857-861. doi:10.1016/S0190-9622(83)70198-2
39. Stewart RH. A Modern View of the Interstitial Space in Health and Disease. *Front Vet Sci*. 2020;7:609583. doi:10.3389/fvets.2020.609583
40. McClure W, Aldrich C. Time required for disappearance of intradermally injected salt solution. *J Am Med Assoc*. 1923;81(4):293. doi:10.1001/jama.1923.02650040033011
41. Zhang J, Huang S, Zhu Z, Gatt A, Liu J. E-selectin in vascular pathophysiology. *Front Immunol*. 2024;15:1401399. doi:10.3389/fimmu.2024.1401399
42. Pigott R, Dillon LP, Hemingway IH, Gearing AJH. Soluble forms of E-selectin, ICAM-1 and VCAM-1 are present in the supernatants of cytokine activated cultured endothelial cells. *Biochem*

Biophys Res Commun. 1992;187(2):584-589. doi:10.1016/0006-291X(92)91234-H
43. Kjærgaard AG, Dige A, Nielsen JS, Tønnesen E, Krog J. The use of the soluble adhesion molecules sE-selectin, sICAM-1, sVCAM-1, sPECAM-1 and their ligands CD11a and CD49d as diagnostic and prognostic biomarkers in septic and critically ill non-septic ICU patients. *APMIS*. 2016;124(10):846-855. doi:10.1111/apm.12585
44. Kaur R, Singh V, Kumari P, Singh R, Chopra H, Emran T Bin. Novel insights on the role of VCAM-1 and ICAM-1: Potential biomarkers for cardiovascular diseases. *Ann Med Surg*. 2022;84:104802. doi:10.1016/j.amsu.2022.104802
45. Herren B, Levkau B, Raines EW, Ross R. Cleavage of β-catenin and plakoglobin and shedding of VE-cadherin during endothelial apoptosis: Evidence for a role for caspases and metalloproteinases. *Mol Biol Cell*. 1998;9(6):1589-1601. doi:10.1091/mbc.9.6.1589
46. Rabiet MJ, Plantier JL, Rival Y, Genoux Y, Lampugnani MG, Dejana E. Thrombin-induced increase in endothelial permeability is associated with changes in cell-to-cell junction organization. *Arterioscler Thromb Vasc Biol*. 1996;16(3):488-496. doi:10.1161/01.ATV.16.3.488
47. Velikova G, Banks RE, Gearing A, et al. Serum concentrations of soluble adhesion molecules in patients with colorectal cancer. *Br J Cancer*. 1998;77(11):1857-1863. doi:10.1038/bjc.1998.309
48. Velikova G, Banks RE, Gearing A, et al. Circulating soluble adhesion molecules E-cadherin, E-selectin, intercellular adhesion molecule-1 (ICAM-1) and vascular cell adhesion molecule-1 (VCAM-1) in patients with gastric cancer. *Br J Cancer*. 1997;76(11):1398-1404. doi:10.1038/bjc.1997.569
49. Flemming S, Burkard N, Renschler M, et al. Soluble VE-cadherin is involved in endothelial barrier breakdown in systemic inflammation and sepsis. *Cardiovasc Res*. 2015;107(1):32-44. doi:10.1093/cvr/cvv144
50. Klimiuk PA, Sierakowski S, Latosiewicz R, et al. Soluble adhesion molecules (ICAM-1, VCAM-1, and E-selectin) and vascular endothelial growth factor (VEGF) in patients with distinct variants of rheumatoid synovitis. *Ann Rheum Dis*. 2002;61(9):804-809. doi:10.1136/ard.61.9.804
51. Dillingh MR, Van Poelgeest EP, Malone KE, et al. Characterization of inflammation and immune cell modulation induced by low-dose LPS administration to healthy volunteers. *J Inflamm*. 2014;11(1):28. doi:10.1186/s12950-014-0028-1
52. Saharinen P, Eklund L, Alitalo K. Therapeutic targeting of the angiopoietin–TIE pathway. *Nat Rev Drug Discov*. 2017;16:635-661. doi:10.1038/nrd.2016.278.
53. Cao Y, Langer R, Ferrara N. Targeting angiogenesis in oncology, ophthalmology and beyond. *Nat Rev Drug Discov*. 2023;22(6):476-495. doi:10.1038/s41573-023-00671-z

CHAPTER 5

Advancing clinical drug development: omics-based immunological characterisation of the intradermal lipopolysaccharide-driven human inflammatory response

Published in: to be submitted

Marella C.E. van Ruissen*[1,2], Juliette A. van den Noort*[1,2], Ingrid Tomljanovic[3], Michelle Osse[1], Manon A. A. Jansen[1,2], Matthijs Moerland[1,2]
**These authors share first authorship.*

1 Centre for Human Drug Research, Leiden, the Netherlands
2 Leiden University Medical Centre, Leiden, the Netherlands
3 Department of Urology, Erasmus University Medical Centre, Rotterdam, The Netherlands

ABSTRACT

Drug development faces high attrition rates. Approximately 90% of clinical drug candidates fail before market authorisation, most commonly due to lack of efficacy. The use of multi-omics, integrating complex biological datasets, is an upcoming strategy to address this challenge. Data from human inflammatory challenge models, such as the intradermal lipopolysaccharide (ID LPS) challenge, are often used to study proof-of-pharmacology in early-phase clinical trials, but may also be leveraged within multi-omics research. Therefore, extending the knowledge of the ID LPS challenge aids more efficient drug development for both proof-of-pharmacology studies and omics-driven drug development. Here we present a transcriptomic and proteomic characterisation of the ID LPS model in humans. Bulk RNA sequencing of skin punch biopsies from healthy participants (N = 6) revealed a robust proinflammatory transcriptomic signature over time after ID LPS, involving mainly innate immune and receptor signalling pathways, including TLR4 signalling. Proteomic profiling of blister fluid from ID LPS treated healthy volunteers (N = 8) demonstrated an inflammatory response with similar temporal clustering and increased expression of inflammatory proteins downstream of TLR4. Furthermore, transcriptome-based analyses revealed overlap between the transcriptomic changes induced by ID LPS and the genetic signatures of inflammatory diseases, supporting the preclinical to clinical translational value of the ID LPS model. The presented research provides a comprehensive framework describing human TLR4-mediated inflammation. Integration of these data into omics-driven drug development strategies could enhance target identification, refine efficacy predictions and enable more informative clinical trial design.

INTRODUCTION

An estimated 90% of drug candidates in clinical development fail to advance to the stage of submission for market authorisation.[1] The major cause for discontinuation of drug development programmes is lack of efficacy in the target population.[2] Traditional drug development programmes commonly employ a single target-based approach, in which drug candidates are identified based on a known molecular target relevant to a single disease.[3] Recent advances in computational and experimental omics methods are driving a shift towards multi-omics approaches that integrate complex biological datasets to combat the high attrition rates in clinical drug development. This potentially enhances target identification, improves efficacy predictions and target validation in clinical trials, thereby optimising the drug development pipeline compared to the traditional single target-based approach.[4–6]

Human inflammatory challenge models used in early-phase clinical trials can also contribute to the optimisation of drug development. By applying such models, mechanistic and pharmacodynamic properties of novel therapeutic compounds can be investigated early in the clinical phase, which contributes to early termination of drugs that demonstrate no signs of potential effectiveness and supports the design of more informative future clinical studies.[7,8] An example of such a human challenge model is the intradermal lipopolysaccharide (ID LPS) model. This model displays mechanistic overlap with a wide variety of diseases, including sepsis, inflammatory lung diseases, and autoimmune disorders, as it induces a transient, innate immune response in the skin.[9–12] Therefore, it can be applied to test immunomodulatory drugs targeting such diseases. The inflammatory response within the model is based on the TLR4-agonistic effects of LPS, which are mainly mediated through nuclear factor kappa-light-chain-enhancer of activated B-cells (NF-KB).[13] Downstream pro-inflammatory cytokines interleukin (IL)-6, IL-8 and tumour necrosis factor (TNF) are detectable after ID LPS exposure in humans. Moreover, recent findings have demonstrated that administration of ID LPS induces an acute dermal influx of neutrophils, followed by recruitment of monocytes and dendritic cells.[9]

While these previous studies have provided valuable insights into the ID LPS challenge response, they focused on quantifying individual cells and cytokines, rather than employing an omics-based approach. An omics-based knowledgebase would enable a deeper and more comprehensive understanding of the molecular networks and pathways activated by the id LPS challenge, including upstream regulators of the immune response and accompanying pathway involvement. Furthermore, correlating the mechanism of action (MoA) and drug target information of drug candidates with such omics data could allow for a more data-driven approach to challenge model selection. This would enable drug candidates to be matched to challenge models that engage overlapping molecular pathways, thereby enhancing the rational design of proof-of-pharmacology studies.

In this manuscript, we characterise the transcriptomic and proteomic profiles of the human inflammatory response to ID LPS. This omics-based framework expands the current understanding of human inflammatory physiology. It also provides a reference for more informed challenge model selection in early-phase clinical trials with immunomodulatory drugs, based on whether the MoA of drug candidates overlaps with targets and pathways driven by ID LPS. Furthermore, it offers a resource for assessing whether anti-inflammatory drug candidates modulate mechanisms relevant to target diseases early in clinical development. Ultimately, these data and insights may contribute to increasing drug development efficiency through future systems biology approaches.

METHODS

This manuscript describes data from two single-centre, open-label, experimental inflammatory challenge studies evaluating TLR4-mediated inflammation following the id injection of LPS. Study A was conducted in November and December 2023 and study B from June 2024 to February 2025 at the Centre for Human Drug Research (Leiden, The Netherlands). Both studies were conducted in accordance with the principles of the Declaration of Helsinki (1975, as revised in 1983) and the Dutch Medical Research Involving Human Subjects Act (WMO). The protocols were approved by the independent Medical Ethics Committee of the Stichting Beoordeling Ethiek Biomedisch Onderzoek (BEBO, Assen, The Netherlands). Furthermore, both studies were prospectively registered: study A in the WHO-recognised Overview of Medical Research in The Netherlands registry (NL-OMON53274) and study B in the EU Clinical Trials Register (2024-512377-27-00). All participants provided written informed consent prior to the initiation of any study-related procedures.

Study design and participant inclusion

We recruited healthy men and women (male:female ratio = 1:1. Study A: n = 6. Study B: n = 8), aged 18-45 years, with a Fitzpatrick skin type I-III. Health status was confirmed by the absence of clinically significant abnormal findings in medical history, physical examination, 12-lead ECG, alcohol breathalyser and clinical laboratory testing (i.e. serum chemistry, haematology, coagulation, urine drug screen and urinalysis) during a medical screening. Participants with a history of pathological scar formation, skin conditions or autoimmune diseases were excluded from participation. The use of medication was not permitted from 7 days prior to dosing until study completion. Furthermore, prolonged sun exposure of the skin was to be avoided from 3 weeks prior to dosing until the end of the study.

LPS challenge

To evaluate the inflammatory skin response, a total of five ID doses of LPS (5 NG LPS/50 µL 0.9% sodium chloride per injection) were administered to the participants in study at five locations on the upper back (Figure 1). In study B, three ID LPS injections (5 NG LPS/50 µL 0.9% sodium chloride per injection) were applied to the forearms. Both studies investigated one additional site that served as an untreated control area (Figure 1).

Transcriptomic profiling

BIOPSY COLLECTION AND PROCESSING FOR RNA SEQUENCING

To characterise the transcriptomic response to the ID LPS challenge, participants in study A underwent sequential biopsy collections prior to ID LPS injection and at 1H, 3H, 6H, 9H and 24H after ID LPS administration. Tissue biopsy samples were obtained from indicated areas (Figure 1). The tissue was embedded in Tissue Tek OCT medium (Sakura Finetek USA, Inc., Torrance, USA), snap frozen in liquid nitrogen, and subsequently stored in a gas phase liquid nitrogen tank.

RNA ISOLATION, SEQUENCING AND DATA PREPROCESSING

Snap-frozen tissue was lysed using RLT lysis buffer with β-mercaptoethanol and RNA was extracted using the RNeasy Plus Micro Kit (Qiagen, CAT. NO. 74034). The extracted RNA concentration was assessed using the Qubit™ RNA Broad range assay (Thermo Fisher, CAT. NO. Q10210) and a minimum of 25 NG/µL was considered acceptable.

A total of 36 human skin biopsy samples that yielded sufficient RNA for sequencing were processed for bulk RNA sequencing by Genomescan BV (Leiden, The Netherlands). RNA libraries were constructed using the NEBNext® Ultra II Directional RNA Library Prep Kit (New England BioLabs, Ipswich, MA, USA, CAT. NO. E7760S/L). Polyadenylated RNA was isolated from total RNA using the NEBNext® Poly(A) MRNA Magnetic Isolation Module (New England BioLabs, Ipswich, MA, USA, CAT. NO. E7490L) via oligo(dT) magnetic bead-based selection. Library preparation included RNA fragmentation, CDNA synthesis, adapter ligation, and PCR amplification of the CDNA library.

Sequencing was performed on the Illumina NovaSeq 6000 platform (Illumina Inc., San Diego, CA, USA) to generate approximately 40 million paired-end reads (2 x 150BP) per sample. Fastp v0.23.2 was used for adapter trimming and removal of low-quality bases. Clean reads were aligned to the GRCh38.p13 human reference genome using STAR v2.7.10. Gene-level raw counts were obtained using HTSeq v2.0.2.

Proteomic profiling

BLISTER FLUID COLLECTION AND PROCESSING FOR PROTEOMIC ANALYSES

To determine the proteomic profile of the ID LPS challenge response, participants in study B underwent blister fluid collection on the forearms prior to ID LPS administration and at 0.5H, 4H and 9H after ID LPS injection (Figure 1). Blister formation was conducted as previously described by Buters et al.[9] After blister formation, blister fluid was collected into Sarstedt tubes containing 50 µL 3% sodium citrate (Sigma-Aldrich, St. Louis, MO, USA) in phosphate buffered saline (Gibco, Thermo Fisher Scientific, Waltham, MA, USA) and immediately kept on ice. The total of 32 samples were centrifuged to obtain the supernatant which was subsequently frozen at -80°C until proteomic analysis at Firalis S.A. (Huningue, France).

The Olink Explore 3072/384 Panel (Olink Proteomics AB, Uppsala, Sweden), consisting of 8 sub-panels in total (Inflammation I+II, Cardiometabolic I+II, Neurology I+II and Oncology I+II), was used to study the relative changes in protein expression for a range of proteins related to inflammatory responses in the obtained blister fluid samples. This panel is a multiplex immunoassay based on proximity extension assay technology and reports normalised protein expression (NPX), an arbitrary unit on a $\log_2$ scale.[14] A total of 9 samples did not pass the quality control (QC)-criteria (a deviation from the median NPX between -0.5 and 0.5 and count > 500 for either incubation or amplification control) for one or more of the subpanels and were therefore excluded from the respective panel analyses (Supplementary Table 1).

Statistical analyses

BASELINE CHARACTERISTICS

Baseline characteristics were summarised using descriptive statistics: means and standard deviations (SDs) for continuous variables, and frequencies and percentages for categorical variables (e.g., sex, skin type).

RNA SEQUENCING ANALYSES

Data visualisation and statistical analyses of the bulk RNA sequencing dataset were performed using R statistical software (v4.4.2). An overview of samples and associated information is provided in Supplementary Table 2. Principal component analysis (PCA) was performed on all features using the PCAplot function from the DESeq2 package (v1.46.0). Differential gene expression analysis was performed using the DESeq2 package with subsequent $\log_2$ fold change (LFC) shrinkage using the apeglm estimator (v1.28.0). Gene set enrichment analysis (GSEA) was conducted on a subset of the Molecular Signatures Database (MSIGDB) v2023.2.Hs using the clusterProfiler package (v4.14.6), including the following: Hallmarks, Reactome, KEGG Medicus, KEGG Legacy, Gene Ontology (MF, BP and CC), PID, Wikipathways and BioCarta. Gene Set Variation Analysis (GSVA) was used for single-sample pathway enrichment with the GSVA package (v2.0.6). Differential expression at the pathway level was assessed using the lmFit function from limma (v3.62.2). Disease gene set enrichment was performed on the Disease Ontology database using DOSE (v4.1.0) and statistically significant sets were filtered using the following thresholds: adjusted *p*-value ≤ 0.0005 and normalised enrichment score (NES) > 0. These were next visualised as a network of the top 30 gene sets using the emapplot function from the enrichplot package (v1.26.6) with custom parameters. For visualisation and clustering purposes, the variance stabilising transformation (VST) was applied using the DESeq2 package. Visualisation was performed using ggplot2 (v3.5.1) and heatmaps were generated using the pheatmap package (v1.0.12). The abundances of 22 immune cell types were quantified by CIBERSORTx using the LM22 signature matrix, B-mode batch correction, 100 permutations and quantile normalisation disabled (https://cibersortx.stanford.edu/, accessed October 2025). The Friedman test was used to assess the differences in absolute scores for each cell type across sample groups, while the Eisinga, Heskes, Pelzer & Te Grotenhuis all-pairs test was applied as post hoc test, as implemented in the PMCMRplus package (v1.9.12). Unless otherwise specified, the statistical significance threshold across all analyses was set at 0.05 and a Benjamini-Hochberg correction was applied to account for multiple testing.

PROTEOMIC ANALYSES

Analyses of Olink protein expression in blister fluid from study B were conducted using R statistical software (v4.4.2), OlinkAnalyze (v4.3.2) and ggplot2 (v3.5.1). PCA was performed using PCA tools::pca (v2.18.0) with default parameters on all features measured by the Inflammation I and II panels, using data from 29 samples which met the QC criteria and were not marked as panel-specific outliers. An overview of samples and associated information is provided in Supplementary Table 3. Subsequently, protein expression was visualised using boxplots and heatmaps depicting NPX values. The relative changes in expression over time were analysed using the Skillings-Mack test followed by the Eisinga, Heskes, Pelzer & Te Grotenhuis post-hoc test on data from participants with complete observations, defined as not yielding any panel-specific outlier samples. Unless otherwise specified, the statistical significance threshold across all analyses was set at 0.05 and a Benjamini–Hochberg correction was applied to account for multiple testing.

RESULTS

Baseline characteristics

In study A, six healthy volunteers aged 20-30 years were included (males n = 3, females n = 3). Study B included eight participants, four males and four females, with a mean age of 24.3 (SD 4.8) years. All included healthy volunteers had Fitzpatrick skin type I-III. Baseline characteristics are presented in Table 1.

TABLE 1 **Baseline characteristics.**

Baseline characteristics*		Study A (N = 6)	Study B (N = 8)
Age (years)		24.5 (4.7)	24.3 (4.8)
Sex, N (%)	Male	3 (50)	4 (50)
	Female	3 (50)	4 (50)
Race, N (%)	White	6 (100)	8 (100)
Fitzpatrick skin type, n (%)	I	1 (16.7)	2 (25)
	II	4 (66.7)	3 (37.5)
	III	1 (16.7)	3 (37.5)

**Mean (SD) for continuous demographic variables and counts (%) for qualitative demographic characteristics.*

Transcriptomic profile

TEMPORAL CLUSTERING AND ENRICHMENT OF INFLAMMATORY PATHWAYS AFTER ID LPS

To characterise the transcriptomic effects of ID LPS injection, we analysed samples across various time points during the inflammatory response. Firstly, we examined sample clustering using PCA, followed by analysis of the most prominent enriched pathways. The PCA plot revealed three well-defined clusters of samples, indicating distinct, time-dependent, LPS-induced transcriptional changes. These clusters included samples from: 1) baseline and 1H post-LPS injection, 2) 3H to 9H post-LPS injection, 3) 24H after ID LPS injection (Figure 2A). T-distributed stochastic neighbour embedding (T-SNE) portrayed similar clustering (Supplementary Figure 1A). As expected based on prior literature, the subsequent single-sample pathway enrichment analysis of the MSIGDB Hallmark gene sets demonstrated that ID LPS predominantly affected pathways involving inflammation and immune responses, such as TNF signalling via NF-KB, complement activation, and IFNA and IFNG responses (Figure 2B). An overview of all significantly altered Hallmark gene sets is provided in Supplementary Figure 1B.

To further investigate the attributes of these inflammatory and immune responses after ID LPS injection, GSEA was performed. A significant positive enrichment of various biologically related subsets of pathways involved in innate immunity peaking at 3-9H post-injection as compared to baseline was observed. Specifically, the activation of innate immune response, leukocyte degranulation, and multiple related pathways, including leukocyte chemotaxis, inflammasome and complement, were enriched post-ID LPS injection (Figure 3A). Furthermore, receptor signalling pathways appeared to be dominant drivers of the inflammatory response. Significant positively enriched gene sets included cytokine- and TLR-signalling starting from 3H post-LPS, as well as JAK-STAT, Fc receptor, and T cell signalling at the later time points (Figure 3B).

CHARACTERISATION OF THE TLR4-DRIVEN INFLAMMATORY RESPONSE AFTER ID LPS INJECTION

TLR4 signalling was studied in further detail since LPS is a TLR4 agonist, as supported by the observed enrichment of innate immune and receptor signalling pathways. Similarly to GSEA, GSVA demonstrated positive enrichment of the TLR4 signalling pathway, including both the MYD88-dependent and the MYD88-independent cascades. This specific transcriptomic response peaked at 6-9H after LPS injection (Figure 4A). The individual genes within the TLR4 signalling pathway that showed significantly increased expression included TLR4, TICAM2, IRAK1 and -4, and downstream effector cytokines such as IL8, IL12B, and IL6 at 3-9H after LPS injection. The expression of several MAPK family members (MAPK10/12/13, MAP2K6) was decreased as compared to baseline (Figure 4B). A network visualisation of the expression of the MYD88-dependent and -independent genes downstream of TLR4 is depicted in Supplementary Figure 2.

Proteomic profile

ID LPS INJECTION INDUCED INFLAMMATION WITH A WELL-DEFINED TEMPORAL PATTERN DRIVEN BY CYTOKINES AND CHEMOKINES

Proteomic analysis was performed on samples from ID LPS injected participants to functionally contextualise the transcriptomic changes induced by ID LPS. PCA on proteins quantified by Olink Inflammation I and II panels revealed four distinct clusters of samples corresponding to the four time points at which the samples were taken: baseline, 0.5H, 4H and 9H after LPS injection. The presence of these clusters indicated LPS-driven proteomic changes occurring in distinct phases over time and confirmed the inflammatory response observed in the transcriptomic data. The PCA loading vectors indicated that cytokines and chemokines are key drivers of the variance associated with the LPS response. Specifically CXCL10, CCL7 and IFNγ contribute most to the separation of samples along PC1 and IL8, TNF, CCL3, and CCL4 primarily drive the separation along PC2 (Figure 5). These proteins also displayed statistically significant increased expression as compared to baseline (data on file).

ID LPS INJECTION INCREASED THE EXPRESSION OF PROTEINS IN THE TLR4 SIGNALLING PATHWAY

Given the importance of TLR4 signalling in the LPS-induced inflammatory response, TLR4-related protein expression over time was subsequently analysed. The expression of proteins downstream of TLR4 indicated that the injection of LPS induced an overall increase in the expression of these proteins, which peaked at 4-9H after injection (Figure 6A). This pattern was supported by statistically significant changes in the expression of these proteins at 4-9H compared to baseline. Specifically, signalling mediators IRAK1 and -4, NFKB1 and JUN display an increased expression after LPS injection, while MAPK13 decreases. All cytokines and chemokines displayed increasing patterns over time after ID LPS injection, with IL8 peaking as early as 0.5H after ID LPS, TNF and CCL4 at 4H, and all other cytokines and chemokines peaking at 9H after injection (Figure 6B). Furthermore, an increasing pattern peaking at 9H after LPS was observed for costimulatory molecules CD40, CD80 and CD86 present on antigen presenting cells (Figure 6A, 6B).

Translational relevance

To assess the translational relevance of the presented transcriptomic and proteomic insights, we studied the patterns of effector cells involved in the ID LPS response based on CIBERSORTx and investigated the overlap of the observed transcriptomic response with available disease gene sets from the Disease Ontology database.

INFLUX OF INFLAMMATORY CELLS AFTER ID LPS INJECTION

Deconvolution of the bulk RNA sequencing dataset using CIBERSORTx revealed a rapid increase in immune cell absolute scores starting at 1H after ID LPS injection and peaking at 9H, indicating increased immune cell infiltration in the skin of study participants (Figure 7A). Specifically, statistically significant rises in neutrophils and activated mast cells were observed at 1-3H after ID LPS, followed by increases in monocytes, activated dendritic cells, M1 macrophages and activated NK cells at 6-9H. At the latest time point (24H), the populations of these innate immune cells declined, while adaptive immune cell subsets, such as resting CD4 memory and CD8 T cells increased. Simultaneously, the mast cells of a resting phenotype and M2 macrophages appear (Figure 7B). Activated CD4 memory T cells and resting NK cells displayed an increasing trend at 6-9H and 24H, respectively, but their low overall mean absolute scores were low (Figure 7A, Supplementary Figure 3A). Supplementary Figure 3B presents all 22 detected cell types and Supplementary Figure 3C complements the post-hoc tested cell types presented in Figure 7B.

OVERLAP OF THE ID LPS RESPONSE WITH TRANSCRIPTOMIC DISEASE SIGNATURES

Finally, we assessed the overlap between the ID LPS transcriptomic response and disease-associated gene sets. Figure 8 displays the top 30 significantly positively enriched disease sets for the 9H vs. baseline comparison based on DOSE analysis of the ID LPS transcriptomic dataset. The full list of significantly positively enriched diseases at 9H vs. baseline is available in Supplementary Table 4. The two major clusters of diseases that overlap with the ID LPS transcriptomic response are viral diseases and autoimmune diseases. These include gene sets related to diseases such as COVID-19, rheumatoid arthritis, systemic lupus erythematosus, and psoriasis. This highlights the potential of the ID LPS model to induce mechanisms that translate to those observed in disease pathophysiology, increasing its translational value.

DISCUSSION

The ID LPS model is a human inflammatory challenge model used to assess proof-of-pharmacology in early-phase clinical trials. While previous studies have characterised its clinical, cellular, and cytokine responses, this manuscript provides the first comprehensive transcriptomic and proteomic characterisation of the human response to ID LPS injection, including the translational relevance.[9,15] ID LPS injection induced a transcriptomic inflammatory response characterised by significant enrichment of innate immunity- and receptor signalling-related pathways, including TLR4 signalling

and its downstream genes. This transcriptomic profile translated to increased expression of inflammatory proteins downstream of TLR4. Furthermore, the transcriptomic responses showed overlap with gene sets specific to inflammatory diseases, highlighting the translational relevance of the model.

Our omics data demonstrated consistent patterns compared to previously reported data from ID LPS studies regarding clinical, cellular, and cytokine levels.[9,15] The clinical study of Buters et al. described time-dependent changes after ID LPS. They reported classical clinical hallmarks of inflammation, including redness and increased skin temperature, at 3-24H after ID LPS. This was accompanied by an early influx of innate immune cells (3-10H), followed by adaptive immune cells (24-48H). Cytokine release (IL-6, IL-8, IL-1β, and TNF) peaking at 3-6H post-LPS was shown to also contribute to the inflammatory response.[9]

The clustering of both our transcriptomic and proteomic data demonstrated clear time-dependent LPS-induced patterns. Proteomic variation along the first two principal components was primarily driven by cytokines and chemokines, with TNF and IL-8 contributing to the variance associated with the early response to ID LPS and CXCL10 and IFNγ driving the variance associated with the later inflammatory response. Moreover, our transcriptomic data mirrored the cellular and cytokine observations from Buters et al., with increased gene expression of IL6, IL8, IL1B, and TNF starting at 1H post-LPS, peaking around 3H, and returning toward baseline thereafter. Novel insights acquired from the present study are strong activation of complement and inflammasome pathways and, when looking at individual genes, several MAPKs. Since these are all described as relevant druggable targets in autoimmune disease, our findings warrant future exploration of those specific biological processes in the context of the LPS response in order to potentially expand the applicability of the ID LPS model.[16–18]

Deconvolutional analysis by CIBERSORTx revealed similar cellular recruitment patterns as reported by Buters et al.,[9,15] with an early influx of neutrophils and monocytes after ID LPS, followed by cytotoxic T cells. CIBERSORTx analysis adds to this knowledge by indicating the functional state of specific cell types and thereby describing the inflammatory response at a more detailed level. For example, the scores of activated dendritic, mast, and NK cells increase between 3-9H post LPS injection and return to a resting state thereafter. In addition, M2 macrophages, contributing to inflammation resolution and tissue repair, appear at 24H after LPS. Lastly, proteomic analyses also aligned with the transcriptomic and prior observations with IL-6, IL-8, and TNF activation after ID LPS injection. Adding to the body of evidence, we identified 16 significantly upregulated proteins downstream of TLR4, including MAPKs, CXCLs, JUN, and IRAK1. These findings further broaden the options for targeted application of the ID LPS model in early-phase clinical studies, as these are all implicated as targets for pharmaceutical immunomodulation.[18–23]

A key strength of the presented work is the joint analysis of transcriptomic and proteomic datasets capturing the acute inflammatory response to ID LPS. The proteomic data confirm the transcriptomic findings and provide the first proteomic-level overview of the physiological inflammatory response to ID LPS. The concordance between transcriptomic and proteomic data strengthens the translational relevance of the ID LPS model for early-phase clinical research. Moreover, this framework, which enables assessment of temporal dynamics and relationships between transcriptomic pathways, cellular responses, and proteomic changes, supports future systems biology approaches for anti-inflammatory and immunomodulatory drug development.[24]

Furthermore, the results of our gene set enrichment analysis on Disease Ontology gene sets expands our understanding of the translational relevance and broader potential applicability of the ID LPS model. We observed an overlap between LPS-induced transcriptomic changes and the gene signatures of inflammatory diseases, including autoimmune diseases such as rheumatoid arthritis and systemic lupus erythematosus. This overlap provides a range of target diseases of drug candidates for which the ID LPS model might be of value in early-phase clinical pharmacological research. Future omics profiling of other experimental human inflammatory models, such as UVB-induced inflammation, or KLH immunisation, could further broaden the available toolbox for translational pharmacological research.[25,26]

Limitations

Several limitations should be taken into consideration when interpreting the data presented in this manuscript. Firstly, the transcriptomic data were generated from the upper back skin biopsies, while the proteomic data were obtained from blister fluid collected from the lower forearms. It is known that there are regional differences in the immunological activity of the skin, with the back having thicker skin, higher cell counts and more adaptive immunity-related cells than the arms,[27] which may contribute to differences between the datasets. However, skin punch biopsies and blister fluid sampling induce only low inflammatory responses and are therefore considered reliable measures to study skin under homeostatic conditions,[28-30] which is underlined by the baseline data presented by Buters et al.,[9] and in our manuscript. Furthermore, the transcriptomic response translates into proteomic changes, indicating that, even though there might be differences in the absolute increases in immune activity between back and forearms, there is no difference in functionality of the immune response.

Secondly, while bulk RNA sequencing and proteomics provide a comprehensive dataset, it inherently does not enable us to directly distinguish which cells, or other factors, contribute to the observed responses and whether they are resident or infiltrating cells. It could therefore be argued that an increased expression of genes or proteins and enrichment of biological pathways is driven by an influx of cells as opposed to gene or protein upregulation or pathway activation. Single-cell approaches could be adopted in the future to provide such insights.[31,32] Furthermore, an expansion of the dataset with metabolomics data from future ID LPS challenge studies would contribute to the application of the ID LPS knowledge base in systems biology.[33]

Thirdly, within this manuscript, we present the first omics-based characterisation of the ID LPS model providing a comprehensive overview of the inflammatory response. Future research could build on this overview by further studying specific genes, pathways and proteins in greater detail. For example, in the transcriptomic analyses of genes downstream of TLR4, we observed decreases in MAPK gene expression as compared to baseline. This could suggest upregulation of resolution and repair processes driven by these MAPKs. These findings argue for additional investigations, including multimodal clinical, cellular and proteomic assessments, into the specific role of MAPKs in the inflammatory response to ID LPS.

CONCLUSION

In conclusion, this manuscript provides a comprehensive transcriptomic and proteomic characterisation of the human inflammatory ID LPS response, offering in-depth insights into the physiology of TLR4-driven inflammation. The strong overlap between transcriptomic and proteomic profiles supports the functional translatability of the model, while the overlap with mechanisms of human inflammatory diseases underscores its broader translational relevance. This dataset can serve as a reference framework to guide challenge model selection in early-phase clinical pharmacology research, enabling MoA-based evaluation of immunomodulatory drug candidates and the design of informative clinical trials. Future integration of these data into systems biology approaches may further accelerate the rational development of anti-inflammatory therapies and improve the translational value of early-phase clinical studies.

FIGURE 1 **Overview of study designs.** (A) Study A: LPS, a TLR4 agonist, was intradermally injected into the skin at five treatment sites on the back of healthy participants. At specified time intervals (pre-LPS injection and at 1H, 3H, 6H, 9H and 24H post-LPS injection) 3-mm biopsy samples were obtained from the LPS challenged regions as well as from the untreated control region, resulting in a total of 6 biopsies per volunteer. (B) Study B: LPS was intradermally injected into the skin at three treatment sites on the lower forearms of healthy participants and one area served as untreated control. At four specified time intervals (pre-LPS injection and at 0.5H, 4H, and 9H post-LPS injection) suction blisters were induced on the designated areas on the forearm. (C) Sample analysis – bulk RNA sequencing was performed on the skin punch biopsy samples. Protein profiling using the Olink platform was conducted on the interstitial fluid obtained from the suction blisters.

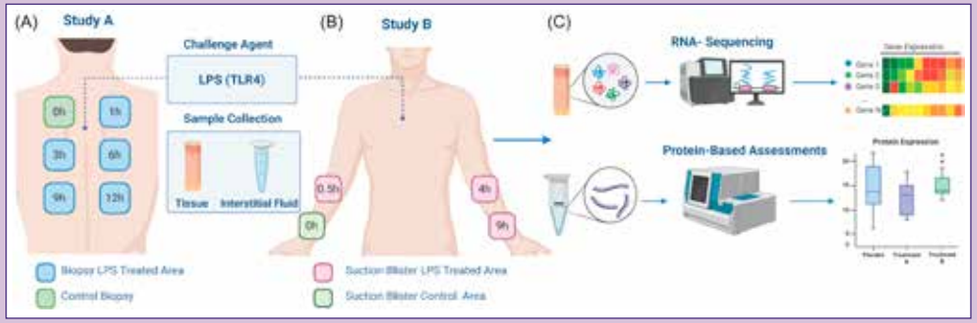

Abbreviations: LPS, lipopolysaccharide; TLR4, Toll-like receptor 4.

FIGURE 2 **Transcriptomic clustering and pathway enrichment characterising the time course of the human response to the ID LPS challenge.** (A) PCA plot of the RNA sequencing dataset (N = 36 samples) visualising global transcriptomic variation over time following ID LPS injection. Samples are coloured by time point at which they were taken. (B) Heatmap showing enrichment scores for a selection of Hallmark gene sets17 significantly altered at 9H after ID LPS injection compared to baseline. The colour gradient (dark blue to red) represents per sample GSVA scores for each of the selected gene sets.

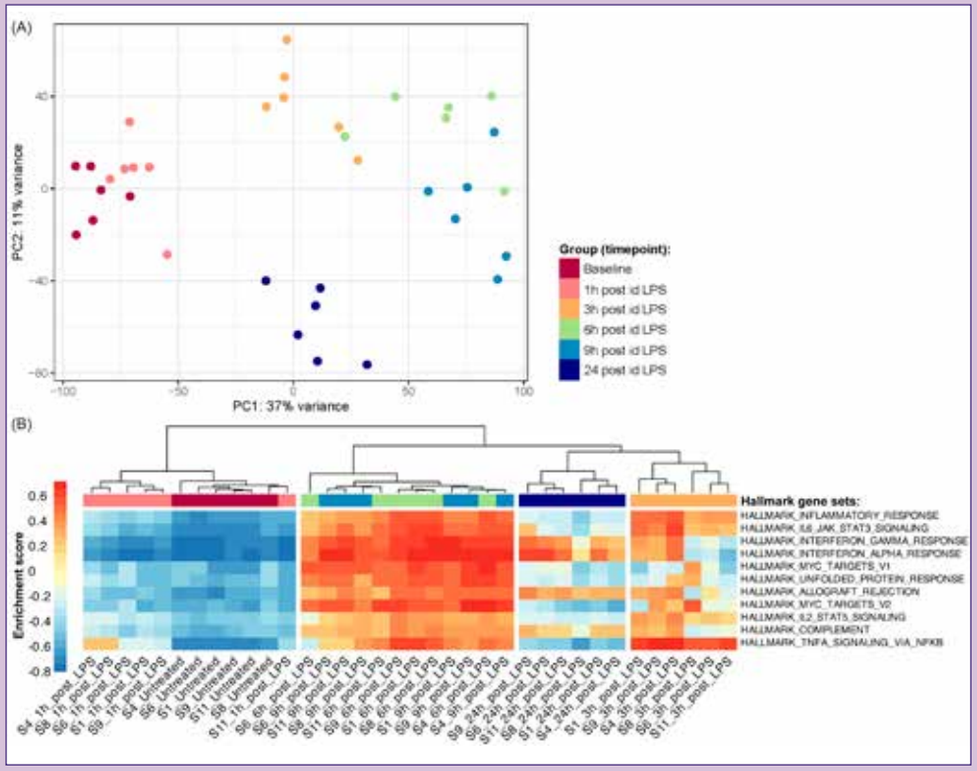

Abbreviations: GSVA, gene set variation analysis; ID LPS, intradermal lipopolysaccharide; PCA, principal components analysis; PC1, first principal component; PC2, second principal component.

FIGURE 3 **Positive enrichment of pathways related to innate immunity and receptor signalling driven by ID LPS injection.** (A) Bar plots displaying GSEA normalized enrichment scores (NES) for 23 selected significantly enriched pathways related to the innate immune response. The bar plots show NES for comparisons of samples taken at multiple time points following ID LPS injection versus the baseline samples. The colour gradient (yellow to purple) represents the -log10 of the adjusted *p*-value, reflecting the significance of the enrichment. The bar length depicts the NES for each gene set. (B) Bar plots displaying GSEA NES for 36 selected significantly enriched pathways related to receptor signalling. The bar plots show NES for comparisons of samples taken at multiple time points following id LPS injection versus the baseline samples. The colour gradient (yellow to purple) represents the -$\log_{10}$ of the adjusted *p*-value, reflecting the significance of the enrichment. The bar length depicts the NES for each gene set.

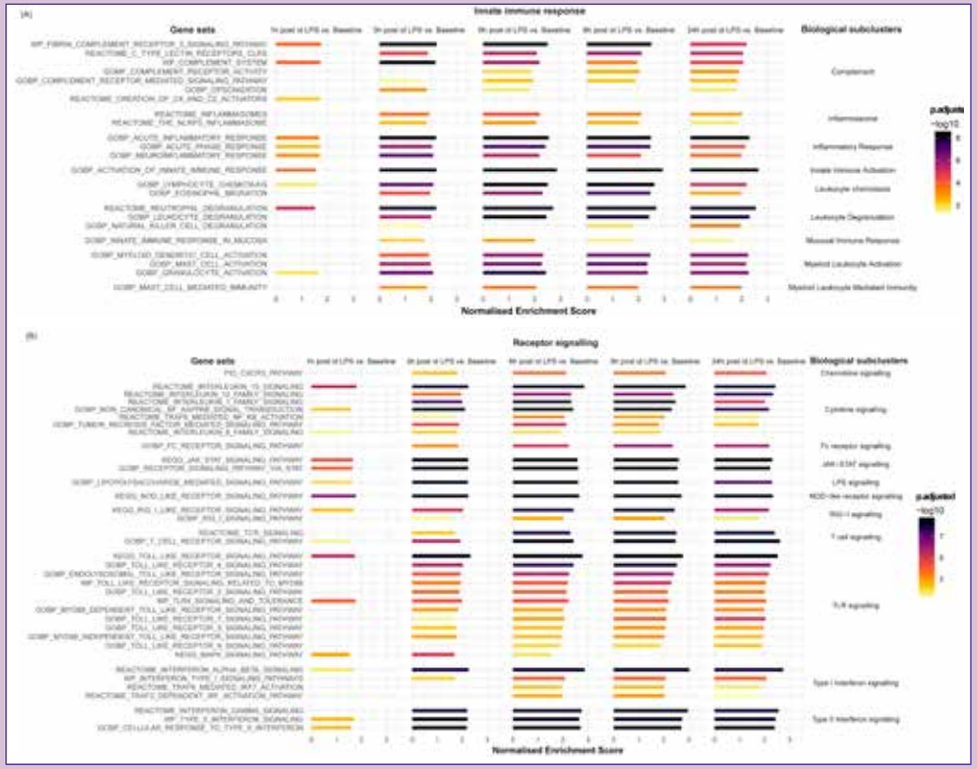

Abbreviations: GSEA, gene set enrichment analysis; id LPS, intradermal lipopolysaccharide; NES, normalised enrichment score; P.ADJUSTED, adjusted p-value.

FIGURE 4 **TLR4-signalling after ID LPS injection.** (A) Boxplots of GSVA single-sample pathway enrichment scores for the TLR4 signalling pathway and its downstream MYD88-independent and -dependent signalling pathways derived from the GOBP database (GO:0034143, GO:0002756, GO:0002755). (B) Heatmaps illustrating the expression of individual differentially expressed genes (9H vs baseline) from the TLR4-driven MYD88-independent and -dependent gene sets derived from the KEGG TLR signalling pathway (hsa04620). The presented genes were significantly altered at 9H after ID LPS injection compared to baseline. The colour gradient (black to red) represents the z-scored expression of each gene from low to high.

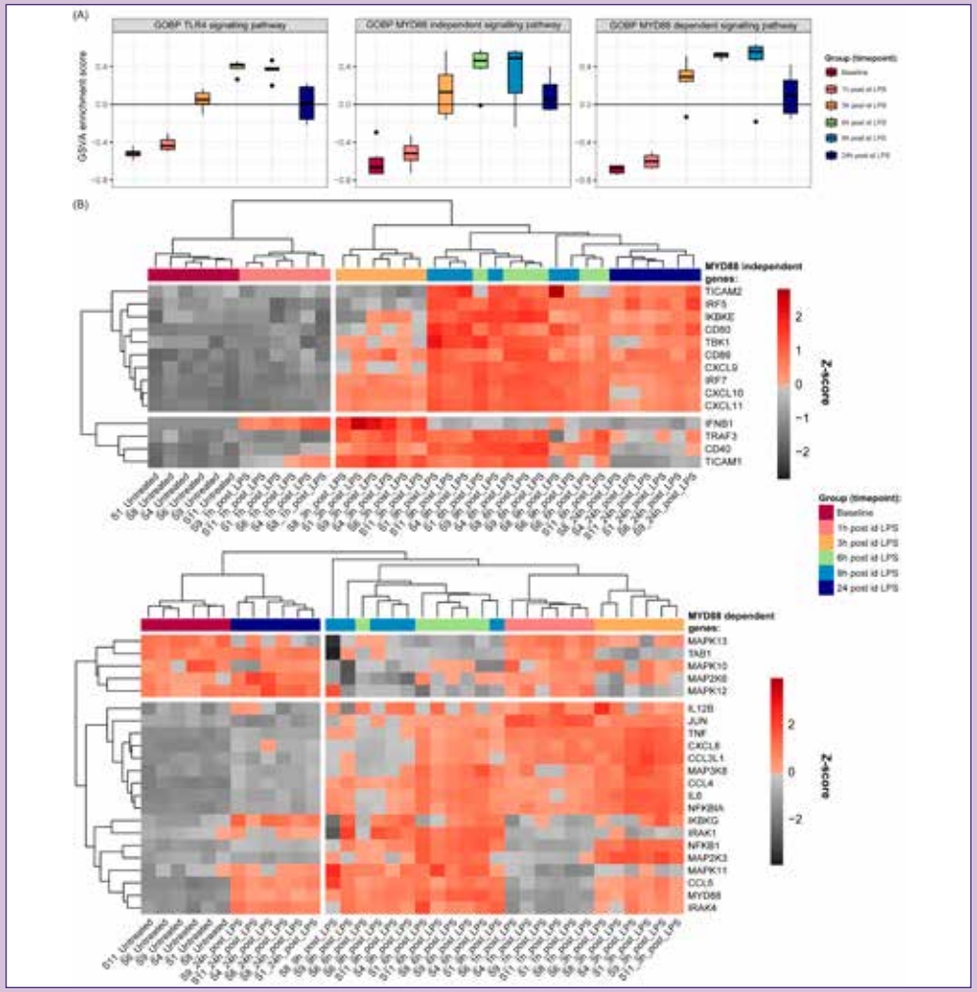

Abbreviations: GSVA, gene set variation analysis; GOBP, Gene Ontology Biological Process; ID LPS, intradermal lipopolysaccharide; KEGG, Kyoto Encyclopedia of Genes and Genomes; MYD88, myeloid differentiation primary response 88; P.ADJUSTED, adjusted p-value; TLR4, Toll-like receptor 4.

FIGURE 5 Proteomic clustering characterising the time course of the human response to the ID LPS challenge. Sample clustering visualised by a PCA plot of the Olink dataset based on proteins measured by the Inflammation I and II panels, excluding panel specific outliers (N = 29 samples). The arrows indicate the top four loading vectors for each principal component, representing proteins contributing most to sample separation.

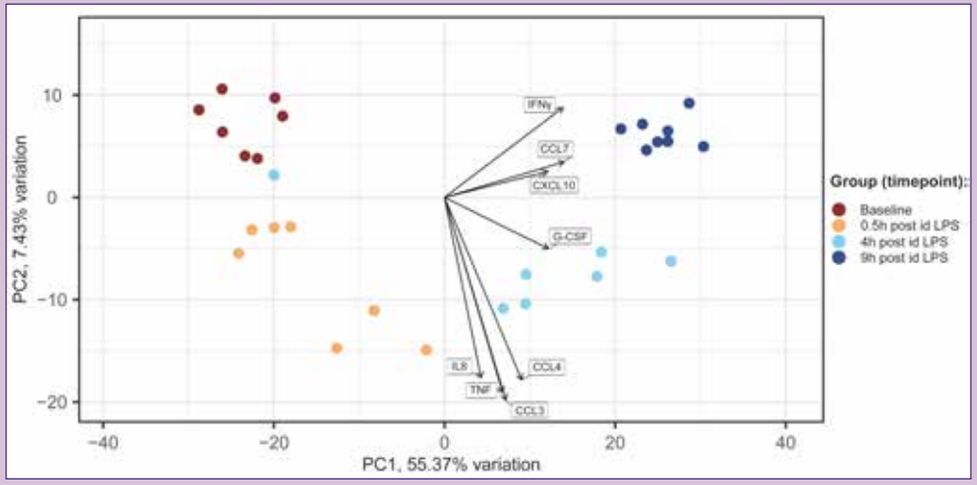

Abbreviations: ID LPS, intradermal lipopolysaccharide; PCA, principal components analysis; PC1, first principal component; PC2, second principal component.

FIGURE 6 Changes in expression of TLR4 signalling cascade proteins after ID LPS injection. (A) Heatmaps showing the expression of MYD88-dependent and MYD88-independent proteins downstream of TLR4 measured using the Olink platform for the comparison of samples at 9H post-ID LPS injection to baseline. The colour gradient (blue to red) represents the per sample normalised protein expression (NPX) for each of the proteins ranging from low to high, with missing values from panel-specific outliers marked black. (B) Boxplots showing the NPX scores of individual proteins corresponding to the MYD88-dependent and -independent subset from the KEGG TLR signalling pathway (hsa04620). The statistical significance of changes in protein expression across different groups (baseline, 0.5H, 4H, and 9H after ID LPS injection) is indicated by asterisks.

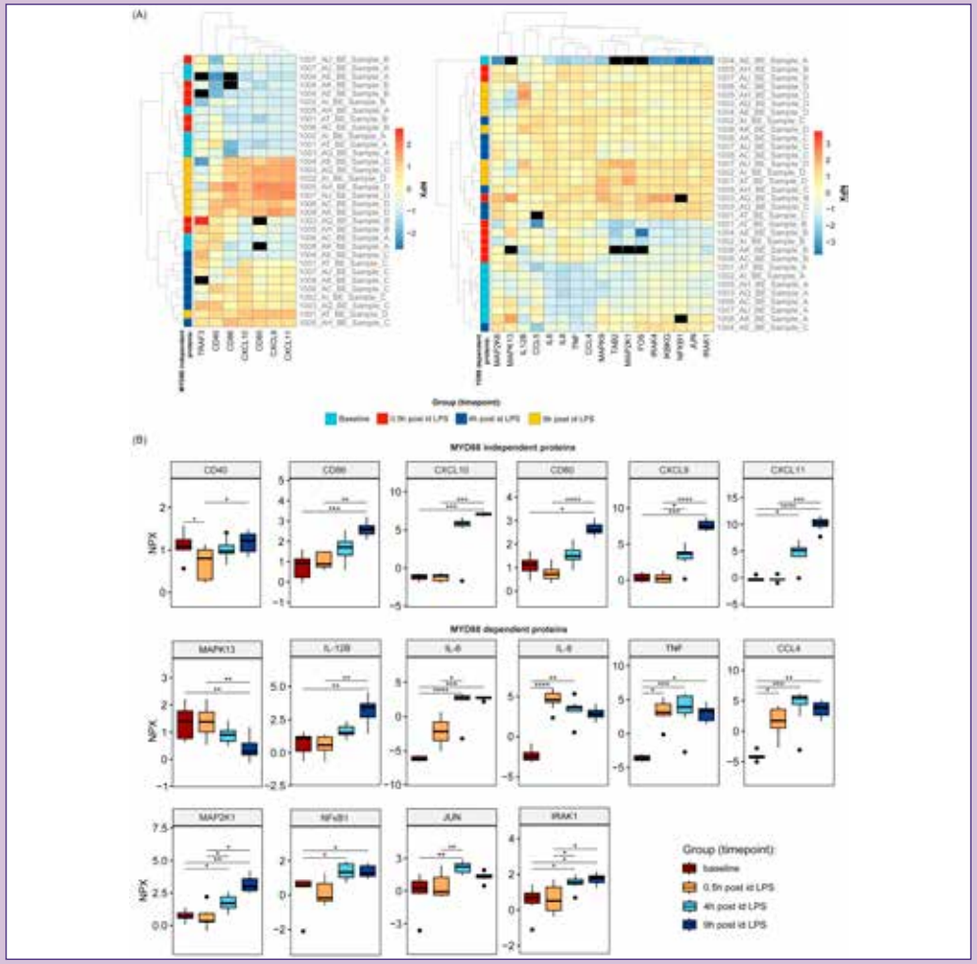

Abbreviations: ID LPS, intradermal lipopolysaccharide; KEGG, Kyoto Encyclopedia of Genes and Genomes; MYD88, myeloid differentiation primary response 88; NPX, normalised protein expression; TLR4, Toll-like receptor 4.

FIGURE 7 **Immune cell infiltration patterns after ID LPS.** (A) Stacked barplot displaying the absolute scores for 22 types of immune cells quantified by CIBERSORTX across all baseline and post-ID LPS samples (N = 36). The bars are sorted by time point and each bar represents a single sample. Colours refer to the individual cell types. (B) Boxplots displaying the changes in relevant immune cells over time after ID LPS injection. Each boxplot represents the median, interquartile range, and 1.5*IQR (whiskers) for each cell type. Asterisks indicate levels of statistical significance for changes between individual time points and baseline. *P.ADJUSTED < 0.05, **P.ADJUSTED < 0.01, ***P.ADJUSTED < 0.001, ****P.ADJUSTED < 0.0001.

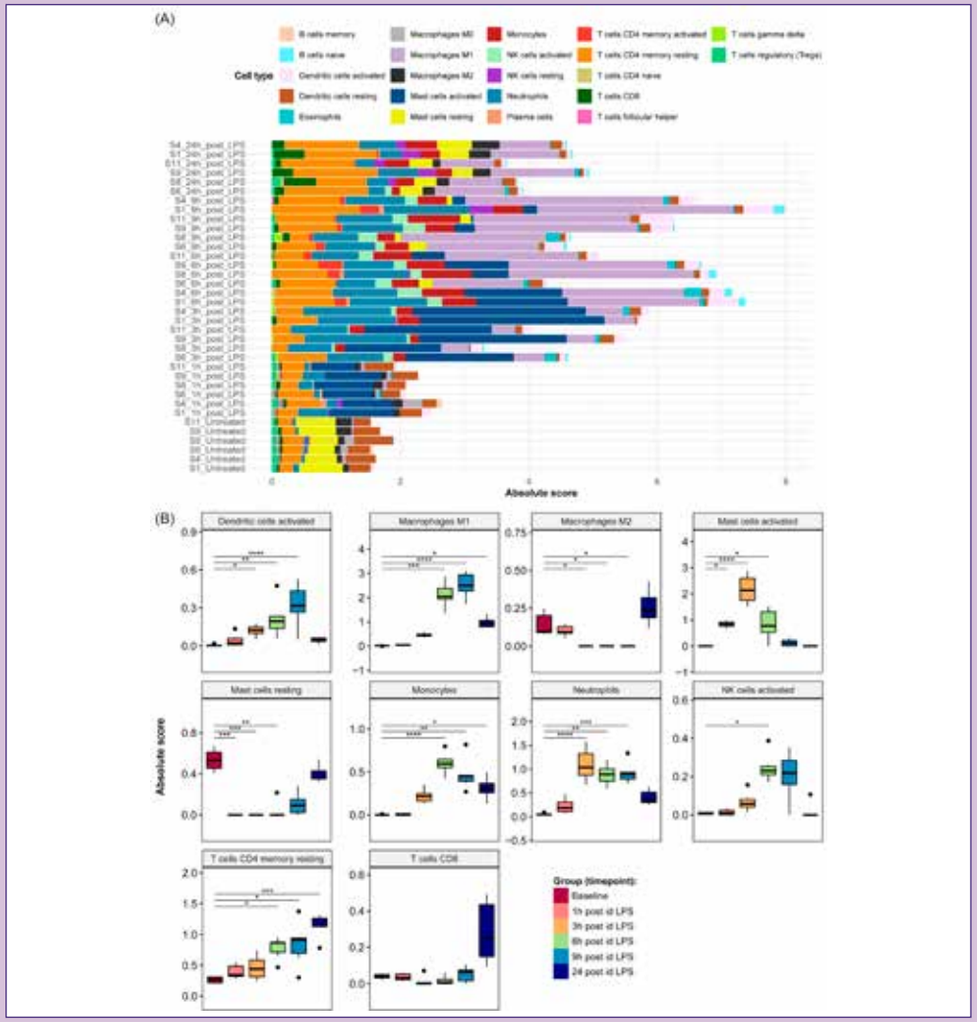

Abbreviations: ID LPS, intradermal LPS; IQR, interquartile range; P.ADJUSTED, adjusted p-value.

FIGURE 8 **Overlap between the transcriptomic response induced by the id LPS model and disease-related gene sets.** Network plot showing the top 30 significantly positively enriched disease sets from the Disease Ontology (DO) database derived using Disease Ontology Semantic and Enrichment analysis (DOSE) for the comparison of samples at 9h post-id LPS injection to baseline. Node sizes indicate the number of core enrichment genes for each gene set, nodes are coloured by NES.

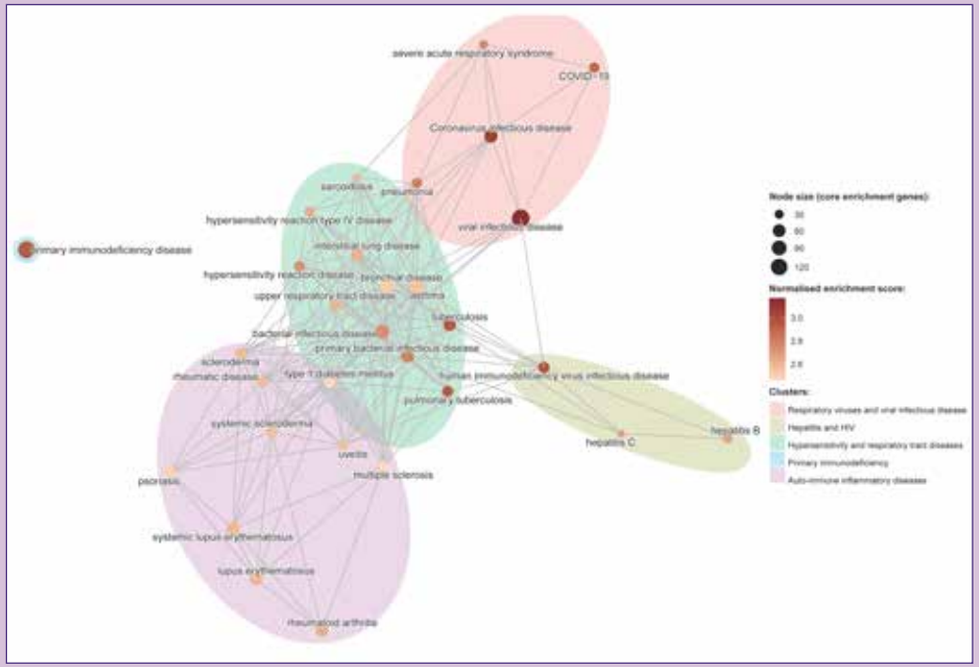

Abbreviations: DO, Disease Ontology; DOSE, Disease Ontology Semantic and Enrichment; id LPS, intradermal lipopolysaccharide; NES, normalised enrichment score.

SUPPLEMENTARY TABLE 1 **Overview of samples analysed using Olink that failed the quality control (QC).**

SampleID	Participant number	Time point	Olink panel	Reason QC failed
CHDR2367A_1001_B	1001	0.5h post id LPS	Neurology II	Out of acceptance criteria for the incubation control for Block B (-0.51)
CHDR2367A_1001_C	1001	4h post id LPS	Cardiometabolic I	Out of acceptance criteria for the amplification control for Block A (-0.57)
CHDR2367A_1003_B	1003	0.5h post id LPS	Cardiometabolic II	Out of acceptance criteria for the incubation control for Block B (0.59)
CHDR2367A_1004_A	1004	Baseline	Oncology II Inflammation II Neurology II	Out of acceptance criteria for the incubation control for Block B (0,61) and C (0.62) Out of acceptance criteria for the incubation control for Block C (0,51) Out of acceptance criteria for the incubation control for Block B (0,88), C (0.7), and D (0.68)
CHDR2367A_1004_B	1004	0.5h post id LPS	Inflammation II	Out of acceptance criteria for the incubation control for Block C (0,57) and out of acceptance criteria for the amplification control for Block C (0,55)
CHDR2367A_1006_D	1006	9h post id LPS	Oncology I	Out of acceptance criteria for the incubation control for Block D (-0,51)
CHDR2367A_1004_A	1008	Baseline	Cardiometabolic II	Out of acceptance criteria for the amplification control for Block B (-0,52)
CHDR2367A_1008_B	1008	0.5h post id LPS	Oncology II	Out of acceptance criteria for the amplification control for Block A (-0,56)
CHDR2367A_1004_C	1008	4h post id LPS	Inflammation II	Out of acceptance criteria for the amplification control for Block A (-0,59) and out of acceptance criteria for the incubation control for Block C (0.6)

SUPPLEMENTARY TABLE 2 **Overview of samples analysed using RNA sequencing.**

SampleID	Sample name	Participant number	Group	Time point
105982-001-001	S1_Untreated	1	Untreated	Baseline
105982-001-007	S4_Untreated	4	Untreated	Baseline
105982-001-013	S6_Untreated	6	Untreated	Baseline
105982-001-019	S8_Untreated	8	Untreated	Baseline
105982-001-025	S9_Untreated	9	Untreated	Baseline
105982-001-031	S11_Untreated	11	Untreated	Baseline
105982-001-002	S1_1h_post_LPS	1	1h_post_LPS	1h post id LPS
105982-001-008	S4_1h_post_LPS	4	1h_post_LPS	1h post id LPS
105982-001-014	S6_1h_post_LPS	6	1h_post_LPS	1h post id LPS
105982-001-020	S8_1h_post_LPS	8	1h_post_LPS	1h post id LPS
105982-001-026	S9_1h_post_LPS	9	1h_post_LPS	1h post id LPS
105982-001-032	S11_1h_post_LPS	11	1h_post_LPS	1h post id LPS
105982-001-037	S1_3h_post_LPS	1	3h_post_LPS	3h post id LPS
105982-001-040	S4_3h_post_LPS	4	3h_post_LPS	3h post id LPS
105982-001-015	S6_3h_post_LPS	6	3h_post_LPS	3h post id LPS
105982-001-021	S8_3h_post_LPS	8	3h_post_LPS	3h post id LPS
105982-001-027	S9_3h_post_LPS	9	3h_post_LPS	3h post id LPS
105982-001-033	S11_3h_post_LPS	11	3h_post_LPS	3h post id LPS
105982-001-004	S1_6h_post_LPS	1	6h_post_LPS	6h post id LPS
105982-001-010	S4_6h_post_LPS	4	6h_post_LPS	6h post id LPS
105982-001-016	S6_6h_post_LPS	6	6h_post_LPS	6h post id LPS
105982-001-022	S8_6h_post_LPS	8	6h_post_LPS	6h post id LPS
105982-001-028	S9_6h_post_LPS	9	6h_post_LPS	6h post id LPS
105982-001-034	S11_6h_post_LPS	11	6h_post_LPS	6h post id LPS
105982-001-038	S1_9h_post_LPS	1	9h_post_LPS	9h post id LPS
105982-001-041	S4_9h_post_LPS	4	9h_post_LPS	9h post id LPS
105982-001-017	S6_9h_post_LPS	6	9h_post_LPS	9h post id LPS
105982-001-023	S8_9h_post_LPS	8	9h_post_LPS	9h post id LPS
105982-001-029	S9_9h_post_LPS	9	9h_post_LPS	9h post id LPS
105982-001-035	S11_9h_post_LPS	11	9h_post_LPS	9h post id LPS
105982-001-039	S1_24h_post_LPS	1	24h_post_LPS	24h post id LPS
105982-001-042	S4_24h_post_LPS	4	24h_post_LPS	24h post id LPS
105982-001-018	S6_24h_post_LPS	6	24h_post_LPS	24h post id LPS
105982-001-024	S8_24h_post_LPS	8	24h_post_LPS	24h post id LPS
105982-001-030	S9_24h_post_LPS	9	24h_post_LPS	24h post id LPS
105982-001-036	S11_24h_post_LPS	11	24h_post_LPS	24h post id LPS

SUPPLEMENTARY TABLE 3 Overview of samples analysed using Olink.

SampleID	Sample name (NPX ID)	Participant number	Group	Time point
CHDR2367A_1001_A	S1001_AT_BE_SAMPLE_A	1001	A	Baseline
CHDR2367A_1002_A	S1002_AI_BE_SAMPLE_A	1002	A	Baseline
CHDR2367A_1003_A	S1003_AQ_BE_SAMPLE_A	1003	A	Baseline
CHDR2367A_1004_A	S1004_AE_BE_SAMPLE_A	1004	A	Baseline
CHDR2367A_1005_A	S1005_AH_BE_SAMPLE_A	1005	A	Baseline
CHDR2367A_1006_A	S1006_AC_BE_SAMPLE_A	1006	A	Baseline
CHDR2367A_1007_A	S1007_AI_BE_SAMPLE_A	1007	A	Baseline
CHDR2367A_1008_A	S1008_AK_BE_SAMPLE_A	1008	A	Baseline
CHDR2367A_1001_B	S1001_AT_BE_SAMPLE_B	1001	B	0.5h post id LPS
CHDR2367A_1002_B	S1002_AI_BE_SAMPLE_B	1002	B	0.5h post id LPS
CHDR2367A_1003_B	S1003_AQ_BE_SAMPLE_B	1003	B	0.5h post id LPS
CHDR2367A_1004_B	S1004_AE_BE_SAMPLE_B	1004	B	0.5h post id LPS
CHDR2367A_1005_B	S1005_AH_BE_SAMPLE_B	1005	B	0.5h post id LPS
CHDR2367A_1006_B	S1006_AC_BE_SAMPLE_B	1006	B	0.5h post id LPS
CHDR2367A_1007_B	S1007_AI_BE_SAMPLE_B	1007	B	0.5h post id LPS
CHDR2367A_1008_B	S1008_AK_BE_SAMPLE_B	1008	B	0.5h post id LPS
CHDR2367A_1001_C	S1001_AT_BE_SAMPLE_C	1001	C	4h post id LPS
CHDR2367A_1002_C	S1002_AI_BE_SAMPLE_C	1002	C	4h post id LPS
CHDR2367A_1003_C	S1003_AQ_BE_SAMPLE_C	1003	C	4h post id LPS
CHDR2367A_1004_C	S1004_AE_BE_SAMPLE_C	1004	C	4h post id LPS
CHDR2367A_1005_C	S1005_AH_BE_SAMPLE_C	1005	C	4h post id LPS
CHDR2367A_1006_C	S1006_AC_BE_SAMPLE_C	1006	C	4h post id LPS
CHDR2367A_1007_C	S1007_AI_BE_SAMPLE_C	1007	C	4h post id LPS
CHDR2367A_1008_C	S1008_AK_BE_SAMPLE_C	1008	C	4h post id LPS
CHDR2367A_1001_D	S1001_AT_BE_SAMPLE_D	1001	D	9h post id LPS
CHDR2367A_1002_D	S1002_AI_BE_SAMPLE_D	1002	D	9h post id LPS
CHDR2367A_1003_D	S1003_AQ_BE_SAMPLE_D	1003	D	9h post id LPS
CHDR2367A_1004_D	S1004_AE_BE_SAMPLE_D	1004	D	9h post id LPS
CHDR2367A_1005_D	S1005_AH_BE_SAMPLE_D	1005	D	9h post id LPS
CHDR2367A_1006_D	S1006_AC_BE_SAMPLE_D	1006	D	9h post id LPS
CHDR2367A_1007_D	S1007_AI_BE_SAMPLE_D	1007	D	9h post id LPS
CHDR2367A_1008_D	S1008_AK_BE_SAMPLE_D	1008	D	9h post id LPS

SUPPLEMENTARY TABLE 4 Overview of significantly positively enriched disease sets for the 9H vs. baseline comparison based on DOSE analysis.

Disease Ontology ID	Disease description	Gene set size	Normalised enrichment score	Adjusted p-value	qvalue
DOID:934	viral infectious disease	297	3.16661116	9.2821E-10	3.4818E-10
DOID:0080599	Coronavirus infectious disease	124	3.05428267	9.2821E-10	3.4818E-10
DOID:526	human immunodeficiency virus infectious disease	76	2.96871619	9.2821E-10	3.4818E-10
DOID:399	tuberculosis	92	2.95862614	9.2821E-10	3.4818E-10
DOID:2957	pulmonary tuberculosis	67	2.94763117	9.2821E-10	3.4818E-10
DOID:612	primary immunodeficiency disease	215	2.9427233	9.2821E-10	3.4818E-10
DOID:0080600	COVID-19	75	2.8926642	9.2821E-10	3.4818E-10
DOID:552	pneumonia	75	2.80273619	9.2821E-10	3.4818E-10
DOID:0050338	primary bacterial infectious disease	114	2.79301044	9.2821E-10	3.4818E-10
DOID:104	bacterial infectious disease	159	2.74135999	9.2821E-10	3.4818E-10
DOID:2945	severe acute respiratory syndrome	53	2.740682	9.2821E-10	3.4818E-10
DOID:0060056	hypersensitivity reaction disease	81	2.73290488	9.2821E-10	3.4818E-10
DOID:2043	hepatitis B	49	2.67760334	9.2821E-10	3.4818E-10
DOID:1883	hepatitis C	42	2.6751949	9.2821E-10	3.4818E-10
DOID:2916	hypersensitivity reaction type IV disease	68	2.63536594	9.2821E-10	3.4818E-10
DOID:7148	rheumatoid arthritis	126	2.63003828	9.2821E-10	3.4818E-10
DOID:3082	interstitial lung disease	146	2.62021969	9.2821E-10	3.4818E-10
DOID:8857	lupus erythematosus	126	2.59830859	9.2821E-10	3.4818E-10
DOID:974	upper respiratory tract disease	109	2.5934373	9.2821E-10	3.4818E-10
DOID:11335	sarcoidosis	56	2.59045277	9.2821E-10	3.4818E-10
DOID:9074	systemic lupus erythematosus	125	2.58205703	9.2821E-10	3.4818E-10
DOID:1575	rheumatic disease	93	2.57398353	9.2821E-10	3.4818E-10
DOID:419	scleroderma	93	2.57398353	9.2821E-10	3.4818E-10
DOID:13141	uveitis	62	2.56450203	9.2821E-10	3.4818E-10
DOID:418	systemic scleroderma	91	2.55857337	9.2821E-10	3.4818E-10
DOID:2841	asthma	246	2.53895484	9.2821E-10	3.4818E-10
DOID:1176	bronchial disease	250	2.51350306	9.2821E-10	3.4818E-10
DOID:8893	psoriasis	84	2.48355267	9.2821E-10	3.4818E-10
DOID:2377	multiple sclerosis	122	2.46556903	9.2821E-10	3.4818E-10
DOID:9744	type 1 diabetes mellitus	152	2.4598348	9.2821E-10	3.4818E-10
DOID:2825	nose disease	96	2.45946458	9.2821E-10	3.4818E-10
DOID:3083	chronic obstructive pulmonary disease	170	2.45028385	9.2821E-10	3.4818E-10
DOID:3342	bone inflammation disease	221	2.44880843	9.2821E-10	3.4818E-10
DOID:2320	obstructive lung disease	171	2.44585861	9.2821E-10	3.4818E-10
DOID:3213	demyelinating disease	133	2.44008995	9.2821E-10	3.4818E-10
DOID:848	arthritis	208	2.43014055	9.2821E-10	3.4818E-10

(Continuation table 4)

Disease Ontology ID	Disease description	Gene set size	Normalised enrichment score	Adjusted p-value	qvalue
DOID:10952	nephritis	206	2.2561795	9.2821E-10	3.4818E-10
DOID:0050589	inflammatory bowel disease	179	2.21761674	9.2821E-10	3.4818E-10
DOID:1240	leukemia	265	2.09583402	9.2821E-10	3.4818E-10
DOID:3042	allergic contact dermatitis	69	2.5398369	1.1463E-09	4.2999E-10
DOID:3388	periodontal disease	60	2.54689716	2.51E-09	9.4153E-10
DOID:2163	nasal cavity disease	86	2.40866907	2.5992E-09	9.7499E-10
DOID:0111962	combined immunodeficiency	56	2.54375331	2.9759E-09	1.1163E-09
DOID:2773	contact dermatitis	71	2.52040165	3.4657E-09	1.3E-09
DOID:3480	uveal disease	68	2.51381706	3.4883E-09	1.3085E-09
DOID:13406	pulmonary sarcoidosis	40	2.52321523	4.3836E-09	1.6443E-09
DOID:2921	glomerulonephritis	188	2.12963532	4.4074E-09	1.6533E-09
DOID:3770	pulmonary fibrosis	103	2.33768688	4.6738E-09	1.7532E-09
DOID:8692	myeloid leukemia	178	2.16180144	4.8538E-09	1.8207E-09
DOID:9500	leukocyte disease	52	2.48426748	7.0005E-09	2.6259E-09
DOID:0060058	lymphoma	102	2.30715529	8.2898E-09	3.1096E-09
DOID:4989	pancreatitis	83	2.3637283	1.3759E-08	5.1611E-09
DOID:4483	rhinitis	85	2.38792003	1.4237E-08	5.3405E-09
DOID:2789	parasitic protozoa infectious disease	80	2.37988816	1.6775E-08	6.2923E-09
DOID:1398	parasitic infectious disease	93	2.3717704	1.6775E-08	6.2923E-09
DOID:409	liver disease	237	2.00166948	1.8969E-08	7.1156E-09
DOID:0060060	non-Hodgkin lymphoma	90	2.3095508	3.5912E-08	1.3471E-08
DOID:1074	kidney failure	265	1.94705141	4.4599E-08	1.6729E-08
DOID:865	vasculitis	80	2.34634654	4.5652E-08	1.7125E-08
DOID:26	pancreas disease	85	2.3361791	5.1718E-08	1.94E-08
DOID:12894	Sjogren's syndrome	51	2.39396216	7.7713E-08	2.9151E-08
DOID:615	leukopenia	40	2.43076655	7.9797E-08	2.9932E-08
DOID:2218	blood platelet disease	67	2.38465393	7.9797E-08	2.9932E-08
DOID:3310	atopic dermatitis	60	2.40183125	8.7921E-08	3.298E-08
DOID:824	periodontitis	51	2.38514983	9.1721E-08	3.4405E-08
DOID:2723	dermatitis	100	2.25293073	1.246E-07	4.6739E-08
DOID:13241	Behcet's disease	59	2.38426752	1.2708E-07	4.7669E-08
DOID:9119	acute myeloid leukemia	135	2.11506778	1.2708E-07	4.7669E-08
DOID:4960	bone marrow cancer	156	2.09738434	1.2708E-07	4.7669E-08
DOID:1564	fungal infectious disease	73	2.32791256	1.5055E-07	5.6474E-08
DOID:5295	intestinal disease	252	1.89151714	2.8291E-07	1.0612E-07
DOID:4780	anti-basement membrane glomerulonephritis	44	2.40162735	3.8633E-07	1.4492E-07
DOID:9808	Goodpasture syndrome	44	2.40162735	3.8633E-07	1.4492E-07
DOID:1247	blood coagulation disease	104	2.16158561	5.3455E-07	2.0051E-07
DOID:0060180	colitis	106	2.10432737	9.1396E-07	3.4284E-07

(Continuation table 4)

Disease Ontology ID	Disease description	Gene set size	Normalised enrichment score	Adjusted p-value	qvalue
DOID:0050136	systemic mycosis	69	2.29505649	9.1986E-07	3.4505E-07
DOID:1037	lymphoid leukemia	126	2.12296626	9.4767E-07	3.5548E-07
DOID:403	mouth disease	121	2.11479358	1.0223E-06	3.8347E-07
DOID:783	end stage renal disease	133	2.04373809	1.0223E-06	3.8347E-07
DOID:0070004	myeloid neoplasm	122	2.0693986	1.6488E-06	6.1848E-07
DOID:3525	middle cerebral artery infarction	133	2.01564505	1.7723E-06	6.648E-07
DOID:1485	cystic fibrosis	76	2.2566086	1.8311E-06	6.8685E-07
DOID:0050339	commensal bacterial infectious disease	44	2.31236502	2.5822E-06	9.686E-07
DOID:8778	Crohn's disease	61	2.26468272	2.5902E-06	9.7162E-07
DOID:2986	IgA glomerulonephritis	46	2.29462552	4.03E-06	1.5117E-06
DOID:5082	liver cirrhosis	188	1.88458125	4.0526E-06	1.5202E-06
DOID:9952	acute lymphoblastic leukemia	116	2.02901807	4.7086E-06	1.7662E-06
DOID:784	chronic kidney disease	173	1.91511095	5.4668E-06	2.0507E-06
DOID:9675	pulmonary emphysema	44	2.27549098	5.6673E-06	2.1259E-06
DOID:11162	respiratory failure	57	2.25359562	5.7531E-06	2.158E-06
DOID:289	endometriosis	53	2.23033928	5.8634E-06	2.1994E-06
DOID:6432	pulmonary hypertension	176	1.88976729	5.9916E-06	2.2475E-06
DOID:12603	acute leukemia	117	2.0225072	1.0154E-05	3.8087E-06
DOID:2913	acute pancreatitis	44	2.24550105	1.047E-05	3.9273E-06
DOID:3407	carotid artery disease	53	2.19071571	1.2824E-05	4.8105E-06
DOID:633	myositis	56	2.19032564	2.2191E-05	8.3241E-06
DOID:9538	multiple myeloma	86	2.02549342	2.642E-05	9.9105E-06
DOID:0050908	myelodysplastic syndrome	56	2.16221278	3.6189E-05	1.3575E-05
DOID:707	B-cell lymphoma	51	2.11896462	3.7276E-05	1.3983E-05
DOID:3526	cerebral infarction	186	1.79556887	4.113E-05	1.5428E-05
DOID:5041	esophageal cancer	144	1.87935058	4.597E-05	1.7244E-05
DOID:224	transient cerebral ischemia	208	1.7799432	4.8081E-05	1.8036E-05
DOID:11394	adult respiratory distress syndrome	41	2.18127393	4.9385E-05	1.8525E-05
DOID:2473	opportunistic mycosis	61	2.12594748	5.192E-05	1.9476E-05
DOID:219	colon cancer	173	1.78576379	7.8957E-05	2.9618E-05
DOID:3454	brain infarction	224	1.65468477	0.00012075	4.5293E-05
DOID:3021	acute kidney failure	100	1.92321797	0.00013684	5.1332E-05
DOID:229	female reproductive system disease	175	1.74759107	0.00015094	5.662E-05
DOID:2349	arteriosclerosis	139	1.82567446	0.00015305	5.7412E-05
DOID:2237	hepatitis	40	2.06238656	0.00022589	8.4734E-05
DOID:2115	B cell deficiency	43	2.03316344	0.00031422	0.00011787
DOID:341	peripheral vascular disease	66	1.96669852	0.00040564	0.00015216
DOID:7693	abdominal aortic aneurysm	53	1.96181956	0.00042236	0.00015843
DOID:0060005	autoimmune disease of endocrine system	54	1.97695113	0.00048327	0.00018128
DOID:11054	urinary bladder cancer	168	1.64784645	0.00048327	0.00018128

SUPPLEMENTARY FIGURE 1 **Transcriptomic clustering and pathway enrichment characterising the time course of the human response to the ID LPS challenge.** (A) T-distributed stochastic neighbour embedding (T-SNE) plot of the RNA sequencing dataset (N = 36 samples) visualising global transcriptomic variation over time following ID LPS injection. The algorithm was applied to DESeq2 variance-stabilised (VST) counts of 2000 most variably expressed genes using the Rtsne package (v0.16). Samples are coloured by time point at which they were taken. (B) Heatmap showing enrichment scores for all Hallmark gene sets[34] significantly altered at 9H after ID LPS injection compared to baseline. The colour gradient (dark blue to red) represents per sample GSVA scores for each of the selected gene sets.

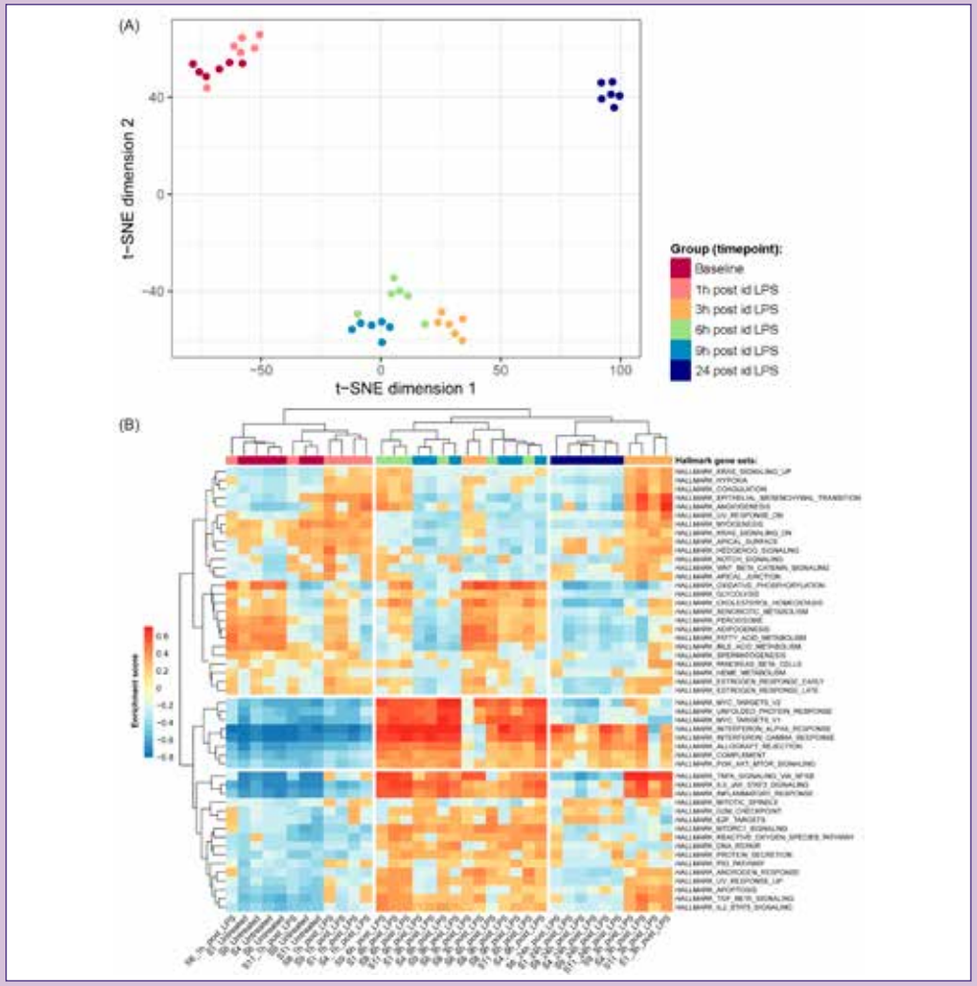

Abbreviations: GSVA, gene set variation analysis; ID LPS, intradermal lipopolysaccharide; T-SNE, t-distributed stochastic neighbour embedding; vst, variance-stabilised.

SUPPLEMENTARY FIGURE 2 **Cytoscape Network visualisation.** Network visualisation generated using Cytoscape,[35] depicting the MYD88-dependent and -independent cascades downstream of increased expression of genes in the TLR4-signalling pathway after id LPS injection as presented by WikiPathways pathway 'TLR-receptor signalling pathway (WP3858)'.[36] The nodes represent individual genes, with fill colours from white to red representing the $\log_2$-fold change in gene expression for 9H after ID LPS compared to baseline.

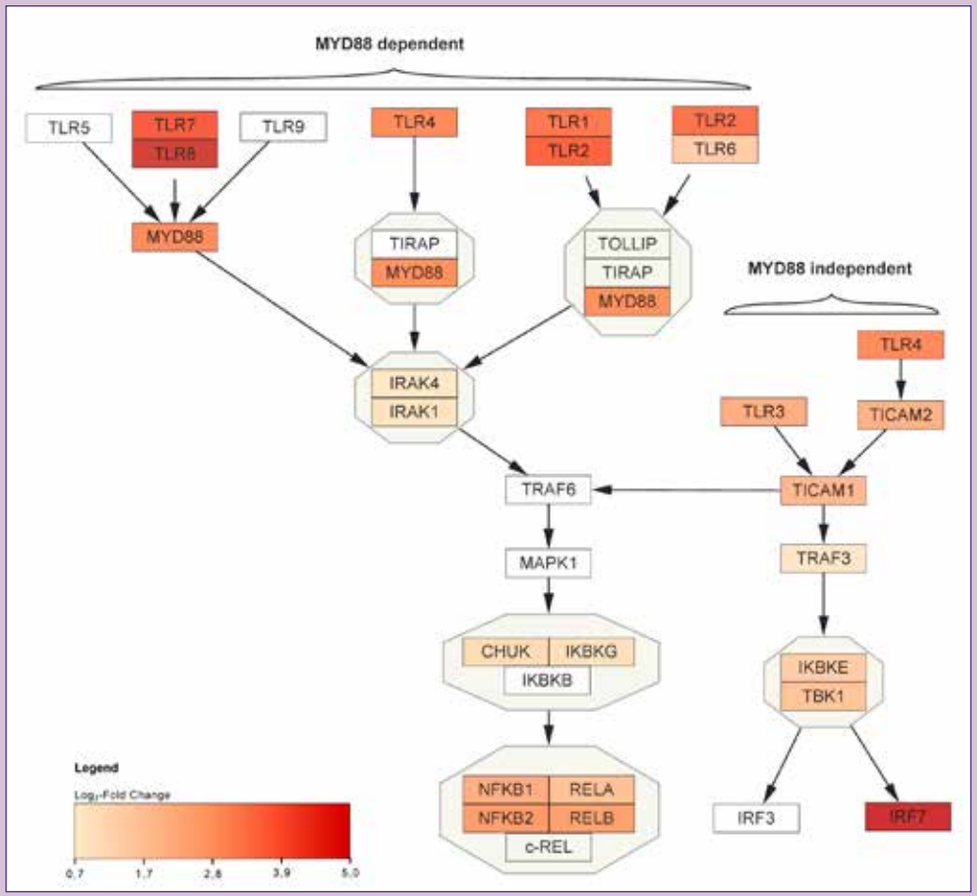

Abbreviations: ID LPS, intradermal lipopolysaccharide; MYD88 = myeloid differentiation primary response 88; TLR = Toll-like receptor.

SUPPLEMENTARY FIGURE 3 **Immune cell infiltration patterns after ID LPS.** (A) Overall mean absolute scores of 22 cell types profiled using CIBERSORTx. (B) Overview of all 22 detected cell types profiled using CIBERSORTx. Each boxplot represents the median, interquartile range, and 1.5*IQR (whiskers) for each cell type. (C) Boxplots displaying the changes in 8 immune cells that were significantly altered in the post-hoc analysis, additional to the ones presented in Figure 7B in the manuscript. Each boxplot represents the median, interquartile range, and 1.5*IQR (whiskers) for each cell type. Asterisks indicate levels of statistical significance for changes between individual time points and baseline. *P.ADJUSTED < 0.05, **P.ADJUSTED < 0.01, ***P.ADJUSTED < 0.001, ****P.ADJUSTED < 0.0001.

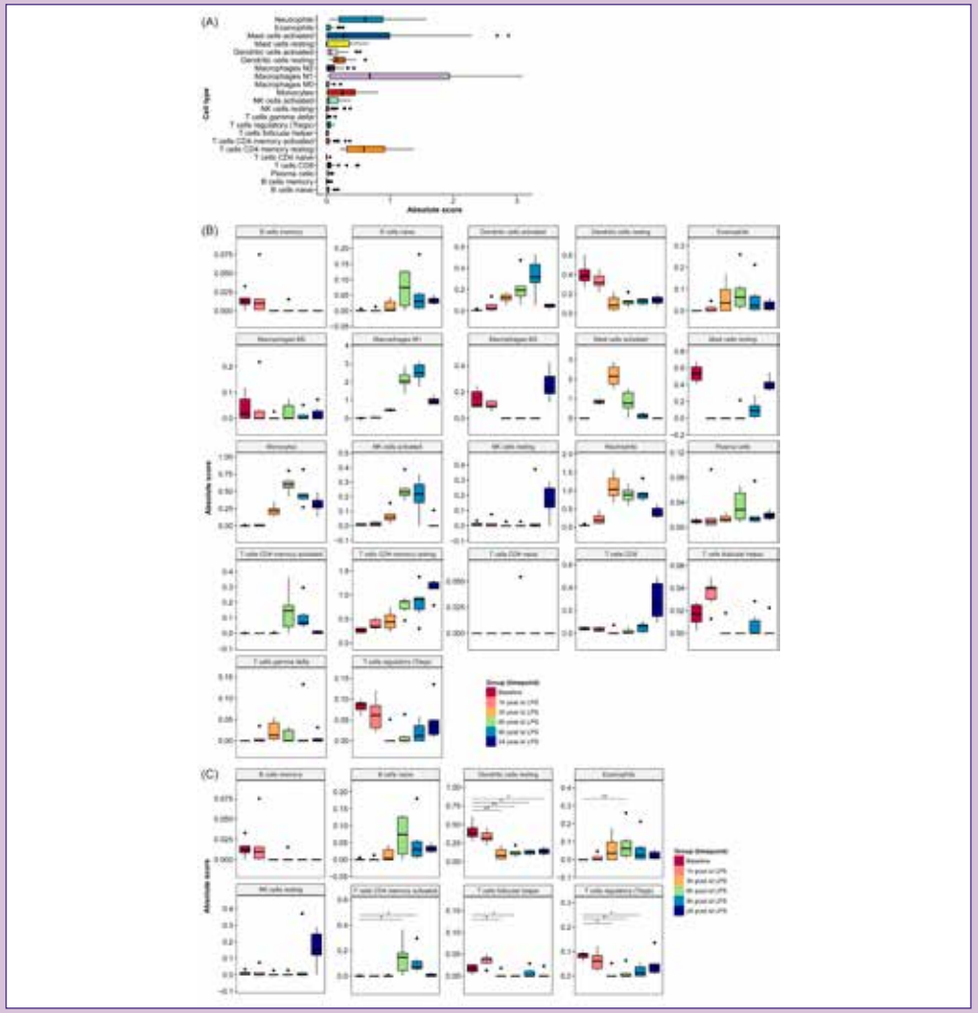

Abbreviations: ID LPS, intradermal lipopolysaccharide; IQR, interquartile range; P.ADJUSTED, adjusted p-value.

REFERENCES

1. Smietana K, Siatkowski M, Møller M. Trends in clinical success rates. *Nat Rev Drug Discov*. 2016;15(6):379-380. doi:10.1038/nrd.2016.85
2. Sun D, Gao W, Hu H, Zhou S. Why 90% of clinical drug development fails and how to improve it? *Acta Pharm Sin B*. 2022;12(7):3049-3062. doi:10.1016/j.apsb.2022.02.002
3. Danhof M, Klein K, Stolk P, Aitken M, Leufkens H. The future of drug development: the paradigm shift towards systems therapeutics. *Drug Discov Today*. 2018;23(12):1990-1995. doi:10.1016/j.drudis.2018.09.002
4. Hughes JP, Rees SS, Kalindjian SB, Philpott KL. Principles of early drug discovery. *Br J Pharmacol*. 2011;162(6):1239-1249. doi:10.1111/j.1476-5381.2010.01127.x
5. Fotis C, Antoranz A, Hatziavramidis D, Sakellaropoulos T, Alexopoulos LG. Network-based technologies for early drug discovery. *Drug Discov Today*. 2018;23(3):626-635. doi:10.1016/j.drudis.2017.12.001
6. Galizzi JP, Lockhart BP, Bril A. Applying systems biology in drug discovery and development. *Drug Metabol Drug Interact*. 2013;28(2):67-78. doi:10.1515/dmdi-2013-0002
7. Hijma HJ, Groeneveld GJ. Analgesic drug development: proof-of-mechanism and proof-of-concept in early phase clinical studies. *Med Drug Discov*. 2021;10:100083. doi:10.1016/j.medidd.2021.100083
8. Schmidt B. Proof of principle studies. *Epilepsy Res*. 2006;68(1):48-52. doi:10.1016/j.eplepsyres.2005.09.019
9. Buters TP, Hameeteman PW, Jansen IME, et al. Intradermal lipopolysaccharide challenge as an acute in vivo inflammatory model in healthy volunteers. *Br J Clin Pharmacol*. 2022;88(2):680-690. doi:10.1111/bcp.14999
10. Yoshino S, Sasatomi E, Ohsawa M. Bacterial lipopolysaccharide acts as an adjuvant to induce autoimmune arthritis in mice. *Immunology*. 2000;99(4):607-614. doi:10.1046/j.1365-2567.2000.00015.x
11. Knapp S. LPS and bacterial lung inflammation models. *Drug Discov Today Dis Models*. 2009;6(4):113-118. doi:10.1016/j.ddmod.2009.08.003
12. Fink MP. Animal models of sepsis. *Virulence*. 2014;5(1):143-153. doi:10.4161/viru.26083
13. Bell E. TLR4 signalling. *Nat Rev Immunol*. 2008;8(4):241. doi:10.1038/nri2301
14. Olink Proteomics AB - assay data. Accessed April 24, 2025. https://olink.com/knowledge/documents
15. Buters TP, Hameeteman PW, Jansen IME, et al. Clinical, Cellular, and Molecular Effects of Corticosteroids on the Response to Intradermal Lipopolysaccharide Administration in Healthy Volunteers. *Clin Pharmacol Ther*. 2022;111(4):964-971. doi:10.1002/cpt.2516
16. Carnazzo V, Rigante D, Restante G, Basile V, Pocino K, Basile U. The entrenchment of NLRP3 inflammasomes in autoimmune disease-related inflammation. *Autoimmun Rev*. 2025;24(7):103815. doi:10.1016/j.autrev.2025.103815
17. Thurman JM, Yapa R. Complement therapeutics in autoimmune disease. *Front Immunol*. 2019;10:672. doi:10.3389/fimmu.2019.00672
18. Zarrin AA, Bao K, Lupardus P, Vucic D. Kinase inhibition in autoimmunity and inflammation. *Nat Rev Drug Discov*. 2021;20(1):39-63. doi:10.1038/s41573-020-0082-8
19. Lamagna C, Gundel C, Chan M, et al. A novel IRAK1/4 dual inhibitor in clinical development blocks Toll-like receptor 4 (TLR4) signaling in human and mouse. *Ann Rheum Dis*. 2020;79:579. doi:10.1136/annrheumdis-2020-eular.3370
20. Yellin M, Paliienko I, Balanescu A, et al. A phase II, randomized, double-blind, placebo-controlled study evaluating the efficacy and safety of MDX-1100, a fully human anti-CXCL10 monoclonal antibody, in combination with methotrexate in patients with rheumatoid arthritis. *Arthritis Rheum*. 2012;64(6):1730-1739. doi:10.1002/art.34330
21. Huang HC, Chen YT, Lin HH, Li ZQ, Yang JM, Tzou SC. Inhibition of IRAK1 Is an Effective Therapy for Autoimmune Hypophysitis in Mice. *Int J Mol Sci*. 2022;23(23):14958. doi:10.3390/ijms232314958
22. Tokunaga R, Zhang W, Naseem M, et al. CXCL9, CXCL10, CXCL11/CXCR3 axis for immune activation–A target for novel cancer therapy. *Cancer Treat Rev*. 2018;63:40-47. doi:10.1016/j.ctrv.2017.11.007

23. Dennison L, Mohan AA, Yarchoan M. Tumor and Systemic Immunomodulatory Effects of MEK Inhibition. *Curr Oncol Rep*. 2021;23(2):23. doi:10.1007/s11912-020-01008-4
24. Azer K, Leaf I. Systems biology platform for efficient development and translation of multitargeted therapeutics. *Front Syst Biol*. 2023;3:1229532. doi:10.3389/fsysb.2023.1229532
25. Siebenga PS, van Amerongen G, Klaassen ES, de Kam ML, Rissmann R, Groeneveld GJ. The ultraviolet B inflammation model: Postinflammatory hyperpigmentation and validation of a reduced UVB exposure paradigm for inducing hyperalgesia in healthy subjects. *Eur J Pain*. 2019;23(5):874-883. doi:10.1002/ejp.1353
26. Saghari M, Gal P, Ziagkos D, et al. A randomized controlled trial with a delayed-type hypersensitivity model using keyhole limpet haemocyanin to evaluate adaptive immune responses in man. *Br J Clin Pharmacol*. 2021;87(4):1953-1962. doi:10.1111/bcp.14588
27. Del Duca E, Pavel AB, Dubin C, et al. Major Differences in Expression of Inflammatory Pathways in Skin from Different Body Sites of Healthy Individuals. *J Invest Dermatol*. 2019;139(10):2228-2232.e10. doi:10.1016/j.jid.2019.04.008
28. Sjöbom U, Christenson K, Hellström A, Nilsson AK. Inflammatory Markers in Suction Blister Fluid: A Comparative Study Between Interstitial Fluid and Plasma. *Front Immunol*. 2020;11:597632. doi:10.3389/fimmu.2020.597632
29. Hu T, Todberg T, Ewald DA, et al. Assessment of Spatial and Temporal Variation in the Skin Transcriptome of Atopic Dermatitis by Use of 1.5 mm Minipunch Biopsies. *J Invest Dermatol*. 2023;143(4):612-620.e6. doi:10.1016/j.jid.2022.10.004
30. Clark KEN, Csomor E, Campochiaro C, et al. Integrated analysis of dermal blister fluid proteomics and genome-wide skin gene expression in systemic sclerosis: an observational study. *Lancet Rheumatol*. 2022;4(7):e507-e516. doi:10.1016/S2665-9913(22)00094-7
31. Jovic D, Liang X, Zeng H, Lin L, Xu F, Luo Y. Single-cell RNA sequencing technologies and applications: A brief overview. *Clin Transl Med*. 2022;12(3):e694. doi:10.1002/ctm2.694
32. Bressan D, Battistoni G, Hannon GJ. The dawn of spatial omics. *Science*. 2023;381(6657):eabq4964. doi:10.1126/science.abq4964
33. Burt T, Nandal S. Pharmacometabolomics in Early-Phase Clinical Development. *Clin Transl Sci*. 2016;9(3):128-138. doi:10.1111/cts.12396
34. Liberzon A, Birger C, Thorvaldsdóttir H, Ghandi M, Mesirov JP, Tamayo P. The Molecular Signatures Database (MSigDB) Hallmark Gene Set Collection. *Cell Syst*. 2015;1(6):417-425. doi:10.1016/j.cels.2015.12.004
35. Shannon P, Markiel A, Ozier O, et al. Cytoscape: A software Environment for integrated models of biomolecular interaction networks. *Genome Res*. 2003;13(11):2498-2504. doi:10.1101/gr.1239303
36. Martens M, Ammar A, Riutta A, et al. WikiPathways: Connecting communities. *Nucleic Acids Res*. 2021;49(D1):D613-D621. doi:10.1093/nar/gkaa1024

SECTION 2

UNCONTROLLED INFLAMMATORY RESPONSES

CHAPTER 6

Adverse immunostimulation in early-phase clinical trials: key findings and recommendations based on the investigator's clinical experience

Published in: Br J Clin Pharmacol. Published online September 19, 2025. doi:10.1002/bcp.70276

Marella C.E. van Ruissen*[1,2], Juliette A. van den Noort*[1,2], Lisanne C.A. Smidt[1,2], Naomi B. Klarenbeek[1,2], Philip H.K. Kremer[1,2], Manon A.A. Jansen[1,2], Jacobus Burggraaf[1,2], Joop M.A. van Gerven[1,2,3], Matthijs Moerland[1,2]

**These authors share first authorship.*

1 Centre for Human Drug Research, Leiden, the Netherlands
2 Leiden University Medical Centre, Leiden, the Netherlands
3 Central Committee on Research Involving Human Subjects (CCMO), The Hague, the Netherlands

ABSTRACT

The emergence of therapeutic proteins has coincided with an increase in acute adverse immunostimulation (AIS). AIS has occurred in clinical trials despite compliance with regulatory guidelines on preclinical evaluation and its incidence is anticipated to increase further. AIS may have significant impact on trial participants and clinical staff exposed to the adversity and can severely hamper progression of investigational medicinal products (IMPs) through drug development programmes. We aim to increase understanding of the mechanistic basis and clinical presentation of AIS by presenting three recent cases of drug-induced AIS in early-phase clinical trials, conducted at the Centre for Human Drug Research (Leiden, The Netherlands), in the context of ICH S6, S8 and Food and Drug Administration guidelines for AIS evaluation. We strongly encourage increased vigilance for AIS during the early stages of the drug development process. Although AIS can probably never be fully mitigated by preclinical studies alone, preclinical evaluations of IMP-induced AIS enables anticipation of its potential occurrence in subsequent clinical studies. The limited information available on the exact mechanisms underlying AIS and uncertainties regarding the relevance of animal species warrant further research into the translatability of the mechanisms underlying AIS between species and models. Implementation of evidence-based, IMP-specific AIS management, mitigation, and monitoring protocols will facilitate AIS recognition and mechanistic understanding, translating into more rational clinical management of AIS. This will improve the overall efficiency of the drug development process while fostering closer collaborative relationship between pharmaceutical companies and investigators, ultimately helping design and conduct high-quality clinical trials that are equally safe and informative.

INTRODUCTION

Although the rapidly expanding field of therapeutic proteins holds great promise for the treatment of a variety of previously untreatable diseases, the testing of such investigational medicinal products (IMPs) has coincided with a notable increase in acute systemic inflammatory reactions, also known as adverse immunostimulation (AIS).[1,2] AIS can be evoked by a variety of IMPs, but it is particularly associated with structurally complex products such as liposomal formulations, antibodies, polyethylene glycol-conjugated proteins, and oligonucleotides (Figure 1).[1,3–6] The rising incidence of AIS occurs despite compliance with regulatory guidelines on preclinical evaluation of AIS.[7] A further rise in the number of AIS cases is anticipated due to increasing structural complexity and target complexity of newly developed IMPs.

AIS is hard to recognise, often misdiagnosed, and underreported.[2,6,8–10] This may be due to the heterogeneous clinical presentation of AIS combined with the absence of a standardised, universally accepted definition and classification system (Figure 1).[8,10] AIS has significant impact on trial participants and clinical staff exposed to such reactions, as symptoms can be severe and unexpected. Consequently, occurrence of unanticipated AIS can hamper progression of the drug development process.

We aim to increase understanding of AIS by presenting the acute clinical manifestation of three recent cases of drug-induced AIS in early-phase clinical trials conducted at the Centre for Human Drug Research. These cases are presented in context of existing guidelines for preclinical AIS evaluation. We also highlight the importance of systematic investigation of IMP-driven AIS, despite its methodological challenges, in preclinical and early clinical drug development phases.

THE REGULATORY LANDSCAPE: EVALUATION OF GUIDELINES

The International Council for Harmonisation of Technical Requirements for Pharmaceuticals for Human Use (ICH) and the United States Food and Drug Administration (FDA) provide three relevant guidelines for the assessment of AIS in preclinical drug development, as summarised in Table 1.

TABLE 1 Summary of current guidelines on the assessment of AIS in drug development.

Guideline	Target pharmaceuticals	Practical guidance on assessing risk of AIS
ICH S6	All pharmaceuticals, excluding biotechnology-derived pharmaceuticals	• Conduct standard toxicity studies. • Expand with fit-for-purpose studies based on findings from standard toxicity studies and IMP-characteristics.
ICH S8	Biotechnology-derived pharmaceuticals	• Conventional toxicity may not be appropriate for biotechnology-derived pharmaceuticals (and thus an opt out is possible). • Monitor injection site reactions. • Study expression of surface antigens on target cells. • Optionally undertake additional testing to clarify issues observed in bullet point 2 and 3.
FDA	All pharmaceuticals	• Fit-for-purpose assays based on IMP-characteristics. • Discuss approaches with relevant authorities.

AIS, adverse immunostimulation; ICH, International Council for Harmonisation of Technical Requirements for Pharmaceuticals for Human Use; IMP, investigational medicinal product; FDA, United States Food and Drug Administration.

The first guideline, effective since 2006, is the ICH S8 titled *'Immunotoxicity studies for human pharmaceuticals'*.[11] ICH S8 is applicable to human pharmaceuticals, excluding biotechnology-derived pharmaceutical products (defined by ICH S6 as *'products derived from characterised cells through the use of a variety of expression systems including bacteria, yeast, insect, plant and mammalian cells'*)[12] and other biologicals. Notably, this guideline does not cover the possibility of target-mediated AIS nor does it provide explicit guidance for the preclinical evaluation of AIS.[11] ICH S8 does state the need for preclinical standard toxicity studies (e.g. assessment of leukocyte counts and globulin levels in serum and pathology of lymphoid organs). This evaluation can be expanded by additional fit-for-purpose immunotoxicity studies *'as appropriate'*, based on findings from standard toxicity studies combined with concerns related to the class, specific properties, and mechanism of action (MoA) of the IMP. The expansion of standard toxicity studies can also be based on clinical information, including outcomes of early-phase clinical trials and the intended patient population. In such cases, ICH S8 recommends immune function studies and immunophenotyping *'before exposure of a large population of patients (Phase III)'* to generate additional data and assess whether *'sufficient data are available to reasonably determine the risk of immunotoxicity'*.[10]

The second guideline reporting on the evaluation of immunotoxicity is ICH S6 titled *'Preclinical safety evaluation of biotechnology-derived pharmaceuticals'* (latest revision published in 2011).[12] ICH S6 provides a framework for the preclinical safety evaluation of biotechnology-derived pharmaceuticals and other biologicals. ICH S6 acknowledges the translational gap between preclinical studies and the in vivo human response for such IMPs; it argues that conventional toxicity testing may not be appropriate due to issues of species specificity, immunogenicity, and unpredicted pleiotropic activity. Therefore, ICH S6 leaves room for certain conventional steps to be omitted during the preclinical testing phase, provided there are rational arguments to support this decision. Regarding AIS, ICH S6 merely includes one paragraph directing investigators to monitor injection site reactions which *'may be indicative of a stimulatory response'* and study the altered expression of surface antigens on target cells *'which has implications for autoimmune potential'*. ICH S6 concludes this paragraph with *'immunotoxicological testing strategies may require screening studies followed by mechanistic studies to clarify such issues'* [of a stimulatory response and autoimmune potential], thus permitting additional immunotoxicity testing. However, directive ICH S6 does not provide clear and imperative guidance for drug development.[12]

Finally, the FDA published a guideline in 2023 (*'Nonclinical Evaluation of the Immunotoxic Potential of Pharmaceuticals - Guidance*

for Industry') which explicitly includes advice for immunotoxicity testing of biotechnology-derived therapeutic proteins.[13] The FDA advises that *'an assessment of the ability of pharmaceuticals to adversely affect the activity of the immune system is an essential component of evaluating the safety of pharmaceuticals'*. According to the FDA, this assessment should include fit-for-purpose assays based on the MoA, target, cellular distribution, and potential to induce immunostimulation in key cell types specific to the IMP. These assessments should *'include appropriate positive and negative controls and have clear, measurable outcomes'* (e.g. cytokine release or complement activation, see Figure 1). This guideline distinguishes itself from the ICH guidelines by explicitly paying attention to systemic hypersensitivity reactions and underlining that immunotoxicity is an essential component in the development of IMPs. It also provides the active recommendation *'that sponsors discuss their proposed approaches, with the appropriate review division'* to aid conducting adequate preclinical immunotoxicity studies, thereby providing a solid framework before proceeding to the clinical phase.[13]

CASE DESCRIPTIONS

At the Centre for Human Drug Research (Leiden, The Netherlands), we conducted multiple clinical studies evaluating IMPs with a potential risk for AIS over the past few years. In three of these studies, IMPs evoked AIS despite adherence to the applicable preclinical and clinical guidelines, proper evaluation of the available preclinical work, and approval from the local authorities (Table 1). All three cases occurred in first-in-human (FIH), randomised, double-blind, placebo-controlled clinical trials with immune-targeting IMPs, intended to inhibit immune responses using various methods. All studies were approved by the Medical Ethics Committee 'Stichting Beoordeling Ethiek Biomedisch Onderzoek' (Assen, the Netherlands) and conducted in accordance with the principles of the Declaration of Helsinki, the ICH E6 guideline (*'Guideline for Good Clinical Practice'*), and ethical principles as referenced in EU Directive 2001/20/EC.[14–16] Participants provided written informed consent prior to any study-related procedures. They were evaluated through extensive medical examination prior to inclusion and were excluded if they previously experienced adverse reactions or allergic reactions to medication, or if they had active infections.

Case X

Case X concerned an immune-targeting, monoclonal antibody (mAb) with a mutated Fc domain. In 4-week Good Laboratory Practice (GLP) rat and monkey toxicology studies, the IMP was well tolerated at doses substantially higher than the dose level administered in humans. Observations included non-adverse lactate dehydrogenase decreases in rats and non-specific reversible skin- and organ mononuclear and mixed cell infiltration in monkeys, but no signs of severe toxicity. AIS-related preclinical evaluations included complement activation assays, Fc-γ receptor binding, and immunophenotyping in monkeys. Based on the outcomes of these additional experiments, the risk for complement activation and Fc receptor interactions was considered low. The FIH starting dose was chosen based on the predicted human dose with minimal pharmacological activity (<5%), as well as a substantial safety factor from the defined no observed adverse effect level (NOAEL) in cynomolgus monkeys.

In the first cohort, 8 participants were dosed with the IMP with a 2-hour intravenous (IV) infusion. In line with expectations there were indications of pharmacological activity, but no signs of AIS were observed. Upon a 3x dose increase in the second cohort, the first participant, a healthy, 26-year-old female with no active allergies or previous exposure to mAbs, showed quickly spreading urticaria at ~90 minutes after start of the infusion. Vital signs in semi-recumbent position were normal, with no other symptoms besides urticaria. Upon standing upright, the participant showed orthostatic hypotension with a blood pressure drop to 72/41 mmHg, resulting in dizziness and near-syncope. The infusion was immediately stopped, and the blood pressure recovered shortly after returning to the semi-recumbent position. Clemastine (2 MG IV) was administered for symptom relief and the urticaria fully resolved ~2 hours after

stopping the infusion. Following the first case, three additional cases of infusion-rate dependent urticaria, orthostatic hypotension, bradycardia, and/or vasovagal symptoms or syncope occurred. All symptoms presented within 2 hours after the start of the infusion and resolved within 4 hours after stopping. We observed no significant changes in leukocytes or CRP. The results of additional analysis of banked clinical samples (pre-dose and post-dose) showed elevated levels of complement activation products (C3a, C4a), but no significant changes in tryptase, cytokines (IFN-γ and IL-6) or IGE (Table 2). Lowering the infusion rate and addition of premedication (H_1-, H_2-antagonists and paracetamol) decreased the severity of the reaction but did not result in full prevention of symptoms.

TABLE 2 Overview of the characteristics of the investigated IMPs and the clinical presentation of AIS in the reported early-phase clinical trials.

	Case X	Case Y	Case Z
IMP	• Single-arm, IgG4 mAb • Mutated Fc-domain	• Synthetic oligonucleotide mixture	• IgG1, mAb • Functional Fc-domain
Clinical signs and symptoms	Infusion rate-dependent: • Urticaria • Orthostatic hypotension • Bradycardia • Vasovagal collapse	In highest dose cohort: • Fever • Shivering • Nausea • Headache	Dose-dependent: • Fever • Chest pain • Dizziness
Time course after start of dosing	• Occurrence ≤ 2H • Resolution ≤ 4H	• Occurrence ≤ 3h • Resolution ≤ 24h	• Occurrence ≤ 10h • Resolution ≤ 24H
Laboratory safety data	• No significant changes in leukocytes/CRP	• Leukocytosis	• CRP elevation
Post-AIS additional analyses	• C3a, C4a elevated (*in vivo*) • IFN-γ, IL-6 induction (*in vivo*) • No tryptase (*in vivo*)	• CRP elevation (*in vivo*) • TNF, IL-10, and IL-8 induction (in + *ex vivo*)	• TNF, IL-6, and IL-8 induction (*in + ex vivo*)

CRP, C-reactive protein; IGG1, immunoglobulin G1; IGG4, immunoglobulin G4; IL-6, interleukin 6; IL-8, interleukin 8; IMP, investigational medicinal product; mAb, monoclonal antibody; TNF, tumour necrosis factor.

Case Y

Case Y involves a chemically synthesised, single-stranded, oligonucleotide mixture without immune-activating excipients or modifications. The single and multiple dose toxicity of the drug substance was studied in mice, rats, and cynomolgus monkeys at doses substantially higher than the human equivalent doses administered during the clinical trial. The IMP demonstrated no immune-related or other relevant safety concerns in animals. Pharmacodynamic (PD) activity was studied preclinically in target-specific studies and assays, where the IMP showed adequate and dose-related inhibition of the selected endpoints. The initial dose for the FIH was determined based on expected minimal pharmacological activity (<5%), while also ensuring a significant safety margin based on the established NOAEL in rats.

In the FIH study >20 healthy volunteers were dosed with Y at escalating dose levels. At the highest planned dose level (>10x higher than the starting dose), the last dosed participant, a 24-year-old female healthy volunteer without abnormalities in her pre-dose clinical and laboratory safety examinations, developed fever and headache starting 0.5-3 hours after dosing. The symptoms were accompanied by leukocytosis (mainly neutrophils) and CRP elevation, which were mild in nature. Three other participants, both male and female with ages ranging from 23-43 years, also displayed mild and transient leukocyte increases compared to baseline and two of them reported headaches. After these observations, levels of circulating cytokines were determined in plasma samples from all volunteers in this trial. No inter-individual elevations in levels of cytokines were seen at baseline in any of the participants except for elevated IFN-γ and IL-10 in the 24-year-old female, which may indicate low-grade pre-existing immune activation. All the four described participants displayed mildly increased TNF, IL-6, IL-8, and IL-10 compared to baseline (Table 2).

Case Z

Case Z originated from a targeted humanised IGG1K mAb of 150 KDA with an intact Fc domain. In agreement with the local authorities and in compliance with the ICH guidelines, preclinical evaluation of this IMP was performed through human in vitro toxicology and animal pharmacology testing, without formal GLP animal toxicology studies. In line with ICH-S6 the rationale for omitting animal toxicology studies was based on the lack of target expression in healthy animals and the known lack of effects resulting from off-target properties of a mAb in such studies. The preclinical pharmacology studies in mice showed no behavioural or physical abnormalities. The PD effects of this IMP were favourable in multiple animal models of inflammation and autoimmune diseases and in ex vivo assays. In vitro safety assays showed no effect on cell activation or function, nor on a wide range of human FcγRs/FcRns interactions. Additionally, in vitro cytokine release assays showed IMP dose-dependent production of IL-8 and TNF, but this was assessed as lower than for other mAbs already in use in the clinic for similar indications. The starting dose was selected based on the preclinical evaluations, clinical data from two other IgGs with intact Fc domains, and the fact that there is little to no target expression in healthy volunteers.

In the FIH study, 37 volunteers were dosed with the IMP. After a 3-fold dose escalation in cohort 2, initial hints of adversity were seen in two participants (out of six) including shivers, elevated body temperature, increased CRP, TNF, and IL-6. A decrease in the infusion rate resulted in a reduction in adverse symptoms in cohort 3 (repeat dose). After another 3-fold dose escalation, all three participants treated with the IMP in cohort 4 experienced adverse events including fever, chest discomfort, odynophagia, dizziness, headache, eructation, leukopenia, and cytokine increases (TNF, IL-6, IL-8). In cohort 5, the cohort 4 dose was repeated and combined with pre-medication (H_1-antagonist, proton pump inhibitor). Despite the premedication, similar, though milder, adverse events still occurred. All described symptoms occurred between 2 and 9 hours after the start of the infusion (Table 2).

DISCUSSION AND RECOMMENDATIONS

These cases illustrate that AIS can arise despite adherence to existing guidelines. Previously, numerous cases of AIS in clinical research, particularly in relation to mAbs, have been described in literature.[1,17,18] Furthermore, it can be argued that the publicly available reports of AIS in clinical research are just the tip of the iceberg, as negative safety findings in early-phase clinical trials are often not published. This indicates that the occurrence of AIS is widespread and requires attention.[19,20]

All three cases involved immune-targeting IMPs designed to inhibit immune-responses through various mechanisms. The preclinical development process as envisaged in the regulatory framework was followed in the cases described, but additional experiments such as assessment of the risk of complement activation (in relevant species) and Fc receptor interactions, and/or cytokine release assays (compared to registered products) did not identify significant safety concerns. These findings indicate that the occurrence of AIS in early clinical trials is unlikely to be fully prevented by preclinical studies alone. Carrying out preclinical evaluations of the ability of a compound to evoke AIS (including the potential role of target expression) prior to FIH dosing is important, as it allows anticipation of potential AIS occurrence in clinical studies. However, in their efforts to gain this information, pharmaceutical companies are strongly hampered by the limited methodologies available and the translational gap between preclinical assays and human studies.[2,12,21]

Differences in AIS sensitivity between species are a major concern, particularly for endpoints such as complement activation, where compounds that induce small increases in complement proteins in animal species can cause large AIS responses in humans.[22,23] The limited information available on the exact mechanisms behind AIS and uncertainties regarding the relevance of animal species for individual safety endpoints warrant further research into the translatability of the mechanisms underlying AIS between species and models.[2,10] To this end, systematic assessments comparing biomarkers of AIS in

preclinical studies with those in early-phase clinical studies could provide valuable insights for drug development.

The limited predictability of AIS requires clinical researchers to anticipate its potential occurrence by implementing evidence-based, IMP-specific AIS management, mitigation and monitoring protocols (Table 3). Such protocols need to cover practical instructions, including relevant additional biomarker analyses to conduct upon occurrence of AIS.[24] The availability of such protocols will facilitate clinical management and contribute to a better mechanistic understanding of the nature of IMP-driven AIS. Ultimately, this may translate into a more efficient and safe clinical drug development process, while also providing relevant insights into the predictive value of the available preclinical package.

Preclinical to clinical IMP-driven AIS translation, prediction, recognition and management requires a strong collaborative relationship between the pharmaceutical company and the investigator, ensuring rational, evidence-based decision making in high-quality clinical trials (Table 3). Increased attention to potential AIS in the early clinical drug development process not only facilitates more prudent clinical trial conduct for both trial participants and staff, but will also result in a more efficient development process, with lower chances of delays due to unexpected adversity. Based on our experience, we recommend that AIS risk is assessed early in the development process, based on theoretical grounds as well as all available preclinical data on the IMP. Pharmaceutical companies and investigators should thoroughly discuss the potential ability of the IMP to drive AIS, guided by IMP-specific properties such as class, structure, MoA and target, and reach an AIS risk score that translates into AIS mitigation, management and monitoring plans for the upcoming clinical study.[24]

In conclusion, we strongly encourage strong vigilance for AIS at early stages in the drug development process. Close collaboration between pharmaceutical companies and clinical investigators is critical for systematic evaluation of AIS biomarkers in the late preclinical and early clinical drug evaluation phase. Implementation of IMP-specific AIS management and evaluation protocols will help in the design and conduct of high-quality clinical trials and in improving understanding of the unanswered translational questions related to AIS, while ensuring the efficiency of the development process.

TABLE 3 Overview of the presented recommendations for (pre)clinical evaluation of IMPs and the intended effects.

Recommendations	Effect
Extensive discussions between pharmaceutical company and investigator on the IMP's potential to evoke AIS.	• To anticipate the occurrence of AIS in clinical trials. • To limit participant burden by creating evidence-based, IMP-specific management protocols and mitigation plans prior to FIH dosing. • To avoid delays in study conduct and drug development programme due to unanticipated adversity.
Systematic evaluation in case of AIS occurrence, including standardised blood sampling strategies (e.g., tryptase, cytokines).	• To gain understanding of the mechanisms underlying IMP-related AIS. • To allow for informed decision-making regarding further clinical development of the IMP.

AIS, adverse immunostimulation; FIH, first-in-human; IMP, investigational medicinal product.

FIGURE 1 **Indicators of AIS at different stages of the drug development process.** Indicators of AIS may arise during all phases of the drug development process. For in vitro, studies these indicators consist of cytokine release, complement activation, and immune complex - Fc-γ receptor interactions. For animal studies, they include abnormalities in standard toxicity testing, injection site reactions, autoimmunity-related altered expression of surface antigens on target cells, and elevated levels of cytokines and/or complement.[13] In clinical trials, AIS has a heterogeneous presentation. Symptoms include, but are not limited to, dyspnoea, back pain, gastro-intestinal symptoms, skin reactions, headache, and alterations in vital signs.

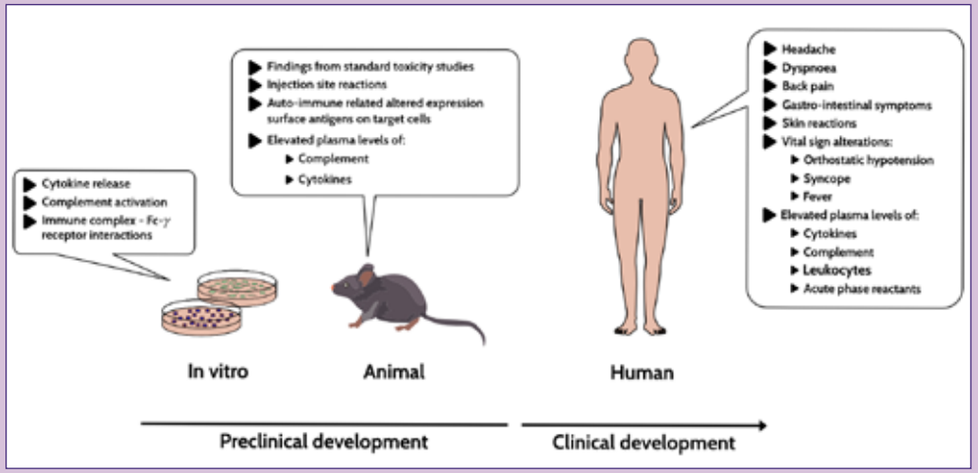

Abbreviations: AIS, adverse immunostimulation.

REFERENCES

1. Baldo BA. Immune-and Non-Immune-Mediated Adverse Effects of Monoclonal Antibody Therapy: A Survey of 110 Approved Antibodies. *Antibodies*. 2022;11(1):17. doi:10.3390/antib11010017
2. Reijers JAA, Malone KE, Bajramovic JJ, Verbeek R, Burggraaf J, Moerland M. Adverse immunostimulation caused by impurities: The dark side of biopharmaceuticals. *Br J Clin Pharmacol*. 2019;85(7):1418-1426. doi:10.1111/bcp.13938
3. Bruno JG. Potential inherent stimulation of the innate immune system by nucleic acid aptamers and possible corrective approaches. *Pharmaceuticals (Basel)*. 2018;11(3):62. doi:10.3390/ph11030062
4. Ibrahim M, Ramadan E, Elsadek NE, et al. Polyethylene glycol (PEG): The nature, immunogenicity, and role in the hypersensitivity of PEGylated products. *J Control Release*. 2022;351(August):215-230. doi:10.1016/j.jconrel.2022.09.031
5. Bakos T, Mészáros T, Kozma GT, et al. mRNA-LNP COVID-19 Vaccine Lipids Induce Complement Activation and Production of Proinflammatory Cytokines: Mechanisms, Effects of Complement Inhibitors, and Relevance to Adverse Reactions. *Int J Mol Sci*. 2024;25(7):3595. doi:10.3390/ijms25073595
6. Szebeni J. Complement activation-related pseudoallergy: A stress reaction in blood triggered by nanomedicines and biologicals. *Mol Immunol*. 2014;61(2):163-173. doi:10.1016/j.molimm.2014.06.038
7. Descotes J. Safety immunopharmacology: Evaluation of the adverse potential of pharmaceuticals on the immune system. *J Pharmacol Toxicol Methods*. 2012;66(2):79-83. doi:10.1016/j.vascn.2012.05.001
8. Elzagallaai AA, Rieder MJ. Pathophysiology of drug hypersensitivity. *Br J Clin Pharmacol*. 2024;90(8):1856-1868. doi:10.1111/bcp.15645
9. Reber LL, Hernandez JD, Galli SJ. The pathophysiology of anaphylaxis. *J Allergy Clin Immunol*. 2017;140(2):335-348. doi:10.1016/j.jaci.2017.06.003
10. Baldo BA. MRGPRX2, drug pseudoallergies, inflammatory diseases, mechanisms and distinguishing MRGPRX2- and IgE/FcεRI-mediated events. *Br J Clin Pharmacol*. 2023;89(11):3232-3246. doi:10.1111/bcp.15845
11. ICH. ICH S8 Guideline: Immunotoxicity Studies for Human Pharmaceuticals.; 2005. https://www.ema.europa.eu/en/ich-s8-immunotoxicity-studies-human-pharmaceuticals-scientific-guideline. Accessed January 24, 2024.
12. ICH. ICH S6(R1) Guideline: Preclinical Safety Evaluation of Biotechnology-Derived.; 2011. https://www.ema.europa.eu/en/ich-s6-r1-preclinical-safety-evaluation-biotechnology-derived-pharmaceuticals-scientific-guideline. Accessed January 24, 2024.
13. FDA. Nonclinical Evaluation of the Immunotoxic Potential of Pharmaceuticals Guidance for Industry.; 2023. https://www.fda.gov/regulatory-information/search-fda-guidance-documents/nonclinical-evaluation-immunotoxic-potential-pharmaceuticals. Accessed January 24, 2024.
14. ICH. ICH guideline E6(R2): Guideline for good clinical practice. Published online 2016. https://www.ema.europa.eu/en/ich-e6-good-clinical-practice-scientific-guideline. Accessed January 24, 2024.
15. Directive 2001/20/EC. Directive (EU) 2001/20/EC of the European Parliament and of the Council of 4 April 2001 on the approximation of the laws, regulations and administrative provisions of the Member States relating to the implementation of good clinical practice in the conduct of clinical trials on medicinal products for human use. https://eur-lex.europa.eu/eli/dir/2001/20/oj. Accessed March 18, 2024.
16. Declaration of Helsinki. World Medical Association declaration of Helsinki: Ethical principles for medical research involving human subjects. *JAMA*. 2013;310(20):2191-2194. doi:10.1001/jama.2013.281053
17. Fülöp T, Mészáros T, Kozma GT, Szebeni J, Józsi M. Infusion reactions associated with the medical application of monoclonal antibodies: The role of complement activation and possibility of inhibition by factor H. *Antibodies*. 2018;7(1):14. doi:10.3390/antib7010014
18. Isabwe GAC, Garcia Neuer M, de las Vecillas Sanchez L, Lynch DM, Marquis K, Castells M. Hypersensitivity reactions to therapeutic monoclonal antibodies: Phenotypes and endotypes. *J Allergy Clin Immunol*. 2018;142(1):159-170.e2. doi:10.1016/j.jaci.2018.02.018

19. Mitra-Majumdar M, Kesselheim AS. Reporting bias in clinical trials: Progress toward transparency and next steps. *PLoS Med*. 2022;19(1):e1003894. doi:10.1371/journal.pmed.1003894
20. Song F, Parekh-Bhurke S, Hooper L, et al. Extent of publication bias in different categories of research cohorts: A meta-analysis of empirical studies. *BMC Med Res Methodol*. 2009;9(1):79. doi:10.1186/1471-2288-9-79
21. Maggi E, Vultaggio A, Matucci A. Acute infusion reactions induced by monoclonal antibody therapy. *Expert Rev Clin Immunol*. 2011;7(1):55-63. doi:10.1586/eci.10.90
22. Dezsi L, Meszaros T, Orfi E, et al. Complement activation-related pathophysiological variations of symptoms and mediators. *Molecules*. 2019;24(18):3283. doi:10.3390/molecules24183283
23. Szebeni J, Alving CR, Rosivall L, et al. Animal models of complement-mediated hypersensitivity reactions to liposomes and other lipid-based nanoparticles. *J Liposome Res*. 2007;17(2):107-117. doi:10.1080/08982100701375118
24. van den Noort JA, Meijs AC, Klarenbeek NB, Moerland M. Navigating adverse immunostimulation: A practical guide for clinical researchers. *Br J Clin Pharmacol*. Published online September 12, 2025. doi:10.1002/bcp.70268

CHAPTER 7

Summary, future directions and conclusion

Drug development is a lengthy and costly process, with high attrition rates as major contributor. Lack of efficacy in patient populations is accountable for approximately half of the candidate drug failures.[1–4] Drug development could therefore benefit from insights into drug effects early in the clinical phase. This can be achieved by evaluating proof-of-pharmacology in early-phase clinical studies using human challenge models that mimic mechanisms relevant to disease pathophysiology. Besides demonstrating proof-of-pharmacology, such studies also inform the design of future clinical trials (e.g. supporting drug target, dose, and endpoint selection), thereby facilitating efficient progression of promising drug candidates to later-stage clinical development.[5–7] This approach ultimately reduces attrition rates and loss of scarce resources and investments, while increasing efficiency of clinical drug development programmes.

In recent years, the use of human challenge models has received growing interest.[8] However, in the field of immunology, the development of models inducing inflammation is still in its infancy.[9,10] Examples of such models are the allyl isothiocyanate (AITC) skin challenge and the intradermal lipopolysaccharide (ID LPS) challenge. These challenges are based on the induction of transient, mild inflammation under controlled circumstances by topical administration of the pro-inflammatory stimuli AITC or LPS.[9–11] These inflammatory models also elicit underexplored immune-mediated vascular responses, potentially relevant to a multitude of diseases targeted by current drug development programmes.[9,11,12]

In contrast to human challenge models inducing inflammation under controlled circumstances, undesirable uncontrolled inflammatory responses are also occasionally encountered in clinical pharmacological studies. These responses induced by investigational medicinal products (IMPS) are known as adverse immunostimulation (AIS).[13,14] Although the incidence of AIS appears to be rising, clear regulatory guidance and a standardised framework for its assessment are not yet available.

This thesis describes research ultimately aimed at advancing immunological clinical drug development. Section 1 explores mechanisms of vascular and inflammatory effects of controlled inflammation in human challenge models. Section 2 examines three first-in-human studies of IMPS that displayed AIS, within the context of existing regulatory guidance.

SECTION 1: CONTROLLED INFLAMMATORY RESPONSES

Proof-of-pharmacology studies conducted early in clinical development could enhance the efficiency of drug development programmes. However, a practical difficulty in implementing proof-of-pharmacology during phase I clinical studies is the lack of the target disorder in healthy participants. Human challenge models aid overcoming this problem by inducing pathways overlapping with pathophysiological processes and the mechanism of action or the target of drug candidates.[5–7]

Given the increasing prevalence of immunological diseases, the growing number of immunological drug targets, and the corresponding increase in immunomodulating drug candidates, the field of immunology could particularly benefit from proof-of-pharmacology approaches.[15,16] It is therefore no surprise that inflammatory challenge models have been gaining ground over the past years.[9,10,17] Examples of such models are the AITC and ID LPS model.[9,10]

AITC — Findings and future perspectives

AITC is a natural substance that produces the pungent taste of cruciferous vegetables, such as garlic, mustard and wasabi. Dermal application of AITC induces neurogenic inflammation through agonism of the transient receptor potential cation channel A1 (TRPA1). The principal read-out of this challenge is the vasodilatory response. Some researchers simultaneously studied pain intensity to assess safety and potential applicability of AITC as a model for pain.[10,11,18] Other aspects of the TRPA1-induced neurogenic inflammation, such as cytokine release and cell attraction, have not been studied thus far.

Preclinical research indicates that the vasodilatory response observed after dermal AITC application is mediated through agonism of TRPA1 on dermal sensory nerves. The vasoactive neuropeptides released after TRPA1 agonism stimulate nitric oxide (NO) production in endothelial cells, which results in the relaxation of vascular smooth muscle cells.[19,20] It is assumed that these mechanisms apply to the observed vasodilatory response in humans as well. However, the exact mechanistic pathway, including all contributing mediators, leading to vasodilation in humans is not yet fully explored. Given the incomplete knowledge on the vasodilatory mechanisms and other aspects of TRPA1-induced inflammation, the current clinical pharmacological applicability of the model is limited to testing pharmacodynamic effects of direct TRPA1 antagonists.[21–23]

In chapter 2, we aimed to study the effects of the NO-driven vasodilatory challenge whole-body heat stress (WBHS)[24] on the effects of the AITC skin challenge. Ideally, this broadens its applicability by further elucidating the downstream mechanisms of AITC-induced vasodilation. We measured dermal blood flow in healthy volunteers at four occasions: (1) baseline, (2) following dermal AITC administration, (3) during WBHS and (4) after AITC administration during WBHS. As expected, both AITC and WBHS independently increased dermal perfusion. Interestingly, their combined vasodilatory effect was smaller than the sum of their individual effects. This might be explained by a potential overlap between their NO-mediated vasodilatory pathways.[25]

We cannot draw specific conclusions about this overlap because the study lacked distal NO-related biomarkers to inform us about the individual and combined mechanistic effects of the two challenges. The short half-life and low topical concentrations of such markers, combined with the complexity of performing a methodologically reliable assessment, prevented us from measuring such biomarkers in the setting of our dynamic clinical trial.[26,27] Another approach to further elucidate the vasodilatory pathways would be to apply pharmacological interventions targeting specific components of the vasodilatory pathway. Currently, no such compounds meeting Good Manufacturing Practice-standards are available. If these become available in the future, similarly designed studies could aim to pharmacologically target the assumed vasodilatory pathways, for example by specific nitric oxide synthetase blockers.

Despite these limitations, the study demonstrated the feasibility of applying AITC, WBHS and their combination in the setting of an early-phase clinical trial. Moreover, the observed vasodilatory responses were consistent with prior research employing each challenge individually, supporting their reproducibility and generalisability within the studied population.[11,28,29] This enhances the applicability of the models in early-phase clinical trials.

As TRPA1 agonist inducing NO-mediated vasodilation, AITC is pre-eminently suitable for assessing the pharmacodynamic effects of TRPA1 antagonistic drug candidates.[11] This model could therefore facilitate translation of preclinical findings about the TRPA1 antagonistic properties of the candidate drugs to the clinical phase and support more efficient and informative drug development.[5–7]

In chapter 3, we applied AITC to study proof-of-pharmacology of TRPA1 antagonist BI 1839100 in a first-in-human single-ascending dose study. Additionally, in vitro and in vivo data demonstrating TRPA1 antagonistic properties of BI 1839100 were presented and clinical safety and pharmacokinetics (PK) of BI 1839100 were studied. The clinical study indicated that BI 1839100 was safe and well tolerated in single oral doses up to 300 MG in healthy participants, with predominantly mild adverse events (AEs) and no imbalance in AEs incidence between active and placebo groups. PK analyses revealed a dose-proportional increase in drug exposure (40 MG - 300 MG). At higher doses an increasing half-life accompanied by a reduced fractional excretion of BI 1839100 in urine was observed. This might indicate saturation of renal excretion, for example saturation of active tubular secretion as is often observed for example in the excretion of metformin, methotrexate and several antibiotics.[30]

To assess BI 1839100's TRPA1 engagement in humans we performed the AITC skin challenge in two dose groups (40 MG and 120 MG) prior to dosing and at the time of the maximal BI 1839100 plasma concentration. BI 1839100 dose-dependently suppressed the AITC-induced dermal blood flow and dermal response size compared to placebo, indicating TRPA1 target engagement.[31] Comparable findings were reported for another TRPA1 antagonist (GDC-0334) that underwent a phase I study with an AITC skin challenge. It had a similar safety profile and fully inhibited the AITC-induced vasodilatory response in the highest dose group.[32] This full inhibition was not

achieved in our study, despite anticipating this based on the GDC-0334 study and preclinical IC_{50}- and IC_{90}-values of calcium influx inhibition by BI 1839100 in AITC stimulated HEK293 cells. This discrepancy could be explained by the fact that we only performed the AITC skin challenge in two dose groups. Therefore, it is possible that the data from the in vitro AITC experiment are not fully translatable to the in vivo human vasodilatory response and that higher doses of BI 1839100 might have achieved complete inhibition. Furthermore, it can be envisioned that AITC displays off-target activity leading to vasodilation that was not inhibited by partial TRPA1 antagonism by BI 1839100. For example, it is known that AITC initiates mild vasodilation in TRPA1 knock out rats via transient receptor potential cation channel subfamily V member 1 (TRPV1) signalling.[11] Additionally, secondary pathway activation of nuclear factor kappa-light-chain-enhancer of activated B-cells (NF-κB) inflammatory signalling and inhibition of voltage-gated CA^{2+} in vascular smooth muscle cells following TRPA1 agonism might lead to vasodilation.[33,34] However, the findings from the GDC-0334 oppose this theory of off-target vasodilatory activity of AITC. Regardless of achieving full inhibition of AITC-induced vasodilation in the first-in-human studies of TRPA1-antagonists, future research in patient populations will reveal the translation to clinical efficacy. It can be envisioned that drug exposure concentrations far below those needed to achieve 100% inhibition of AITC-induced vasodilation already induce beneficial effects for patients.

The findings in our study reinforce the value of the AITC skin challenge as translational tool to bridge between preclinical and clinical research and to demonstrate target engagement. The observed incomplete translatability of preclinical to clinical findings highlights the importance of conducting thorough human in vivo challenge studies to characterise pharmacodynamic responses of novel therapeutics. Additionally, such data from clinical studies can guide data-driven informed dose selection in subsequent development stages. Overall, investigators and drug developers should be encouraged to apply the AITC skin challenge in the early stages of clinical development of drug candidates, specifically TRPA1 antagonists or NO-targeting agents, to enhance efficiency and informativeness of their drug development programmes.[35-37]

The molecular aspects of TRPA1-induced inflammation are understudied and represent an interesting potential extension of the AITC skin challenge. Rodent studies show that TRPA1 activation contributes to leukocyte infiltration, cytokine release and cutaneous immune cell activation.[38] TRPA1 also contributes to histamine-dependent pruritus, a key symptom that negatively influences the quality of life of atopic dermatitis and allergic contact dermatitis patients.[39,40] In humans, however, the extent to which inflammatory phenomena occur after topical AITC administration is unclear. Erythema typically resolves within one hour after AITC application, suggesting a short-lived mild inflammatory response. Yet one study reported hyperpigmentation as post-inflammatory sign at 64 hours after AITC, implying more sustained inflammation.[10,41] Future clinical studies could therefore focus on unravelling the inflammatory aspects of the AITC challenge, including cellular- and cytokine-level effects. This may broaden its applicability to studying time courses of AITC-induced inflammation and the potential modulation of this inflammatory response by pharmaceuticals under development for diseases such as atopic dermatitis.

LPS – Findings and future perspectives

Another inflammatory human challenge model suitable for assessing proof-of-pharmacology in early-phase clinical drug development is the ID LPS model. Injection of ID LPS induces a Toll-like receptor 4 (TLR4)-mediated, transient, localised innate immune response consisting of two major components. Namely, a vascular component, characterised by increased dermal perfusion and erythema, and an inflammatory component, involving the recruitment of immune cells and cytokine production. Although the immunological clinical endpoints of the ID LPS challenge have been extensively studied,[9,12] its potential as a model for controlled induction of vascular responses and the transcriptomic and proteomic profiles underlying its clinical effects remained largely unexplored.

Vascular responses, including vascular leakage, are a feature of the pathophysiology of numerous acute and chronic diseases and contribute to both morbidity and disease progression.[42,43] As

multiple vascular response- and leakage-targeting drug candidates are currently under development,[44–46] there is a clear opportunity for studying proof-of-pharmacology in early-phase clinical research using human challenge models that mimic these pathophysiological processes. However, such models have not been developed yet.

Chapter 4 aimed to fill this gap by characterising the ID LPS challenge as model for vascular responses and vascular leakage in healthy volunteers. By integrating data on vasodilation, skin volume changes, endothelial activation, and protein extravasation, we demonstrated that ID LPS injection elicits an objectifiable vascular response accompanied by vascular leakage. Specifically, we reported increased skin volumes based on dermal imaging and increased albumin and total protein concentrations in blister fluid as markers of vascular leakage after ID LPS injection. Additionally, we demonstrated the presence of vascular hyperpermeability after LPS, including relative increases in endothelial activation markers (e.g. ICAM-1 and VCAM-1) and an increased number of neutrophils in blister fluid.[47]

A major strength of the ID LPS model is its simultaneous induction of measurable inflammatory and vascular responses. This mimics pathophysiological mechanisms that are also seen in disease, as diseases displaying increased vascular permeability almost invariably also involve inflammation. In sepsis, for example, systemic inflammation leads to endothelial dysfunction, tight-junction disruption and marked peripheral and pulmonary vascular leakage.[48] Similarly, although these concern chronic conditions as opposed to acute inflammatory hits, the inflammatory states in cancer and diabetes are associated with impaired endothelial barrier integrity and increased microvascular permeability.[42,43] Thus, the combined inflammatory and vascular profile of the ID LPS model offers important translational relevance for a wide range of diseases. A further strength of the model is its controlled, high-precision ability to assess localised vascular leakage over time, without the logistical and safety limitations of systemic challenges in healthy volunteers, such as seen in the intravenous LPS challenge.[49]

During the development of a human challenge model for such vascular responses, we would ideally demonstrate that the ID LPS-induced vascular responses are modifiable by vascular-targeting drugs. As no approved drugs are available on the market, we were unable to do that. However, unpublished data indicate that an experimental mitogen-activated protein kinase inhibitor can fully suppress LPS-induced increases in skin volume, suggesting that plasma extravasation after ID LPS can indeed be pharmacologically modified. Given the expanding pipeline of vasculature-targeted drugs, generation of confirmatory data should only be a matter of time.[44–46]

Besides increasing efficiency of drug development by studying proof-of-pharmacology using human challenge models, applying an omics approach could also combat the high attrition rates in clinical drug development. By integrating biological, computational and pharmacological knowledge, such approaches enable pathway- and mechanism-focused research into disease biology and mechanisms of action (MoAs) and pharmacodynamic effects of drug candidates in a clinical environment.[50,51] This approach enhances target identification and improves efficacy predictability and target validation in clinical trials. Thereby the drug development pipeline could be optimised as compared to traditional development strategies.[51–53] Interestingly, data derived from human challenge models can be integrated in such novel omics approaches. This aids optimisation of human challenge model selection based on alignment between target expression and MoA engagement of drug candidates in the omics data.[6]

Chapter 5 presents a comprehensive omics framework characterising the human response to ID LPS injection, including transcriptomic, proteomic, and translational perspectives. We demonstrated that ID LPS injection induces a transcriptomic inflammatory signature in skin tissue, marked by enrichment of innate immunity- and receptor signalling-related pathways, including TLR4 signalling and its downstream genes. These transcriptomic changes also translated to proteomic changes including significantly increase expression of inflammatory proteins downstream of TLR4. Importantly, the transcriptomic dataset displayed substantial overlap with the annotated gene sets of a range of immunological and inflammatory diseases, underlining the translational relevance of the ID LPS model for drug development.

Collectively, these findings provide a reference to guide challenge model selection in early-phase clinical trials of immunomodulatory

drugs. This should be performed based on whether the MoA of drug candidates overlaps with targets and pathways driven by ID LPS, and whether these display overlap with the annotated gene sets of diseases relevant to the tested drugs. Moreover, these insights offer a resource for assessing whether anti-inflammatory drug candidates modulate mechanisms relevant to target diseases early in clinical development.

Future research could build on these findings by further elucidating the contributions of individual cells to the transcriptomic changes observed. Focussing on specific elements of the observed inflammatory response (e.g. complement and inflammasome activation), which may represent druggable targets, is another interesting future direction research could take.[54–56] Ultimately, integrating these data with existing data on both the human ID LPS response and inflammatory disease biology could support a systems biology approach to anti-inflammatory drug development to further enhance drug development programmes.[50,57]

SECTION 2: UNCONTROLLED INFLAMMATORY RESPONSES

AIS – Observations and recommendations

In contrast to human inflammatory challenge models that induce mild, transient inflammatory responses in a controlled setting, AIS represents an uncontrolled inflammatory reaction that can occur during clinical studies.[14,58] These reactions are caused by the IMP itself. In recent years, the increasing structural complexity of immunomodulatory drugs, especially of bispecific or Fc-engineered antibodies, has been associated with an increase in AIS incidence.[13,14] AIS can result from multiple mechanisms, including IMP structure- or formulation-issues, exaggerated pharmacological activity (on- and off-target), or anti-drug-antibody-induced immune complex formation.[13,59,60] Despite the growing incidence of AIS in early-phase clinical trials, with great impact on study participant safety and efficiency of drug development programmes, no comprehensive evidence-based guidance or framework for its prediction, prevention, and evaluation currently exists.[61] Furthermore, early-phase clinical trials in which AIS occurs are often not published, limiting our collective knowledge and potential scientific progression in this area.[62]

Chapter 6 of this thesis presents lessons learned from three clinical cases of drug-induced AIS, in the context of the current regulatory guidance. We illustrated that AIS can arise despite adherence to the existing FDA- and ICH- guidelines for preclinical and clinical risk assessment of drug candidates. This highlights the limited predictability of AIS and the need for a more refined approach. Furthermore, currently there is no regulatory obligation to study specific details upon AIS occurrence in clinical studies, preventing us from learning from the incidents.[60,63,64]

To address this problem, we proposed that it is crucial for clinical researchers and pharmaceutical companies to extensively discuss the IMP's potential to evoke AIS during the design of the first clinical study. Furthermore, local regulatory agencies can be actively approached to weigh in on the discussions. Such discussions enable timely extension of the preclinical knowledge on the IMP's characteristics (if needed) and aid anticipation on the potential occurrence of AIS. This anticipation includes the implementation of evidence-based, IMP-specific AIS management, mitigation, and monitoring protocols.[65] Such dedicated protocols should include practical instructions detailing procedures for detection and management of AIS, complemented by a description of relevant biomarker analyses to conduct upon AIS occurrence.[66]

Future studies that apply enhanced collaboration between investigators, pharmaceutical companies and local regulators, combined with comprehensive management protocols and analysis of AIS (if it occurs), will benefit from more effective management of AIS and a simultaneous increase in the understanding of mechanisms underlying IMP-induced AIS. Ultimately, this knowledge supports informed, data-driven decision making in the continuation or modification of the drug development programme, improving further clinical development.

CONCLUSION

Throughout this thesis we aimed to expand knowledge of controlled and uncontrolled inflammatory responses within early-phase clinical pharmacological research, ultimately advancing immunological clinical drug development.

The studies employing the AITC model demonstrated that the induction of controlled inflammation in healthy volunteers can effectively be used to assess pharmacodynamic effects and target engagement in early-phase clinical trials. Furthermore, we characterised the ID LPS model for vascular leakage, thereby broadening its utility for future early-phase clinical trials. The accompanying multi-omics analyses of the ID LPS response provided in-depth mechanistic insights and links the model to disease-relevant pathways, strengthening its translational value for drug development. Together, these advances expand the knowledge and applicability of controlled human inflammatory challenge models, enabling informative proof-of-pharmacology studies for immune-targeting drug candidates in early-phase drug development.

In parallel, our evaluation of three clinical cases of AIS underscored that uncontrolled inflammatory responses remain difficult to predict and evaluate, despite existing regulatory guidance. These findings highlight the need for systematic AIS management protocols, evaluation strategies and enhanced collaborations between investigators, sponsors and regulatory authorities. These approaches improve anticipation on AIS, management of AIS and aid data-driven decision making in the drug development programme.

It is hoped that the insights gained from this thesis contribute to the informational and translational value of early-phase clinical pharmacological studies in the future. Ultimately, this will translate into safer, more efficient and more informative drug development programmes, reducing resource usage while enabling faster delivery of effective therapies to patients.

REFERENCES

1. Sun D, Gao W, Hu H, Zhou S. Why 90% of clinical drug development fails and how to improve it? *Acta Pharm Sin B*. 2022;12(7):3049-3062. doi:10.1016/j.apsb.2022.02.002
2. Harrison RK. Phase II and phase III failures: 2013-2015. *Nat Rev Drug Discov*. 2016;15(12):817-818. doi:10.1038/nrd.2016.184
3. Smietana K, Siatkowski M, Møller M. Trends in clinical success rates. *Nat Rev Drug Discov*. 2016;15(6):379-380. doi:10.1038/nrd.2016.85
4. DiMasi JA, Grabowski HG, Hansen RW. Innovation in the pharmaceutical industry: New estimates of R&D costs. *J Health Econ*. 2016;47:20-33. doi:10.1016/j.jhealeco.2016.01.012
5. Schmidt B. Proof of principle studies. *Epilepsy Res*. 2006;68(1):48-52. doi:10.1016/j.eplepsyres.2005.09.019
6. Chen C. Opportunities and pitfalls in clinical proof-of-concept: principles and examples. *Drug Discov Today*. 2018;23(4):776-787. doi:10.1016/j.drudis.2018.01.045
7. Hijma HJ, Groeneveld GJ. Analgesic drug development: proof-of-mechanism and proof-of-concept in early phase clinical studies. *Med Drug Discov*. 2021;10:100083. doi:10.1016/j.medidd.2021.100083
8. Adams-Phipps J, Toomey D, Więcek W, et al. A Systematic Review of Human Challenge Trials, Designs, and Safety. *Clinical Infectious Diseases*. 2023;76(4):609-619. doi:10.1093/cid/ciac820
9. Buters TP, Hameeteman PW, Jansen IME, et al. Intradermal lipopolysaccharide challenge as an acute in vivo inflammatory model in healthy volunteers. *Br J Clin Pharmacol*. 2022;88(2):680-690. doi:10.1111/bcp.14999
10. Andersen HH, Lo Vecchio S, Gazerani P, Arendt-Nielsen L. Dose-response study of topical allyl isothiocyanate (mustard oil) as a human surrogate model of pain, hyperalgesia, and neurogenic inflammation. *Pain*. 2017;158(9):1723-1732. doi:10.1097/j.pain.0000000000000979
11. Joseph V, Yang X, Gao SS, et al. Development of AITC-induced dermal blood flow as a translational in vivo biomarker of TRPA1 activity in human and rodent skin. *Br J Clin Pharmacol*. 2021;87(1):129-139. doi:10.1111/bcp.14370
12. Buters TP, Hameeteman PW, Jansen IME, et al. Clinical, Cellular, and Molecular Effects of Corticosteroids on the Response to Intradermal Lipopolysaccharide Administration in Healthy Volunteers. *Clin Pharmacol Ther*. 2022;111(4):964-971. doi:10.1002/cpt.2516
13. Reijers JAA, Malone KE, Bajramovic JJ, Verbeek R, Burggraaf J, Moerland M. Adverse immunostimulation caused by impurities: The dark side of biopharmaceuticals. *Br J Clin Pharmacol*. 2019;85(7):1418-1426. doi:10.1111/bcp.13938
14. Baldo BA. Immune-and Non-Immune-Mediated Adverse Effects of Monoclonal Antibody Therapy: A Survey of 110 Approved Antibodies. *Antibodies*. 2022;11(1):17. doi:10.3390/antib11010017
15. Fauconnier A, Melis M, Berenbeck M, Pio B, Croisier T. Trends in the drug target landscape for autoimmune diseases. *Nat Rev Drug Discov*. 2025;24(6):415-416. doi:10.1038/d41573-025-00061-7
16. Conrad N, Misra S, Verbakel JY, et al. Incidence, prevalence, and co-occurrence of autoimmune disorders over time and by age, sex, and socioeconomic status: a population-based cohort study of 22 million individuals in the UK. *The Lancet*. 2023;401(10391):1878-1890. doi:10.1016/S0140-6736(23)00457-9
17. van der Kolk T, Assil S, Rijneveld R, et al. Comprehensive, Multimodal Characterization of an Imiquimod-Induced Human Skin Inflammation Model for Drug Development. *Clin Transl Sci*. 2018;11(6):607-615. doi:10.1111/cts.12563
18. Pozsgai G, Bodkin J V., Graepel R, Bevan S, Andersson DA, Brain SD. Evidence for the pathophysiological relevance of TRPA1 receptors in the cardiovascular system in vivo. *Cardiovasc Res*. 2010;87(4):760-768. doi:10.1093/cvr/cvq118
19. Eberhardt M, Dux M, Namer B, et al. H2S and NO cooperatively regulate vascular tone by activating a neuroendocrine HNO-TRPA1-CGRP signalling pathway. *Nat Commun*. 2014;5:4381. doi:10.1038/ncomms5381
20. Wang Z, Ye D, Ye J, et al. The TRPA1 channel in the cardiovascular system: Promising features and challenges. *Front Pharmacol*. 2019;10:1253. doi:10.3389/fphar.2019.01253

21. Wong BJ. Sensory nerves and nitric oxide contribute to reflex cutaneous vasodilation in humans. *Am J Physiol Regul Integr Comp Physiol*. 2013;304(8):651-656. doi:10.1152/ajpregu.00464.2012.
22. Andrei SR, Ghosh M, Sinharoy P, Damron DS. Stimulation of TRPA1 attenuates ischemia-induced cardiomyocyte cell death through an eNOS-mediated mechanism. *Channels*. 2019;13(1):192-206. doi:10.1080/19336950.2019.1623591
23. Holowatz LA, Houghton BL, Wong BJ, et al. Nitric oxide and attenuated reflex cutaneous vasodilation in aged skin. *Am J Physiol Heart Circ Physiol*. 2003;284(5):H1662-H1667. doi:10.1152/ajpheart.00871.2002
24. Kellogg DL, Zhao JL, Wu Y. Roles of nitric oxide synthase isoforms in cutaneous vasodilation induced by local warming of the skin and whole body heat stress in humans. *J Appl Physiol*. 2009;107(5):1438-1444. doi:10.1152/japplphysiol.00690.2009
25. van Ruissen MCE, van Kraaij SJW, Gal P, et al. Open-Label Interventional Study in Healthy Volunteers to Evaluate NO-Mediated Vasodilation by Dermal Allyl Isothiocyanate Challenge and Whole-Body Heat Stress. *J Exp Pharmacol*. 2024;16:285-294. doi:10.2147/JEP.S473217
26. Hunter RA, Storm WL, Coneski PN, Schoenfisch MH. Inaccuracies of nitric oxide measurement methods in biological media. *Anal Chem*. 2013;85(3):1957-1963. doi:10.1021/ac303787p
27. Coneski PN, Schoenfisch MH. Nitric oxide release: Part III. Measurement and reporting. *Chem Soc Rev*. 2012;41(10):3753-3768. doi:10.1039/c2cs15271a
28. Gemae MR, Akerman AP, McGarr GW, et al. Myths and methodologies: Reliability of forearm cutaneous vasodilatation measured using laser-Doppler flowmetry during whole-body passive heating. *Exp Physiol*. 2021;106(3):634-652. doi:10.1113/EP089073
29. Luetkemeier MJ, Allen DR, Huang M, et al. Skin tattooing impairs sweating during passive whole body heating. *J Appl Physiol*. 2020;129(5):1033-1038. doi:10.1152/japplphysiol.00427.2019
30. van Ginneken CAM, Russel FGM. Saturable Pharmacokinetics in the Renal Excretion of Drugs. *Clin Pharmacokinet*. 1989;16(1):38-54. doi:10.2165/00003088-198916010-00003
31. van Ruissen MCE, van Kraaij SJW, Wolfova J, et al. Proof of Pharmacology, Safety, and Pharmacokinetics of the Novel TRPA1 Antagonist BI 1839100: A Randomized, Placebo-Controlled, Parallel Group, First-In-Human Study in Healthy Male Participants. *Clin Transl Sci*. 2025;18(8):e70290. doi:10.1111/cts.70290
32. Balestrini A, Joseph V, Dourado M, et al. A TRPA1 inhibitor suppresses neurogenic inflammation and airway contraction for asthma treatment. *J Exp Med*. 2021;218(4):e20201637. doi:10.1084/JEM.20201637
33. Yao K, Dou B, Zhang Y, et al. Inflammation—the role of TRPA1 channel. *Front Physiol*. 2023;14:1093925. doi:10.3389/fphys.2023.1093925
34. Alvarez-Collazo J, Alonso-Carbajo L, López-Medina AI, et al. Cinnamaldehyde inhibits L-type calcium channels in mouse ventricular cardiomyocytes and vascular smooth muscle cells. *Pflugers Arch*. 2014;466(11):2089-2099. doi:10.1007/s00424-014-1472-8
35. Hu Z, Zhang Y, Yu W, et al. Transient receptor potential ankyrin 1 (TRPA1) modulators: Recent update and future perspective. *Eur J Med Chem*. 2023;257:115392. doi:10.1016/j.ejmech.2023.115392
36. Li H, Förstermann U, Xia N, Kuntic M, Münzel T, Daiber A. Pharmacological targeting of endothelial nitric oxide synthase dysfunction and nitric oxide replacement therapy. *Free Radic Biol Med*.. 2025;237:455-472. doi:10.1016/j.freeradbiomed.2025.06.009
37. Mason RP, Cockcroft JR. Targeting nitric oxide with drug therapy. *J Clin Hypertens*. 2006;8(12 Suppl 4):40-52. doi:10.1111/j.1524-6175.2006.06041.x
38. Gouin O, L'Herondelle K, Lebonvallet N, et al. TRPV1 and TRPA1 in cutaneous neurogenic and chronic inflammation: pro-inflammatory response induced by their activation and their sensitization. *Protein Cell*. 2017;8(9):644-661. doi:10.1007/s13238-017-0395-5
39. Maglie R, de Araujo DSM, Antiga E, Geppetti P, Nassini R, De Logu F. The role of trpa1 in skin physiology and pathology. *Int J Mol Sci*. 2021;22(6):1-13. doi:10.3390/ijms22063065
40. Ständer S, Yosipovitch G, Bushmakin AG, et al. Examining the association between pruritus and quality of life in patients with atopic dermatitis treated with crisaborole. *J Eur Acad Dermatol Venereol*. 2019;33(9):1742-1746. doi:10.1111/jdv.15712
41. Lawrence E, Syed H, Al Aboud K. Postinflammatory Hyperpigmentation. StatPearl Publishing; 2024. https://www.ncbi.nlm.nih.gov/books/NBK559150/. Accessed November 14, 2025.
42. Wautier JL, Wautier MP. Vascular Permeability in Diseases. *Int J Mol Sci*. 2022;23(7):3645. doi:10.3390/ijms23073645
43. Park-Windhol C, D'Amore PA. Disorders of Vascular Permeability. *Annu Rev Path*. 2016;11:251-281. doi:10.1146/annurev-pathol-012615-044506
44. Okada Y. Potential Therapeutic Strategies and Drugs That Target Vascular Permeability in Severe Infectious Diseases. *Biol Pharm Bull*. 2024;47(3):549-555. doi:10.1248/bpb.b24-00028
45. Darwish I, Conrad Liles W. Emerging therapeutic strategies to prevent infection-related microvascular endothelial activation and dysfunction. *Virulence*. 2013;4(6):572-582. doi:10.4161/viru.25740
46. Hajitou A, Pasqualini R, Arap W. Vascular targeting: Recent advances and therapeutic perspectives. *Trends Cardiovasc Med*. 2006;16(3):80-88. doi:10.1016/j.tcm.2006.01.003
47. van Ruissen MCE, van Diemen M, Botros L, et al. Breaking Barriers: Characterization of the Intradermal Lipopolysaccharide Challenge as an In Vivo Model for Controlled Induction of Vascular Leakage in Healthy Volunteers. *Clin Pharmacol Ther*. Published online November 15, 2025. doi:10.1002/cpt.70126
48. McMullan RR, McAuley DF, O'Kane CM, Silversides JA. Vascular leak in sepsis: physiological basis and potential therapeutic advances. *Crit Care*. 2024;28(1):97. doi:10.1186/s13054-024-04875-6
49. Dillingh MR, Van Poelgeest EP, Malone KE, et al. Characterization of inflammation and immune cell modulation induced by low-dose LPS administration to healthy volunteers. *J Inflam*. 2014;11(1):28. doi:10.1186/s12950-014-0028-1
50. Azer K, Leaf I. Systems biology platform for efficient development and translation of multitargeted therapeutics. *Front Syst Biol*. 2023;3:1229532. doi:10.3389/fsysb.2023.1229532
51. Galizzi JP, Lockhart BP, Bril A. Applying systems biology in drug discovery and development. *Drug Metabol Drug Interact*. 2013;28(2):67-78. doi:10.1515/dmdi-2013-0002
52. Hughes JP, Rees SS, Kalindjian SB, Philpott KL. Principles of early drug discovery. *Br J Pharmacol*. 2011;162(6):1239-1249. doi:10.1111/j.1476-5381.2010.01127.x
53. Fotis C, Antoranz A, Hatziavramidis D, Sakellaropoulos T, Alexopoulos LG. Network-based technologies for early drug discovery. *Drug Discov Today*. 2018;23(3):626-635. doi:10.1016/j.drudis.2017.12.001
54. Carnazzo V, Rigante D, Restante G, Basile V, Pocino K, Basile U. The entrenchment of NLRP3 inflammasomes in autoimmune disease-related inflammation. *Autoimmun Rev*. 2025;24(7):103815. doi:10.1016/j.autrev.2025.103815
55. Thurman JM, Yapa R. Complement therapeutics in autoimmune disease. *Front Immunol*. 2019;10(4):672. doi:10.3389/fimmu.2019.00672
56. Zarrin AA, Bao K, Lupardus P, Vucic D. Kinase inhibition in autoimmunity and inflammation. *Nat Rev Drug Discov*. 2021;20(1):39-63. doi:10.1038/s41573-020-0082-8
57. Burt T, Nandal S. Pharmacometabolomics in Early-Phase Clinical Development. *Clin Transl Sci*. 2016;9(3):128-138. doi:10.1111/cts.12396
58. Suntharalingam G, Perry MR, Ward S, et al. Cytokine Storm in a Phase 1 Trial of the Anti-CD28 Monoclonal Antibody TGN1412. *N Engl J Med*. 2006;355(10):1018-1028. doi:10.1056/NEJMoa063842
59. Mease KM, Kimzey AL, Lansita JA. Biomarkers for nonclinical infusion reactions in marketed biotherapeutics and considerations for study design. *Curr Opin Toxicol*. 2017;4:1-15. doi:10.1016/j.cotox.2017.03.005
60. FDA. Nonclinical Evaluation of the Immunotoxic Potential of Pharmaceuticals Guidance for Industry.; 2023. https://www.fda.gov/regulatory-information/search-fda-guidance-documents/nonclinical-evaluation-immunotoxic-potential-pharmaceuticals. Accessed January 24, 2024.
61. Descotes J. Safety immunopharmacology: Evaluation of the adverse potential of pharmaceuticals on the immune system. *J Pharmacol Toxicol Methods*. 2012;66(2):79-83. doi:10.1016/j.vascn.2012.05.001
62. Mitra-Majumdar M, Kesselheim AS. Reporting bias in clinical trials: Progress toward transparency and next steps. *PLoS Med*. 2022;19(1):e1003894. doi:10.1371/journal.pmed.1003894
63. ICH. ICH S8 Guideline: Immunotoxicity Studies for Human Pharmaceuticals.; 2005. https://www.ema.europa.eu/en/ich-s8-immunotoxicity-studies-human-pharmaceuticals-scientific-guideline. Accessed January 24, 2024.

64. ICH. ICH S6(R1) Guideline: Preclinical Safety Evaluation of Biotechnology-Derived.; 2011. https://www.ema.europa.eu/en/ich-s6-r1-preclinical-safety-evaluation-biotechnology-derived-pharmaceuticals-scientific-guideline. Accessed January 24, 2024.
65. van Ruissen MCE, van den Noort JA, Smidt LCA, et al. Adverse immunostimulation in early phase clinical trials: Key findings and recommendations based on the investigator's clinical experience. *Br J Clin Pharmacol*. Published online September 19, 2025. doi:10.1002/bcp.70276
66. van den Noort JA, Meijs AC, Klarenbeek NB, Moerland M. Navigating adverse immunostimulation: A practical guide for clinical researchers. *Br J Clin Pharmacol*. Published online September 12, 2025. doi:10.1002/bcp.70268

CHAPTER 8

Nederlandse samenvatting

INTRODUCTIE

De toepassing van farmacologische challenge-modellen in vroege fase medicijnonderzoek

De ontwikkeling van geneesmiddelen is een tijdrovend en kostbaar proces. De ontdekking van een nieuw medicijn tot zijn toelating tot de markt duurt doorgaans 10 tot 15 jaar en de kosten bedragen 1 tot 2 miljard euro (inclusief de kosten van alle mislukte kandidaat-geneesmiddelen). Van alle kandidaat-geneesmiddelen in de klinische onderzoeksfase haalt naar schatting 90% de toelating tot de markt niet, waarbij meer dan 50% van deze mislukkingen is toe te schrijven aan een gebrek aan werkzaamheid in de patiëntenpopulatie. Door de kennis over de farmacodynamische effecten en werkzaamheid van kandidaat-geneesmiddelen in de vroegste klinische onderzoeksfase te vergroten, zou het geneesmiddelontwikkelingsproces efficiënter en doeltreffender kunnen worden gemaakt.

Het toepassen van farmacologische proof-of-pharmacology experimenten in vroege fase geneesmiddelenstudies is een van de mogelijke strategieën om deze kennis te verkrijgen. De data uit zulke studies kunnen bijdragen aan het vroegtijdig stopzetten van de ontwikkeling van kandidaat-geneesmiddelen die geen tekenen van werkzaamheid vertonen. Daarnaast dragen ze bij aan de efficiënte verdere ontwikkeling van veelbelovende kandidaat-geneesmiddelen. Men is namelijk meer geïnformeerd over de effecten van een middel en kan daardoor betere toekomstige klinische studies ontwerpen met adequate selectie van geneesmiddeltargets, doseringen en relevante eindpunten. Deze aanpak leidt idealiter tot een vermindering van het aantal kandidaat-geneesmiddelen dat in late onderzoeksfasen afvalt vanwege een gebrek aan werkzaamheid.

Een praktische hindernis die overwonnen moet worden bij het uitvoeren van zulke proof-of-pharmacology experimenten in fase I geneesmiddelenstudies, is dat gezonde deelnemers niet de ziekte of aandoening hebben waarvoor waarvoor een geneesmiddel ontwikkeld wordt. Farmacologische of fysiologische challenge-modellen kunnen toegepast worden om deze hindernis te overwinnen. Zulke modellen bootsen namelijk door de toediening van een kunstmatige stimulus pathofysiologische processen, gerelateerd aan het werkingsmechanisme van een kandidaat-geneesmiddel of de ziekte waarvoor deze ontwikkeld wordt, mechanistisch na. Hierdoor is in een vroege fase dus al kennis te verkrijgen over de farmacodynamische effecten van kandidaat-geneesmiddelen.

Inflammatoire challenge-modellen

De laatste jaren is er steeds meer belangstelling voor het gebruik van dergelijke challenge-modellen in gezonde mensen. De ontwikkeling van inflammatoire modellen die gecontroleerde ontstekingen induceren staat echter nog in de kinderschoenen, terwijl het immunologische vakgebied in het bijzonder kan profiteren van meer vroege fase geneesmiddelstudies met een proof-of-pharmacology benadering. Het is namelijk bekend dat de prevalentie van immunologische ziekten toeneemt en tegelijkertijd wordt er een continu groeiend scala aan immunologische geneesmiddeltargets geïdentificeerd. Dit leidt logischerwijs tot een toename van het aantal immunomodulerende kandidaat-geneesmiddelen dat momenteel onderzocht wordt. Deze zouden profijt kunnen hebben van de inzet van humane challenge-modellen.

Voorbeelden van zulke inflammatoire modellen zijn de allylisothiocyanaat (AITC) huid challenge en de intradermale lipopolysaccharide (ID LPS) challenge. Door de lokale toediening van de pro-inflammatoire stimuli AITC of LPS wekken deze modellen onder gecontroleerde omstandigheden een tijdelijke, milde, lokale ontstekingsreactie op. Naast de primaire ontstekingsreactie wekken deze ontstekingsmodellen ook onderbelichte immuun-gemedieerde vasculaire reacties op, die relevant zijn voor een groot aantal ziektes waarop huidige geneesmiddelontwikkelingsprogramma's zich richten.

Ongewenste ontstekingsreacties in vroege fase medicijnonderzoek

In tegenstelling tot de beschreven gecontroleerde inflammatoire challenge-modellen in gezonde mensen, komen in klinisch-farmacologische studies ook wel eens ongewenste, ongecontroleerde

ontstekingsreacties voor die worden veroorzaakt door kandidaat-geneesmiddelen. Deze reacties staan bekend als ongewenste immuunstimulatie (OIS). OIS kan mechanistisch worden onderverdeeld in drie categorieën:

1 IgE-gemedieerde overgevoeligheidsreacties. Deze treden meestal op na herhaalde blootstelling aan het kandidaat-geneesmiddel. Deze reactie ontstaat door basofielen- en mestceldegranulatie na antigeenspecifieke IgE-binding aan hun FcεRI-receptoren.
2 Complementactiverings-gerelateerde pseudoallergie (CARPA). CARPA ontstaat door onbedoelde activering van de complementcascade na initiële blootstelling aan het geneesmiddel.
3 Cytokine release syndroom (CRS). CRS wordt gekenmerkt door een acute en overmatige afgifte van pro-inflammatoire mediatoren (TNF, IL-6, IL-1β, IFN-γ) bij blootstelling aan geneesmiddelen. Dit wordt gevolgd door wijdverspreide activering van immuuncellen en systemische ontsteking.

De klinische manifestatie van OIS is heterogeen en varieert van milde symptomen (bijvoorbeeld jeuk en buikpijn) tot levensbedreigende reacties (bijvoorbeeld shock met hypotensie, acute ademnood en meervoudig orgaanfalen). De vaak niet-specifieke aard van de symptomen bemoeilijkt de detectie van vroege stadia en milde verschijningsvormen van OIS. Hoewel de incidentie van OIS in klinische studies de afgelopen jaren lijkt toe te nemen, bestaan er nog geen duidelijke richtlijnen of een gestandaardiseerd kader voor de beoordeling van OIS.

DOEL VAN DIT PROEFSCHRIFT

Dit proefschrift beschrijft onderzoek dat gericht is op het bevorderen van immunologische klinische geneesmiddelontwikkeling. In deel 1 van dit proefschrift worden de gecontroleerde vasculaire en inflammatoire effecten van de AITC en ID LPS-challenge mechanistisch onderzocht. In deel 2 worden huidige regulatoire overwegingen aangaande OIS geëvalueerd en worden inzichten besproken die zijn verkregen uit drie first-in-human studies waarin OIS optrad.

DEEL 1: GECONTROLEERDE ONTSTEKINGSREACTIES

Bevindingen in dit proefschrift en bijbehorende toekomstperspectieven

AITC–ACHTERGROND

AITC is een natuurlijke stof die de scherpe smaak van kruisbloemige groenten, zoals knoflook, mosterd en wasabi, veroorzaakt. Het AITC challenge-model is gebaseerd op dermale toediening van AITC. Dit veroorzaakt een neurogene ontstekingsreactie die wordt gemedieerd door afgifte van calciumafhankelijke neuropeptiden na activering van het transient receptor potential cation kanaal A1 (TRPA1). De belangrijkste uitleesmaat van dit challenge-model is de lokale vasodilatoire respons. De verhoogde perfusie wordt gekwantificeerd met behulp van laser speckle contrast beeldvorming. Sommige onderzoekers hebben ook de pijnintensiteit bestudeerd om de veiligheid en mogelijke toepasbaarheid van AITC als challenge-model voor pijn te onderzoeken. Andere aspecten van de door TRPA1-geïnduceerde neurogene ontstekingsreactie, zoals bijvoorbeeld cytokine-afgifte en celattractie, zijn tot nu toe niet onderzocht.

Preklinisch onderzoek in cellen en in dieren wijst uit dat de vasodilatoire respons die wordt waargenomen na dermale AITC-toediening wordt gemedieerd door agonisme van TRPA1 specifiek aanwezig op dermale sensorische zenuwen. De vasoactieve neuropeptiden die vrijkomen na TRPA1-agonisme stimuleren de productie van stikstofmonoxide (NO) in endotheelcellen. Het effect daarvan is relaxatie van vasculaire gladde spiercellen en dus vasodilatatie. Er wordt aangenomen dat deze mechanismen ook van toepassing zijn bij mensen. Echter, het exacte mechanisme, inclusief alle bijdragende mediatoren, is in mensen nog niet volledig onderzocht. Gezien deze onvolledige kennis over de vasodilatoire mechanismen en andere inflammatoire aspecten van TRPA1-geïnduceerde ontsteking, is de huidige klinisch-farmacologische toepasbaarheid van het model beperkt tot het testen van farmacodynamische effecten van directe TRPA1-antagonisten.

AITC – MECHANISTISCHE EXPLORATIES VAN VASODILATATIE

In hoofdstuk 2 van dit proefschrift hebben we de effecten van een NO-gedreven vasodilatoire challenge (systemische warmtestress) op de vasodilatoire effecten van de AITC challenge bestudeerd. Op deze manier wilden we meer inzicht bieden in de vasodilatoire mechanismen van de AITC challenge bij mensen, om zo de toepasbaarheid van deze challenge te verbreden. In dit hoofdstuk hebben we de dermale bloedstroom vier keer gemeten bij gezonde vrijwilligers: (1) vóór en (2) na dermale toediening van AITC, (3) tijdens systemische warmtestress en (4) na toediening van AITC tijdens systemische warmtestress. Zoals verwacht op basis van eerdere onderzoeken zorgden zowel AITC als systemische warmtestress onafhankelijk van elkaar voor een toename van de dermale perfusie. Een interessante observatie was dat hun vasodilatoire effect kleiner was wanneer de challenges tegelijkertijd gebruikt werden dan de som van hun vasodilatoire effecten als de challenges los van elkaar werden toegepast. Deze observatie kan worden verklaard door een mogelijke overlap tussen de NO-gemedieerde vasodilatoire mechanismen van de twee challenges.

Over de exacte bijdragende factoren in deze overlap kunnen we geen specifieke conclusies trekken omdat onze studie geen distale NO-gerelateerde biomarkers bevatte. Zulke biomarkers zouden informatie kunnen verschaffen over de individuele en gecombineerde mechanistische effecten van de twee challenges. De korte halfwaardetijd en lage lokale concentraties van dergelijke markers, in combinatie met de complexiteit van het uitvoeren van methodologisch betrouwbare laboratoriumtests voor zulke markers, beletten ons om deze biomarkers te meten. Een andere benadering om de vasodilatoire mechanismen verder te verduidelijken, is de toepassing van farmacologische interventies die gericht zijn op specifieke componenten van de vasodilatoire mechanismen. Momenteel zijn er geen Good Manufacturing Practice (GMP)-kwaliteit medicijnen hiervoor beschikbaar. Als deze in de toekomst beschikbaar komen, zouden soortgelijke studies zich kunnen richten op het farmacologisch moduleren van mediatoren binnen de veronderstelde vasodilatoire routes, zoals specifieke NO-synthetase-blokkers. Ondanks deze beperkingen heeft de studie de haalbaarheid aangetoond van het toepassen van AITC, systemische warmtestress en hun combinatie in het kader van een vroege fase klinische studie. Bovendien waren de waargenomen vasodilatoire reacties consistent met eerder onderzoek waarbij beide middelen afzonderlijk werden toegepast. Dit ondersteunt de reproduceerbaarheid en generaliseerbaarheid van de twee challenges binnen de onderzochte populatie en vergroot de toepasbaarheid van deze challenges in vroege fase klinische studies.

AITC – FARMACODYNAMISCHE EFFECTEN VAN EEN TRPA1-ANTAGONISTISCH KANDIDAAT-GENEESMIDDEL

Als TRPA1-agonist die NO-gemedieerde vasodilatatie induceert, is AITC bij uitstek geschikt voor het beoordelen van de farmacodynamische effecten van TRPA1-antagonistische kandidaat-geneesmiddelen. Dit model kan daarom de vertaling van preklinische bevindingen over de TRPA1-antagonistische eigenschappen van kandidaat-geneesmiddelen naar de klinische fase vergemakkelijken en een efficiënter en informatiever geneesmiddelontwikkelingsproces ondersteunen.

In hoofdstuk 3 hebben we de AITC challenge toegepast om de farmacologische werking van TRPA1-antagonist BI 1839100 te onderzoeken in een first-in-human studie in gezonde mannen. Daarnaast lieten we in vitro- en in vivo-gegevens zien die de TRPA1-antagonistische eigenschappen van BI 1839100 aantonen en werden de klinische veiligheid en farmacokinetiek van BI 1839100 onderzocht. Het klinische onderzoek wees uit dat voor gezonde mannen enkele doseringen BI 1839100 tot 300 MG veilig waren en goed werden verdragen. Er waren overwegend milde bijwerkingen (zoals hoofdpijn en vermoeidheid) en er was geen verschil in de incidentie van bijwerkingen tussen de BI 1839100 en de placebogroepen. Farmacokinetische analyses toonden een dosis-proportionele toename van de blootstelling aan het geneesmiddel (40 MG - 300 MG). Bij hogere doses werd een toenemende halfwaardetijd waargenomen, gepaard gaande met een verminderde fractionele uitscheiding van BI 1839100 in de urine. Dit zou kunnen duiden op verzadiging van de renale uitscheiding, bijvoorbeeld verzadiging van de actieve tubulaire secretie zoals ook wordt waargenomen bij andere geneesmiddelen (bv. metformine, methotrexaat en verschillende antibiotica).

Om de TRPA1-binding van BI 1839100 in mensen te bestuderen, hebben we de AITC challenge uitgevoerd in twee doseringsgroepen (40 MG en 120 MG). Eenmaal werd dit gedaan voorafgaand aan de toediening van BI 1839100 en vervolgens werd dit herhaald op de T_{max}. We zagen dat BI 1839100 op een dosisafhankelijke manier de intensiteit en grootte van de door AITC-geïnduceerde toegenomen dermale bloedstroom onderdrukte. Dit wijst er op dat BI 1839100 bindt aan zijn target in gezonde mensen (proof-of-pharmacology). Vergelijkbare bevindingen werden gerapporteerd voor een andere TRPA1-antagonist (GDC-0334) die in het verleden ook een fase I studie met een AITC challenge onderging. GDC-0334 had een vergelijkbaar veiligheidsprofiel en remde de door AITC geïnduceerde vasodilatoire respons volledig in de hoogste doseringsgroep. Deze volledige remming werd in onze studie niet bereikt, ondanks dat we dit hadden verwacht op basis van de GDC-0334-studie en preklinische data (nl. IC_{50}- en IC_{90}-waarden van calciuminflux-remming door BI 1839100 in AITC-gestimuleerde HEK293-cellen). Deze discrepantie kan worden verklaard door het feit dat we de AITC-huidtest slechts in twee doseringsgroepen hebben uitgevoerd en het waarschijnlijk is dat de in vitro data niet één-op-één vertaalbaar zijn naar de in vivo vasodilatoire respons in mensen. Daarom is het mogelijk dat met hogere doses BI 1839100 volledige remming hadden kunnen bereiken. Daarnaast kan worden beargumenteerd dat AITC off-target activiteit vertoont die leidt tot vasodilatatie die niet wordt geremd door TRPA1-antagonisme door BI 1839100. Het is bijvoorbeeld bekend dat AITC via transient receptor potential cation kanaal V1 (TRPV1)-signalering milde vasodilatatie in TRPA1-knock-out ratten initieert. Ook zou de secundaire activatie van nuclear factor kappa-light-chain-enhancer of activated B-cells (NF-κB) inflammatoire signalering en de remming van spanningsafhankelijke Ca^{2+} in vasculaire gladde spiercellen na TRPA1-agonisme kunnen leiden tot vasodilatatie. De volledige inhibitie die bereikt werd in de GDC-0334 studie spreekt deze argumentatie tegen. Ongeacht of er volledige remming van AITC-geïnduceerde vasodilatatie wordt bereikt in first-in-human studies met TRPA1-antagonisten, zal toekomstig onderzoek in patiënten de vertaling naar klinische werkzaamheid gaan aantonen. Het is namelijk goed mogelijk dat bij lagere geneesmiddelconcentraties, onder de benodigde concentraties om volledige remming van AITC-geïnduceerde vasodilatatie te bewerkstelligen, al gunstige effecten voor patiënten teweeg worden gebracht.

De bevindingen in onze studie versterken de waarde van de AITC challenge als translationeel instrument tussen preklinisch en klinisch onderzoek en als middel om TRPA1-target binding aan te tonen. De waargenomen onvolledige transleerbaarheid van de preklinische naar klinische bevindingen benadrukt het belang van grondig proof-of-pharmacology onderzoek in mensen om de farmacodynamische reacties van kandidaat-geneesmiddelen te karakteriseren. Bovendien kunnen gegevens uit zulke klinische studies als leidraad dienen voor een evidence-based, geïnformeerde doseringskeuze in latere geneesmiddelstudies. Dit verbetert idealiter de efficiëntie en informatieve waarde van geneesmiddelontwikkelingsprogramma's. Onderzoekers en geneesmiddelontwikkelaars doen er daarom goed aan om de AITC challenge toe te passen in de vroege stadia van de klinische ontwikkeling van met name hun TRPA1-antagonistische of NO-gerichte kandidaat-geneesmiddelen.

Tot slot zouden de moleculaire aspecten van TRPA1-geïnduceerde ontsteking, die tot nu toe onderbelicht zijn, een interessante mogelijke uitbreiding van de AITC challenge zijn. Studies in knaagdieren tonen aan dat TRPA1-activering bijdraagt aan leukocyteninfiltratie, cytokine-afgifte en activering van immuuncellen in de huid. TRPA1 draagt ook bij aan histamine-afhankelijke jeuk, een belangrijk symptoom dat de kwaliteit van leven van patiënten met atopische dermatitis en allergische contact dermatitis negatief beïnvloedt. Bij mensen is het echter onduidelijk in hoeverre ontstekingsverschijnselen optreden na lokale toediening van AITC. Erytheem verdwijnt doorgaans binnen een uur na toediening van AITC, wat wijst op een kortdurende milde ontstekingsreactie. Maar er is één onderzoek dat hyperpigmentatie als post-inflammatoir teken tot 64 uur na AITC rapporteerde, wat duidt op langdurigere aanwezigheid van de ontstekingsreactie. Toekomstige klinische studies zouden zich daarom kunnen richten op de nadere ontrafeling van ontstekingsaspecten van de AITC challenge, inclusief de effecten op cellulair en cytokine niveau. Hiermee zou de toepasbaarheid van het model kunnen worden uitgebreid, zodat er naast vasodilatoire responsen ook

andere aspecten van de AITC geïnduceerde inflammatoire respons bestudeerd kunnen worden, inclusief de mogelijke modulatie van deze responsen door geneesmiddelen voor ziekten zoals atopische dermatitis.

LPS–ACHTERGROND

Een ander inflammatoir humaan challenge-model dat geschikt is voor het bestuderen van de farmacologische werking van kandidaat-geneesmiddelen in de vroege fase van hun klinische ontwikkeling is het ID LPS-model. Injectie van ID LPS induceert een door Toll-like receptor 4 (TLR4) gemedieerde kortdurende, lokale immuunrespons. Deze response bestaat uit twee belangrijke componenten: een vasculaire component, gekenmerkt door verhoogde dermale perfusie en erytheem, en een inflammatoire component, waarbij lokaal immuun cellen worden gerekruteerd en cytokines worden geproduceerd. De cellulaire infiltratie volgt een temporeel patroon met een snelle toename van neutrofielen, gevolgd door influx van monocyten, dendritische cellen en T-cellen. Deze respons gaat gepaard met de lokale toename van cytokines zoals IL-1β, IL-6, IL-8, IFN-γ en TNF. Hoewel deze immunologische klinische eindpunten uitgebreid zijn onderzocht, was het model nog niet goed gekarakteriseerd voor gecontroleerde inductie van vasculaire responsen en ook niet voor de RNA en eiwit profielen die ten grondslag liggen aan de klinische effecten van ID LPS.

LPS–EEN MODEL VOOR VASCULAIRE LEKKAGE

Vasculaire reacties, waaronder vasculaire lekkage, zijn een kenmerk van de pathofysiologie van talrijke acute en chronische ziekten en dragen bij aan zowel morbiditeit als ziekteprogressie. Aangezien er momenteel meerdere kandidaat-geneesmiddelen in ontwikkeling zijn die gericht zijn op vasculaire responsen en lekkage, is er markt voor om in vroeg stadium klinisch onderzoek te doen naar hun farmacologische werking. Dit kan gedaan worden met behulp van challenge-modellen die mechanistisch gezien relevante vasculaire pathofysiologische processen nabootsen.

Hoofdstuk 4 had als doel om de ID LPS-challenge te karakteriseren als model voor zulke vasculaire reacties en vasculaire lekkage bij gezonde mensen. Door data over vasodilatatie, veranderingen in het huidvolume, endotheliale activering en eiwitextravasatie te integreren, hebben we in dit hoofdstuk aangetoond dat LPS-injectie een objectiveerbare vasculaire reactie teweegbrengt die gepaard gaat met vasculaire lekkage. We rapporteerden namelijk een toename van het huidvolume en een toename van de albumine en totale eiwit concentraties in blaarvocht, als markers van vasculaire lekkage na LPS-injectie. Daarnaast hebben we de aanwezigheid van vasculaire hyperpermeabiliteit na LPS aangetoond, waaronder een relatieve toename van endotheliale activeringsmarkers (bijv. ICAM-1 en VCAM-1) en een toename van het aantal neutrofielen in blaarvocht.

Een belangrijk voordeel van ons ID LPS-model is dat het tegelijkertijd meetbare ontstekingsreacties en vasculaire reacties induceert. Dit bootst pathofysiologische mechanismen die ook voorkomen bij ziekten goed na, aangezien de ziekten die gepaard gaan met verhoogde vasculaire permeabiliteit vrijwel altijd ook inflammatie met zich meebrengen. Bij sepsis bijvoorbeeld leidt systemische ontsteking tot endotheliale dysfunctie, verstoring van de tight junctions en aanzienlijke perifere en pulmonale vasculaire lekkage. Daarnaast, hoewel het bij de volgende voorbeelden om chronische aandoeningen gaat in tegenstelling tot acute ontstekingen, gaan ontstekingsreacties bij kanker en diabetes gepaard met een verminderde integriteit van de endotheliale barrière en een verhoogde microvasculaire permeabiliteit. Het gecombineerde inflammatoire en vasculaire profiel van het ID LPS-model is dus translationeel relevant voor een breed scala aan ziekten. Een ander sterk punt van het model is de gecontroleerde en nauwkeurige lokale beoordeling van vasculaire lekkage in de loop van de tijd, zonder de logistieke en veiligheidsbeperkingen van systemische challenge-modellen bij gezonde vrijwilligers, zoals bij de intraveneuze LPS-challenge.

Idealiter zouden we ook aantonen dat de door ID LPS-geïnduceerde vasculaire reacties kunnen worden beïnvloed door geneesmiddelen met een vasculair target. Dit was echter op dit moment niet mogelijk omdat zulke geneesmiddelen niet op de markt beschikbaar zijn. Echter, uit niet-gepubliceerde data blijkt dat een experimentele mitogen-activated protein kinase (MAPK)-remmer de door ID LPS-geïnduceerde toename van het huidvolume

volledig kan onderdrukken. Dit suggereert dat in ieder geval de LPS-geïnduceerde vaatlekkage farmacologisch kan worden beïnvloed. Gezien de pijplijn van kandidaat-geneesmiddelen die zich op vasculaire reacties richten is het hopelijk slechts een kwestie van tijd voordat uitgebreide benchmarking voor alle uitleesmaten van de ID LPS-challenge als vasculair model gedaan kan worden.

LPS–EEN OMICS-KARAKTERISATIE VAN HET MODEL

Naast het verhogen van de efficiëntie van geneesmiddelontwikkeling door het bestuderen van proof-of-pharmacology met behulp van humane challenge-modellen, kan de toepassing van een omics-benadering ook het hoge percentage mislukkingen bij de klinische ontwikkeling van kandidaat-geneesmiddelen tegengaan. Dergelijke omics-benaderingen integreren biologische, computationele en farmacologische kennis. Hierdoor worden nieuwe inzichten mogelijk in de biologie van ziekten en de werkingsmechanismen van kandidaat-geneesmiddelen, waarbij de nadruk ligt op pathways en mechanismen. Dit verbetert de identificatie van medicijn targets, de voorspelbaarheid van de werkzaamheid van kandidaat-geneesmiddelen en de validatie van targets in een klinische setting. Data die verzameld zijn in studies met humane challenge-modellen kunnen ook gebruikt worden bij dergelijke benaderingen.

Hoofdstuk 5 presenteert een uitgebreide omics-karakterisatie van de menselijke respons op ID LPS-injectie. We hebben aangetoond dat na ID LPS-injectie op RNA niveau veranderingen optreden aangaande de inflammatoire reactie in huidweefsel. Deze veranderingen worden gekenmerkt door een toename van aangeboren immuniteit- en receptorsignalerings-gerelateerde pathways, waaronder TLR4-signalering en daaronder vallende genen. Dit RNA profiel vertaalde zich ook naar een eiwit profiel met een significante toename van ontstekingseiwitten gerelateerd aan TLR4. Daarnaast zagen we dat de RNA dataset een aanzienlijke overlap vertoonde met de geannoteerde genensets van een reeks immunologische en inflammatoire ziekten. Dit onderstreept de translationele relevantie van het ID LPS-model voor de ontwikkeling van geneesmiddelen voor een breed scala aan inflammatoire ziekten.

De gepresenteerde data kunnen gebruikt worden om op een geïnformeerde wijze challenge-modellen in vroege fase klinische studies van immunomodulerende geneesmiddelen te selecteren. Men kan namelijk zien of het werkingsmechanisme van kandidaat-geneesmiddelen overlapt met de targets en pathways die worden beïnvloed door ID LPS, en ook of die overlappen met geannoteerde genensets van voor het middel relevante ziekten. Bovendien biedt hoofdstuk 5 een hulpmiddel om in een vroeg stadium van de klinische ontwikkeling te beoordelen of kandidaat-ontstekingsremmende geneesmiddelen mechanismen moduleren die relevant zijn voor de ziekte waarvoor ze ontwikkeld worden.

Toekomstig onderzoek zou op deze bevindingen kunnen voortbouwen door de bijdragen van individuele cellen aan de waargenomen transcriptieveranderingen verder te verduidelijken. Een andere interessante richting die het onderzoek in de toekomst zou kunnen inslaan, is het focussen op specifieke elementen van de waargenomen ontstekingsreactie die mogelijk bruikbare targets voor geneesmiddelen vormen (bijvoorbeeld complement- en inflammasoom-activering). Uiteindelijk zou de integratie van deze gegevens met bestaande kennis over zowel de ID LPS-reactie bij mensen, als de biologie van ontstekingsziekten een systeem-biologische benadering van de ontwikkeling van ontstekingsremmende geneesmiddelen kunnen ondersteunen om geneesmiddelontwikkelingsprogramma's verder te verbeteren.

DEEL 2: ONGECONTROLEERDE ONTSTEKINGSREACTIES

Bevindingen in dit proefschrift en bijbehorende toekomstperspectieven

OIS - ACHTERGROND

In tegenstelling tot inflammatoire challenge-modellen bij mensen, die in een gecontroleerde omgeving milde, voorbijgaande ontstekingsreacties opwekken, vertegenwoordigt OIS een onge-

controleerde ontstekingsreactie die tijdens klinische studies kan optreden. Deze reacties worden veroorzaakt door het kandidaat-geneesmiddel zelf. De afgelopen jaren is de toenemende structurele complexiteit van immunomodulerende geneesmiddelen, met name bispecifieke of Fc-gemodificeerde antilichamen, in verband gebracht met een toename van het aantal gevallen van OIS.

Ondanks die toenemende incidentie van OIS in vroege fase klinische geneesmiddelstudies, met grote gevolgen voor de veiligheid van deelnemers aan studies en de efficiëntie van de ontwikkeling van geneesmiddelen, bestaat er momenteel geen uitgebreide, evidence-based richtlijn of kader voor de anticipatie en preventie ervan. Bovendien worden vroege fase klinische studies waarin OIS voorkomt vaak niet gepubliceerd, wat onze collectieve kennis en potentiële wetenschappelijke vooruitgang op dit gebied beperkt.

OIS – LESSEN DIE WE KUNNEN TREKKEN UIT DRIE KLINISCHE CASES

Hoofdstuk 6 van dit proefschrift presenteert de lessen die zijn getrokken uit drie klinische casussen van door kandidaat-geneesmiddelen veroorzaakte OIS, in de context van de huidige regulatoire richtlijnen. We hebben laten zien dat OIS kan optreden ondanks naleving van de bestaande FDA- en ICH-richtlijnen voor preklinische en klinische risicobeoordeling van kandidaat-geneesmiddelen. Dit benadrukt de beperkte voorspelbaarheid van OIS en de noodzaak van een meer verfijnde aanpak. Bovendien is er momenteel geen verplichting om specifieke details te bestuderen wanneer OIS zich voordoet in klinische studies, waardoor we onvoldoende kunnen leren van de incidenten.

Daarom stelt hoofdstuk 6 voor dat het van cruciaal belang is dat klinische onderzoekers en farmaceutische bedrijven tijdens het ontwerp van de eerste klinische studie uitgebreid overleggen over het potentieel van het kandidaat-geneesmiddel om OIS te veroorzaken. Bovendien kunnen lokale regelgevende instanties actief worden benaderd om deel te nemen aan deze discussies. Dergelijke discussies maken het mogelijk om, indien nodig, de preklinische kennis over de kenmerken van het kandidaat-geneesmiddel tijdig uit te breiden en helpen bij het anticiperen op het mogelijk optreden van OIS. Dit omvat de implementatie van evidence-based, geneesmiddel-specifieke protocollen voor de klinische behandeling van OIS. Dergelijke specifieke protocollen moeten praktische instructies bevatten met gedetailleerde procedures voor de detectie en de beoordeling van OIS, aangevuld met een beschrijving van relevante biomarkeranalyses die moeten worden uitgevoerd wanneer OIS optreedt.

Toekomstige studies waarin wordt ingezet op een betere samenwerking tussen onderzoekers, farmaceutische bedrijven en lokale regelgevende instanties, in combinatie met uitgebreide behandelingsprotocollen en analyse van OIS (indien deze zich voordoet), zullen profiteren van een effectievere behandeling van OIS. Tegelijkertijd zal het inzicht over de mechanismen die ten grondslag liggen aan de door het kandidaat-geneesmiddel-geïnduceerde OIS toenemen. Dergelijke kennis ondersteunt weloverwogen, evidence-based besluitvorming over de voortzetting of wijziging van geneesmiddelontwikkelingsprogramma's, waardoor de verdere klinische ontwikkeling wordt verbeterd.

CONCLUSIE

In dit proefschrift hebben we ons gericht op het vergroten van de kennis over gecontroleerde en ongecontroleerde ontstekingsreacties in vroeg stadium klinisch-farmacologisch onderzoek, met als uiteindelijk doel het bevorderen van immunologische klinische geneesmiddelontwikkeling.

De studies waarbij gebruik werd gemaakt van het AITC model hebben aangetoond dat de inductie van gecontroleerde ontstekingen bij gezonde vrijwilligers effectief kan worden gebruikt om farmacodynamische effecten en geneesmiddeltarget binding te beoordelen in gezonde vrijwilligers. Daarnaast hebben we het ID LPS-model gekarakteriseerd voor vasculaire lekkage voor toekomstige vroege fase klinische onderzoeken. De bijbehorende omics-analyses van de ID LPS-respons leverden diepgaande mechanistische inzichten op en koppelen het model aan ziekte-gerelateerde pathways, waardoor de translationele waarde voor geneesmiddelontwikkeling wordt versterkt. Samen vergroten deze vorderingen de kennis en toepasbaar-

heid van gecontroleerde human inflammatoire challenge-modellen waardoor informatievere proof-of-pharmacology-studies mogelijk worden voor immuungerichte kandidaat-geneesmiddelen in de vroege fase van geneesmiddelontwikkeling.

Tegelijkertijd onderstreepte onze evaluatie van drie klinische gevallen van OIS dat ongecontroleerde ontstekingsreacties moeilijk te voorspellen en mechanistisch te bestuderen zijn, ondanks bestaande regelgevende richtlijnen. Deze bevindingen benadrukken de noodzaak van systematische OIS-behandelingsprotocollen, evaluatiestrategieën en verbeterde samenwerking tussen onderzoekers, sponsors en regelgevende instanties. Deze benaderingen verbeteren de anticipatie op OIS, de behandeling van OIS en ondersteunen evidence-based besluitvorming in geneesmiddelontwikkelingsprogramma's.

We hopen dat de inzichten die uit dit proefschrift zijn verkregen bijdragen aan de informatieve en translationele waarde van toekomstige klinisch-farmacologische studies. Idealiter zal dit leiden tot veiligere, efficiëntere en informatievere geneesmiddelontwikkelingsprogramma's, waardoor schaarse middelen doelmatiger worden ingezet en effectieve therapieën voor patiënten sneller beschikbaar kunnen komen.

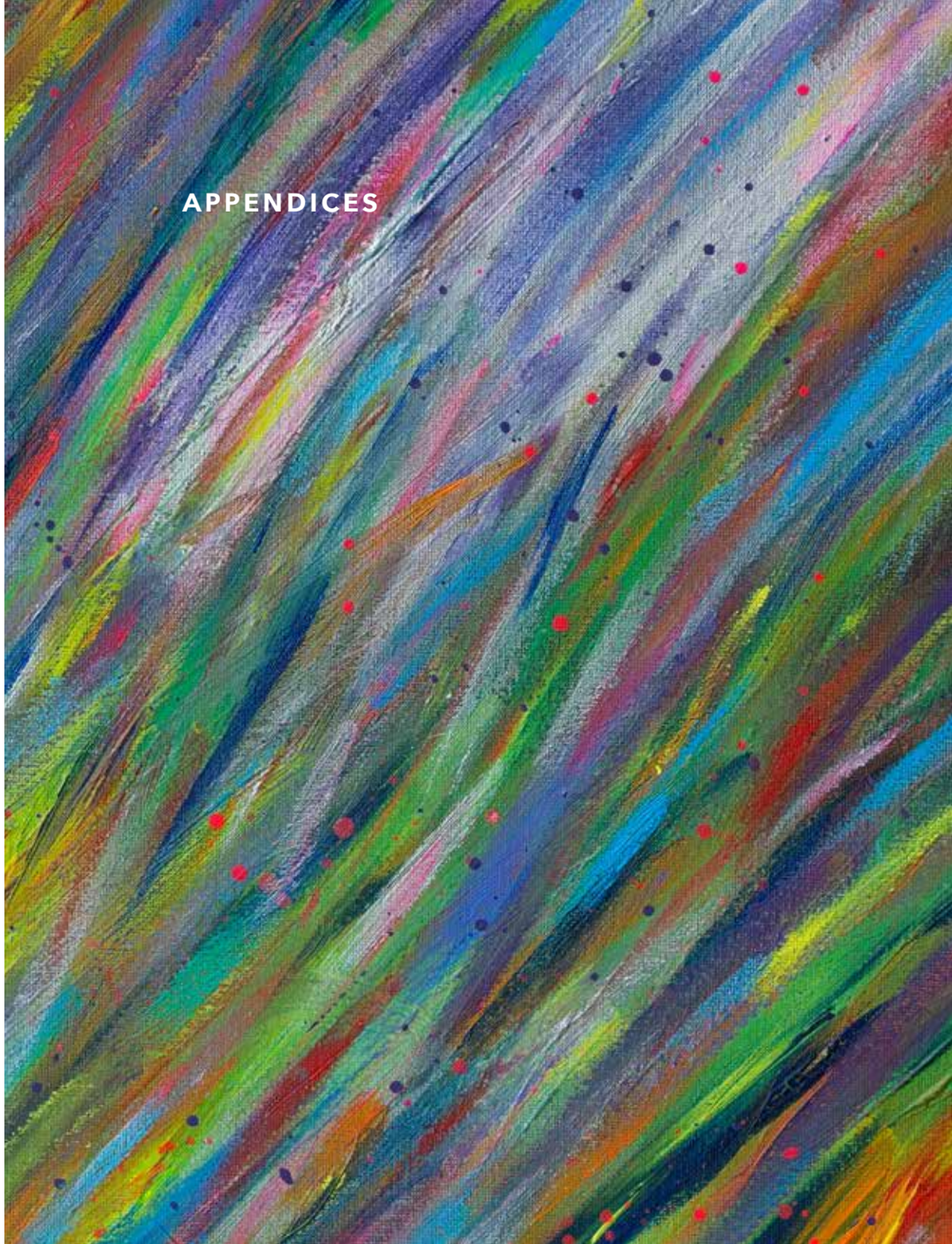

AN OVERVIEW OF THE PHD TRAJECTORY

The PHD trajectory of M.C.E. (Marella) van Ruissen represented an intensive period of growth, during which scientific, collaborative and leadership skills were gradually developed and refined. At the outset, the focus was primarily on designing and conducting clinical pharmacological studies and acquiring basic knowledge of drug development, pharmacokinetics, and pharmacodynamics, while gradually transitioning toward independent initiation and execution of research projects and innovate methodologies. The trajectory was characterised by a strong focus on the development of novel methodologies, the organisation of studies (including a multi-centre patient study), active participation in team science, and contributions to teaching and clinical pharmacology education.

Throughout the PHD, Marel was involved in the innovation of at least four methodological applications to investigate vascular leakage, vasodilation, glycocalyx quality, and thrombocyte activation. This exemplifies her ability to identify unmet methodological needs and address them using acquired scientific knowledge and creativity.

Alongside research, teaching and supervision formed a consistent part of Marel's PHD trajectory. Each year, she taught pharmacodynamic working groups to medical and biopharmaceutical sciences students. Furthermore, she delivered sessions on a variety of subjects relevant to colleagues, including cytokine release syndrome and a range of pharmacological challenge models. She also contributed to the development of educational material on pharmacokinetics and examinations. In addition, she supervised internships of multiple MSc students, providing guidance on a personal and scientific level. This combination of teaching and supervision facilitated Marel's personal development into a knowledgeable researcher with strong leadership skills.

Team science and open science were integral to the PHD trajectory. She delivered presentations regularly during biweekly group meetings, monthly scientific advisory board discussions, and (clinical) pharmacology meetings. These interactions stimulated exchange of knowledge, in-depth reasoning about research design, set-up, conduct, and results. Open communication of study outcomes extended beyond the scientific community, with results being shared directly with study participants and presented to all colleagues of CHDR, where complex data were translated into a broadly accessible and understandable format. These activities emphasised transparency and societal engagement in her clinical pharmacological research.

A key aspect of Marel her PHD trajectory was responsibility for ethical approval processes. Marel took the lead in over five applications submitted to national and local ethical bodies. This required detailed knowledge of the prepared study protocols, familiarity with regulatory frameworks, and interdisciplinary interactions and collaborations. Active participation in ethics committee meetings (METC LDD, METC BEBO, CCMO) was also part of the PHD trajectory. In several instances, she provided advice on the ethical approval of submitted clinical pharmacological studies. These activities reflect not only her procedural knowledge, but also her capability to work with a range of colleagues with different backgrounds, and her understanding of the broader ethical dimensions of early-phase human research.

Leading the organisation of complex studies further illustrated Marel's growing independence. She coordinated the set-up and conduct of over five studies, including the participation in a global multi-centre patient study, which required the establishment of logistic frameworks, cross-site collaboration, and harmonisation of study protocols. These efforts highlight her ability to lead complex logistical operations and demonstrate her suitability for roles requiring large-scale overview and coordination.

Marel's leadership responsibilities expanded in parallel with scientific activities. Within the clinical environment, she guided new physicians in their on-call responsibilities, and she assumed accountability for all non-trial related medications. These roles required the ability to train and support colleagues in a dynamic setting and further reflect her transition from trainee to independent professional.

Participation in national and international immunology- and pharmacology-focused meetings was frequent. These events provided exposure to the latest developments in the field. Her professional and personal growth was further stimulated through the completion of a multitude of courses in clinical pharmacology and project management. This structured training pathway facilitated the development of both technical expertise and essential competencies for managing complex projects and multidisciplinary teams. Furthermore, it enabled Marel to become a certified clinical pharmacologist.

In conclusion, Marel's PHD trajectory was marked by progressive development from a novice researcher to an independent scientist capable of leading diverse research projects. The combination of clinical pharmacological knowledge, methodological innovation, teaching and supervision activities, active ethical participation, and scientific and logistical coordination of clinical studies and research projects illustrates a PHD trajectory that enabled her to develop increasing responsibility and expertise.

CRediT statement of the thesis chapters

A tabular overview of the contributions of the PHD Candidate to each scientific chapter presented in this thesis according to the CRediT taxonomy is depicted in Figure 1.

Dissemination table

Table 1 provides a tabular overview of the dissemination of the scientific research presented in this thesis. The manuscripts are listed in order of publication date (oldest first).

FIGURE 1 **CRediT table for the thesis of M.C.E. van Ruissen.** The contributions of M.C.E. van Ruissen to each scientific chapter in this thesis are listed in the table. The colours represent lead, equal, supporting, and no contribution from dark purple to white. Study preregistration status, and manuscript preprinting and peer reviewed publication status are listed in the table as well.

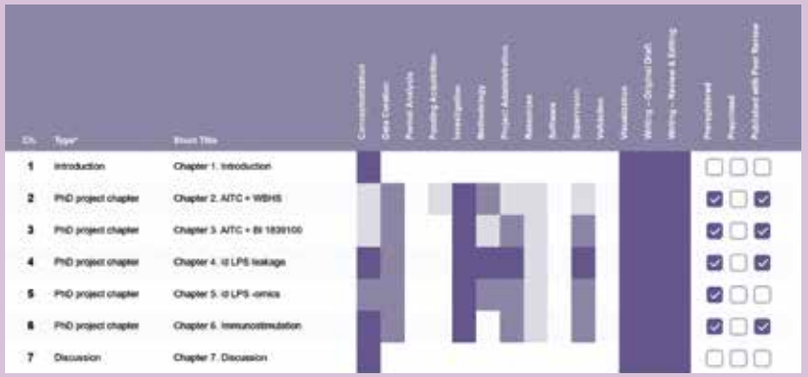

PhD project chapters are the direct result of the PhD project of the PhD candidate.Some theses also include Collaboration Chapters, to which the PhD candidate has contributed but fall outside the PhD project.

TABLE 1 **Dissemination table of scientific research within this PHD thesis.**

Van Ruissen MCE, van Kraaij SJW, Gal P, et al. Open-Label Interventional Study in Healthy Volunteers to Evaluate NO-Mediated Vasodilation by Dermal Allyl Isothiocyanate Challenge and Whole-Body Heat Stress. J Exp Pharmacol. 2024;16:285-294. Published 2024 Sep 17. doi:10.2147/JEP.S473217	
Chapter in this thesis	2
Pre-registration	https://onderzoekmetmensen.nl/nl/trial/50731
Registered report	N/A
Datamanagement plan	Present in study file, not available open source
Study materials	Present in study file, not available open source
Conference contributions of PHD candidate	Moderated poster presentation at NVKFB voorjaarsdag 2022
Open data/figures	Only data publicly available from publication: https://www.dovepress.com/open-label-interventional-study-in-healthy-volunteers-to-evaluate-no-m-peer-reviewed-fulltext-article-JEP
Code/software	Present in study file, not available open source
Preprint	N/A
Publication in peer reviewed journal	https://www.dovepress.com/open-label-interventional-study-in-healthy-volunteers-to-evaluate-no-m-peer-reviewed-fulltext-article-JEP
Other forms of dissemination	Summary of results for all study participants.
Van Ruissen MCE, van Kraaij SJW, Wolfova J, et al. Proof of Pharmacology, Safety, and Pharmacokinetics of the Novel TRPA1 Antagonist BI 1839100: A Randomised, Placebo-Controlled, Parallel Group, First-In-Human Study in Healthy Male Participants. Clin Transl Sci. 2025;18(8):e70290. doi:10.1111/cts.70290	
Chapter in this thesis	3
Pre-registration	https://www.onderzoekmetmensen.nl/nl/trial/51644 https://clinicaltrials.gov/study/NCT05354453?term=NCT05354453&rank=1 EUDRACT: 2021-006294-27
Registered report	N/A
Datamanagement plan	Present in study file, not available open source
Study materials	Present in study file, not available open source
Conference contributions of PHD candidate	N/A
Open data/figures	Only data publicly available from publication: https://ascpt.onlinelibrary.wiley.com/doi/10.1111/cts.70290
Code/software	Present in study file, not available open source
Preprint	N/A
Publication in peer reviewed journal	https://ascpt.onlinelibrary.wiley.com/doi/10.1111/cts.70290

(Continuation table 1)

Other forms of dissemination	Summary of results for all study participants. Publication in CHDR library: https://chdr.nl/library/proof-of-pharmacology-safety-and-pharmacokinetics-of-the-novel-trpa1-antagonist-bi-1839100-a-randomized-placebo-controlled-parallel-group-first-in-human-study-in-healthy-male-participants
Van Ruissen MCE, van den Noort JA, Smidt LCA et al. Adverse immunostimulation in early-phase clinical trials: key findings and recommendations based on the investigator's clinical experience. Br J Clin Pharmacol. Published online ahead of print September 19, 2025. doi:10.1002/bcp.70276	
Chapter in this thesis	6
Pre-registration	The URLs and database registration numbers of the three presented clinical trials cannot be shared to ensure anonymity of the three described compounds.
Registered report	N/A
Datamanagement plan	Present in study files, not available open source
Study materials	Present in study files, not available open source
Conference contributions of PHD candidate	Poster at IUIS 2023 Poster at NVVI-BIS dagen 2023 Poster at ECI 2024
Open data/figures	Only data publicly available from publication: https://bpspubs.onlinelibrary.wiley.com/doi/epdf/10.1002/bcp.70276
Code/software	Present in the study files, not available open source
Preprint	N/A
Publication in peer reviewed journal	https://bpspubs.onlinelibrary.wiley.com/doi/epdf/10.1002/bcp.70276
Other forms of dissemination	Summaries of results for all study participants.
Van Ruissen MCE, van Diemen M, Botros L, et al. Breaking barriers: characterisation of the intradermal lipopolysaccharide challenge as an in vivo model for controlled induction of vascular leakage in healthy volunteers. Clin Pharmacol Ther. Published online November 15, 2025. doi:10.1002/cpt.70126	
Chapter in this thesis	4
Pre-registration	EUDRACT: 2024-512377-27-00
Registered report	N/A
Datamanagement plan	Present in study file, not available open source
Study materials	Present in study file, not available open source
Conference contributions of PHD candidate	Poster at ECI 2024 Poster at ESC congress 2024 Poster at IVBM 2024
Open data/figures	Only data publicly available from publication: https://ascpt.onlinelibrary.wiley.com/doi/10.1002/cpt.70126

(Continuation table 1)

Code/software	Present in study file, not available open source
Preprint	N/A
Publication in peer reviewed journal	https://ascpt.onlinelibrary.wiley.com/doi/10.1002/cpt.70126
Other forms of dissemination	Summary of results for all study participants
Van Ruissen MCE, van den Noort JAA, Tomljanovic I, et al. Advancing Clinical Drug Development: Omics-Based Immunological Characterisation of the Intradermal Lipopolysaccharide-Driven Human Inflammatory Response	
Chapter in this thesis	5
Pre-registration	EUDRACT: 2024-512377-27-00 https://onderzoekmetmensen.nl/nl/trial/53274
Registered report	N/A
Datamanagement plan	Present in study file, not available open source
Study materials	Present in study file, not available open source
Conference contributions of PHD candidate	Oral presentation at Complement Summit 2024 Poster at Dutch complement symposium 2025
Open data/figures	TBD
Code/software	Present in study file, not available open source
Preprint	N/A
Publication in peer reviewed journal	TBD
Other forms of dissemination	Summary of results for all study participants

Overview of courses and other educational activities

Tables 2, 3, and 4 present the courses and training activities completed by M.C.E. van Ruissen during her PHD programme. Table 2 lists the mandatory courses and activities, Table 3 lists the scientific courses and activities, and Table 4 summarises all activities involving transferable skills.

TABLE 2 Overview of mandatory courses and workshops.

Date	Title	Study load
Dec. '21	Responsible research	1.5 EC / 42 hrs
May '22	Scientific Conduct	0.2 EC / 5 hrs
Oct. '22	Leiden University Onboarding Programme (meeting)	0.2 EC / 5 hrs
Feb. '23	Basic Methods and Reasoning in Biostatistics	1.5 EC / 42 hrs
Aug. '25	Leiden University Onboarding Programme (e-learning)	0.2 EC / 5 hrs
TOTAL		3.6 EC / 99 hrs

TABLE 3 Overview of scientific courses, workshops and other training activities.

Date	Title	Study load
Dec. '21–May '22	EU CTR Expert course	0.3 EC / 9 hrs
Dec. '21–Nov. '25	Biweekly Science Meeting	2.9 EC / 80 hrs
Dec. '21–Nov. '25	Weekly Clinical Pharmacology Education Hour	5.7 EC / 160 hrs
Dec. '21–Nov. '25	Monthly scientific advisory board meeting	2.9 EC / 80 hrs
Jan. '22	Medicamenteuze therapie	0.6 EC / 16 hrs
Jan. '22	Clinical Research in the Netherlands–Legislation+ Procedures course	0.3 EC / 8 hrs
Jan. '22–Nov. '25	Clinical Pharmacological Lectures - LUMC/CHDR	1.4 EC / 40 hrs
March '22–June '25	Presentations on AITC+WBHS challenge in healthy volunteers, glycocalyx imaging, healthy volunteers, safety findings in FIH trials, effects of behavioural interventions on IV LPS challenge, PK/PD in a FIH trial, multispectral imaging, mAbs during pregnancy, mechanisms of hyperammonemia.	1.7 EC / 48 hrs
April '22	NVKFB voorjaarsdag, moderated poster presentation	0.3 EC / 8 hrs
April '22	PK-PD course	0.5 EC / 14 hrs
April '22	Contributed to poster presentation EFIC congress	0.1 EC / 2 hrs
April '22–July '25	Scientific advisory board presentations of protocols and results of FIH studies and other clinical pharmacological studies	0.5 EC / 14 hrs
Oct.–Dec. '22	Clinical Development course	1.8 EC / 50 hrs
Nov. '22–Nov. '25	Toxicology education hour - Radboud UMC	1.1 EC / 30 hrs
May '23	Pharmacogenetics in practice course	0.3 EC / 8 hrs
August–Sept. '23	Case Studies in Personalised Medicine (pharmacogenetics) course	0.6 EC / 18 hrs
Sept. '22–Sept. '25	Teaching basic pharmacodynamics–Working group 1+2	0.5 EC / 14 hrs
October '23	Health Technology Assessment Course	0.4 EC / 10 hrs
Nov. '23	Joint Belgian-Dutch Immunology Meeting, poster presentation	0.6 EC / 16 hrs
Nov.–Dec. '23	Peer review article BJCP #1	0.3 EC / 8 hrs
Dec. '23	International Congress of Immunology, poster presentation	1.8 EC / 50 hrs
Jan. '24	Principles in epidemiology course	0.2 EC / 5 hrs
April '24–May '25	Lecture series on microvascular imaging	0.2 EC / 5 hrs
July–Sept. '24	Contributed to poster presentation International Vascular Biology Meeting and poster presentation European Society of Cardiology Congress	0.1 EC / 2 hrs
Sept. '24	European Congress of Immunology, poster presentation	1.4 EC / 40 hrs
Dec. '24–April '25	Contribution to oral presentation complement summit and poster presentation Dutch complement days	0.1 EC / 2 hrs
April–Sept. '25	Development of education about distribution volume	0.4 EC / 10 hrs
June '25	EULAR congress	1.1 EC / 32 hrs
Sept. '25	Peer review article BJCP #2	0.2 EC / 5 hrs
TOTAL		28.3 EC / 784 hrs

TABLE 4 Overview of transferable skills courses, workshops and other training activities.

Date	Title	Study load
Feb. '22–Mrch '23	Traineeship for clinical scientists & physicians–CHDR	0.6 EC / 17 hrs
April '22–Aug. '23	Intervision PHD students	0.4 EC / 10 hrs
July–Nov. '22	METC meetings: Leiden, Den Haag, Delft+stichting BEBO	1.1 EC / 30 hrs
Oct. '22	Teach the Teacher course	0.4 EC / 11 hrs
Feb.–Mrch '23	Development+guidance internship medicine master student	0.4 EC / 10 hrs
Feb.–Mrch '23	Committee meetings: formulary meeting LUMC, antibiotics committee LUMC, Expertgroup Toxicology NVIC/NVZA/NVKFB	0.3 EC / 8 hrs
Feb.–Nov. '23	Guidance internship biopharmaceutical sciences master student	3.9 EC / 108 hrs
June–July '23	Basic project management for PHDs course	0.5 EC / 13 hrs
June–July '23	Effective Communication course	0.4 EC / 10 hrs
Oct. '23	Managing your references using Mendeley course	0.1 EC / 3 hrs
Nov. '23–Jan. '24	Advanced project management for PHDs course	0.6 EC / 17 hrs
Sept. '24	CCMO meeting	0.2 EC / 5 hrs
Sept.–Oct '25	Presenting skills for researchers course	0.7 EC / 20 hrs
TOTAL		9.6 EC / 262 hrs

CURRICULUM VITAE

Marella Cornelia Elizabeth van Ruissen was born on 16 January 1996 in Ede, The Netherlands. From a young age, her curiosity, social engagement, adventurous spirit, and intellect were first signs that made it clear that she would follow a path combining compassion, science, and lifelong exploring. To nurture those talents, Marel took part in various social activities during high school, including chairing the local youth tennis committee, serving on the youth city council, and volunteering in Ghana. After obtaining her Gymnasium diploma in 2014 at CSG Het Streek in Ede, she moved to Amsterdam to study Medicine at the University of Amsterdam. Early in her academic career, she developed an interest in scientific research and published research articles on the effects of probiotics on pneumonia and on the impact of travel on antibiotics use in immunocompromised patients. She obtained her Bachelor's degree *cum laude* in 2017 and continued with the Master of Science in Medicine, also at the University of Amsterdam. Alongside her studies, she became actively involved in the national advocacy organisation for medical students, De Geneeskundestudent. Her roles as general board member and, later, as commissioner of internal affairs allowed her to contribute to improving the academic environment for medical students on a national level. In 2020, she obtained her medical degree and started working as a resident (ANIOS) in the Department of Internal Medicine at the Spaarne Gasthuis, where she worked across various wards and contributed to patient care during the early stages of the COVID-19 pandemic. This period was not just about practising medicine, but also about experiencing the power of calm amidst chaos, of human connections, and of human resilience. In 2021, she joined the Centre for Human Drug Research (CHDR) as research physician and project leader. Simultaneously, she began her PHD trajectory investigating controlled and uncontrolled inflammatory responses under the supervision of dr. M.A.A. Jansen, dr. M. Moerland and prof. dr. J. Burggraaf. During her time at CHDR, she also completed the training programme to become a clinical pharmacologist. In addition to the research projects presented in this thesis, she contributed to numerous other early-phase clinical studies in the fields of immunology, dermatology, psychiatry, and neurology and initiated many exploratory projects on the vascular effects of intradermal lipopolysaccharide. In January 2026, following the completion of her PHD thesis, she began her specialist training in rheumatology in Leiden. An ideal fit to continue nurturing her talents and combining them with her clinical and research interests. Marel is a physician, a clinical pharmacologist, a scientist, and, above all, someone who sees medicine as a calling to unite compassion, science, and lifelong exploring.